Luman/CREB3 is a novel retrograde regulator of sensory neuron regeneration: mechanism of action

A Thesis Submitted to

the College of Graduate Studies and Research

In Partial Fulfillment of the Requirements

For the Degree of Doctor of Philosophy

In the Department of Anatomy and Cell Biology

University of Saskatchewan

Canada

By

Zhengxin Ying

Permission to use

In presenting this thesis in partial fulfillment of the requirements for a Postgraduate degree from the University of Saskatchewan, I agree that the libraries of this University may make it freely available for inspection. I further agree that permission for copying of this thesis in any manner, in whole or in part, for scholarly purposes may be granted by the professor or professors who supervised my thesis work or, in their absence, by the Head of the Department or the Dean of the College in which my thesis work was done. It is understood that any copying or publication or use of this thesis or parts thereof for financial gain shall not be allowed without my written permission. It is also understood that due recognition shall be given to me and to the University of Saskatchewan in any scholarly use which may be made of any material in my thesis.

Requests for permission to copy or to make other use of material in this thesis in whole or part should be addressed to:

Head of the Department of Anatomy and Cell Biology

University of Saskatchewan

Saskatoon, Saskatchewan S7N 5E5

Canada

Abstract

Luman (CREB3, LZIP) is a basic leucine zipper transcription factor involved in regulation of the unfolded protein response (UPR), dendritic cell maturation, and cell migration. But despite reported expression in primary sensory neurons, little is known about its role in the nervous system. Luman mRNA from rat sensory neurons was amplified and its coding sequence was determined. The rat Luman cDNA contains a full-length open reading frame encoding 387 amino acids, and the recombinant protein generated from this clone activated transcription from UPR elements. Quantitative RT-PCR revealed rat Luman transcripts in a variety of rat tissues with the highest levels in nervous system tissue. *In situ* hybridization confirmed the findings and demonstrated that the Luman mRNA hybridization signal localizes to neurons and satellite glial cells in dorsal root ganglia (DRG), the cytoplasm of hepatocytes in liver, and the hippocampal pyramidal cell layers in CA1 and CA3 and the granular cell layer of the dentate gyrus. Luman protein localizes with axonal endoplasmic reticulum (ER) components along the axon length within the sciatic nerve and is activated by sciatic nerve injury. Adult sensory axons also contain Luman mRNA which is translated within the axon and transported to the cell body via the importin-mediated retrograde transport system in response to nerve injury. Further, creation of an N-terminal, C-terminal dual fluorescence-tagged Luman adenoviral construct allowed visualization of the cleavage and retrograde translocation of the N-terminal portion of Luman to the nucleus in real time *in vivo* and *in vitro*. Neuronal or subcellular axonal knockdown of Luman significantly impaired the intrinsic ability of injury-conditioned, but not naïve, sensory neurons to extend the regeneration-associated elongating form of neurites. Sciatic nerve crush injury also induced activation of the UPR in axotomized DRGs, including genes linked to cholesterol biosynthesis. Knockdown of Luman decreased the activation of UPR and cholesterol biosynthesis, and axotomy-inducted increases in neurite outgrowth, which could be largely rescued with either mild UPR inducer treatment or cholesterol supplementation. Together these findings provide novel insights linking remote injury-associated axonal ER responses to the regenerative growth capacity of adult sensory neurons via axonal activation and synthesis of Luman and reveal a role for the UPR in regulation of axotomy-induced neurite outgrowth that is critically dependent on Luman.

Acknowledgements

I would like to express my deepest appreciation to my supervisor, Dr. Valerie Verge, who has been an excellent mentor for me. I want to thank her for inspiring my pursuit of science, and for trusting me and giving me freedom to conduct research. Her advice on both research and on my career has been invaluable. I would also like to express my gratitude to my co-supervisor, Dr. Vikram Misra. His enthusiasm about science and his way of managing scientific activities has motivated me throughout my PhD study.

I would also like to thank my committee members, Drs. Patrick Krone, David Schreyer, Terra Arnason, and Adil Nazarali. Their encouragements, insightful comments, and critical questions have been very helpful in my research.

I would especially like to thank all the lab technicians: Ruiling Zhai, Jayne Johnston, and Noreen Rapin, and colleagues: Nikki McLean, Joelle Nadeau, Rui Zhang, Ajay Rajaram, and Shannon Berko for providing help whenever I needed.

I would like to thank the University of Saskatchewan College of Graduate Studies and Research and the College of Medicine, and China Scholarship Council for kindly providing my PhD scholarship.

I am also very thankful to my family. Words cannot express how grateful I am to my mother for all of the sacrifices that she has made during the pursuit of my degree. I would also like to thank my friends, Mylyne Tham and Peng Zhai, for supporting me throughout the writing process. At the end, special thanks go to my beloved wife Yang Su who has always been my biggest supporter.

In dedication to my mother for

making me be who I am, and my wife for

supporting me all the way!

Contents

List of tables

List of figures

List of abbreviations

ATF3	activating transcription factor 3
ATF6	activating transcription factor 6
bZIP	basic leucine zipper
cAMP	Cyclic adenosine monophosphate
CAT	Chloramphenicol acetyltransferase
CHOP	CCAAT/enhancer-binding protein homologous protein
CNS	Central nervous system
COPII	coat protein II
CREB	cAMP response element-binding protein
DIV	day/days *in vitro*
DLK	dual leucine zipper kinase
DRG	dorsal root ganglion
EDEM	ER degradation-enhancing alpha-mannosidase
eIF2	eukaryotic translation initiation factor 2
ELISA	Enzyme-linked immunosorbent assay
ER	endoplasmic reticulum
ERSE	ER stress response element
GADD34	growth arrest and DNA damage-inducible protein 34
GAP43	growth associated protein 43
GFP	green fluorescent protein
GRP78	glucose-regulated protein 78
HCF	host cell factor
Herp	homocysteine-induced endoplasmic reticulum protein
INSIG	insulin-induced gene
IP	immunoprecipitation
IRE1	inositol-requiring protein 1
JIP	c-Jun amino-terminal kinase-interacting protein
JNK	c-Jun amino-terminal kinase
LDL	low-density lipoprotein

MAPK	mitogen-activated protein kinase
MOI	multiplicity of infection
mTOR	Mammalian target of rapamycin
NF-κB	Nuclear factor kappa-light-chain-enhancer of activated B cells
NGF	nerve growth factor
NLS	nuclear localization signal
PERK	protein kinase RNA-like ER kinase
PNS	Peripheral nervous system
PP1	protein phosphatase
RAGs	regeneration-associated genes
Ran	Ras-related nuclear protein
RanBP	Ran binding protein
RFP	red fluorescent protein
S1P	site-1 protease
S2P	site-2 protease
SCAP	SREBP cleavage activating protein
SEM	standard error of the mean
Sox11	SRY-box containing gene 11
SREBPs	sterol regulatory element-binding proteins
STAT3	signal transducer and activator of transcription 3
UPR	Unfolded protein response
UPRE	UPR element
XBP1	X-box binding protein 1

1 Introduction

1.1 Peripheral nerve regeneration

The peripheral nervous system (PNS) serves to connect the central nervous system (CNS) to the rest of the body, relaying sensory and motor information between brain and spinal cord and the extremities. Unlike the CNS, which is protected by bones and a blood brain barrier, the PNS is more vulnerable to chemical and mechanical insults. Indeed, among trauma patients, 5.1 % have PNS injuries (Noble et al., 1998), compared to 1.8 % having spinal cord injuries (Hasler et al., 2011).

After injury, the PNS is capable of regeneration. Although the earliest study about PNS regeneration dates back to second century A.D. (Terzis et al., 1997), it was not until 1776, that a British chemist and anatomist William Cumberland Cruikshank did an experiment revealing the physiological aspects of nerve regeneration. It was known that after the bilateral severance of the vagus nerves, animals died after a survival period of "many days" (Willis and Feindel, 1681, reprinted in 1966). Cruikshank found that unilateral cutting of the vagus nerve was not lethal, and if some time was given before cutting the other vagus nerve, survival time was increased. After examining the experimental animal, he found that "the divided nerves of the right side (first cut) were firmly united; having their extremities covered with a kind of callous substance; the regenerating nerve, like bone in the same situation, converting the whole of the surrounding extravasated blood into its own substance." (Cruickshank, 1795).

At that time, scientists did not know whether the regeneration was caused by the reunion of the two cut ends of the nerve, or through the outgrowth of new fibres from the end that attached to the cell body. In 1850, the British neurophysiologist Augustus Volney Waller observed the disorganization of the frog hypoglossal nerves after axotomy. He noted, "On the fifth day the tubes (nerve) appear more varicose than usual, and the medulla (axon) more irregular. About the tenth day the medulla forms disorganized, fusiform masses at intervals, and where the white substance of Schwann cannot be detected… After twelve or fifteen days many of the single tubules have ceased to be visible, their granular medulla having been removed by absorption. The branches contain masses of amorphous medulla." (Waller, 1850). This phenomenon, which is now known as Wallerian degeneration, suggested that the regeneration

was due to outgrowth but not reunion. But with increasing experimental evidence supporting reunion at that time, even Waller himself had accepted the reunion theory (Waller, 1861; Ochs, 1977).

The outgrowth and reunion debate, which lasted throughout the last half of the nineteenth century, was ended by a Spanish pathologist, histologist, and neuroscientist Santiago Ramón y Cajal. He improved a silver staining technique created by the Italian physician and scientist Camillo Golgi. This improved staining method, which is called Cajal's stain, is still in use today. With the developed histological and microscopy techniques, Cajal confirmed Waller's observation. "When one interrupts the continuity of a nerve by the scalpel or destructive agents, the peripheral stump degenerates rapidly, but all its constituent factors do not disappear. By a process of progressive liquefaction and absorption, the axon, myelin, and a part of the organs that are close to Schwann's cell are destroyed." He also found that after the severance of a nerve, "from the third day on, and sometimes before, the various collateral and terminal branches that issue from the fibres of the central stump have grown so much that they abandon the chambers formed by the membrane of Schwann and penetrate into the scar." (Ramón y Cajal and May, 1928, reprinted in 1959). Cajal's work established the "neuron doctrine" that the nervous system is made up of individual cells with distinct structure, function and developmental properties. Within this, his work on repair of the nervous system led to the broad acceptance that injured axons grow in order to reconnect to target (outgrowth theory) as opposed to reuniting with the distal severed end of the nerve (reunion debate).

Our understanding of PNS regeneration has since been significantly elucidated. We now know that for regeneration to occur, Wallerian degeneration and the associated influx of macrophages into both the distal nerve stump and the axotomized cell body are necessary (Lu and Richardson, 1991; Niemi et al., 2013), the axon must have intrinsic growth ability, and the growth environment must be permissive. Unfortunately, despite over 200 years research about PNS regeneration, functional recovery after PNS injury is still disappointing (Johnson et al., 2005). Studying the cellular and molecular mechanisms behind PNS regeneration will not only help us understand the nature of this biological event, but also develop better approaches to treat PNS injuries.

1.1.1 Regeneration in PNS and CNS

Unlike the PNS, the CNS has very limited regeneration ability. Scientists once believed that the CNS neurons had lost their intrinsic regeneration ability after development is completed. Cajal stated: "Pathologists consider it an unimpeachable dogma that there is no regeneration of the central paths… A vast series of anatomico-pathological experiments in animals, and an enormous number of clinical cases that have been methodically followed by autopsy, serve as a foundation for this doctrine, which is universally accepted to-day". He believed that "the general attitude is to attribute the regenerative inefficiency of the centres to the absence of cells of Schwann" (Ramón y Cajal and May, 1928, reprinted in 1959). But this doctrine was challenged by the discovery that injured CNS neurons could regrow into peripheral nerve grafts containing Schwann cells (Richardson et al., 1980). Further, with respect to adult sensory neurons, the growth of the central axon of primary sensory neurons into a peripheral nerve graft occurs only if its peripheral axon had also been injured (Richardson and Issa, 1984), suggesting that both the environment and the neuron must be in a growth permissive state if axonal regeneration is to occur in the CNS.

Research into the nonpermissive nature of the CNS environment for axon regrowth led to the identification of several intrinsic factors that inhibit growth in the CNS (McKerracher et al., 1994; Filbin, 2003; Nash et al., 2009) being identified. However, recent studies showed that deletion or blockage of these intrinsic inhibitor factors did not achieve expected CNS axon regeneration *in vivo*, suggesting that the intrinsic growth ability is different between the PNS and CNS. For example, following injury, many CNS neurons fail to induce the expression of the growth-promoting genes which are highly up-regulated in injured PNS neurons (Huebner and Strittmatter, 2009), with proximity of the injury to the cell body perhaps impacting the response in the CNS (Richardson et al., 1984). The CNS axons also have a lower content of translational machinery than do the PNS axons (Verma et al., 2005), which results in less local protein synthesis that plays an important role in PNS regeneration (Gumy et al., 2010).

1.1.2 Permissive growth environment

Oligodendrocyte-derived myelin in the CNS and Schwann cell-derived myelin in the PNS are both nonpermissive to growth as they contain inhibitory molecules (McKerracher et al., 1994; David et al., 1995). But the differential expression of laminin in the adult PNS versus CNS

(David et al., 1995) coupled with the more rapid clearance of myelin debris in the PNS (Vargas and Barres, 2007) are likely to be factors that contribute to the more permissive growth environment for the PNS axon. A positive impact on growth has also been linked to the availability of injury-associated cytokines [reviewed in (Zigmond, 2012)] and growth factors [reviewed in (Boyd and Gordon, 2003)], and activation of their associated signalling pathways.

1.1.2.1 Physical barrier

After CNS injury, the activation of astrocytes and recruitment of microglia lead to the formation of the glial scar (Cregg et al., 2014), which isolates the injury site and minimizes the area of inflammation, but also becomes a physical barrier for axonal outgrowth. However, in the PNS there is no glial scar formed, and Wallerian degeneration is highly effective in removing myelin debris distal to the site of axon injury within 2 weeks. In contrast Wallerian degeneration lasts from months to years in the CNS (Vargas and Barres, 2007). The delayed degeneration in the CNS contributes to the formation of glial scar in human spinal cord (Buss et al., 2004). Not only does the glial scar form a physical barrier, it also contains inhibitory molecules that hinder axon growth (Silver and Miller, 2004). The value of rapid Wallerian degeneration in PNS regeneration has been demonstrated by the *Wld*^{s} mouse. This mouse has delayed Wallerian degeneration (Lunn et al., 1989), which shows impaired regeneration because of the persistence of distal axons (Bisby and Chen, 1990). It was later found out that the *Wld*^{s} phenotype is due to the expression of a chimeric gene that contains the N-terminal 70 amino acids of ubiquitination factor E4B and the nicotinamide mononucleotide adenylyltransferase (Mack et al., 2001).

1.1.2.2 Molecular barrier

The main inhibitory molecules in the glial scar are chondroitin sulfate proteoglycans, a family of extracellular matrix molecules characterized by a protein core with glycosaminoglycan side chains (Morgenstern et al., 2002). Treatment with chondroitinase ABC, an enzyme that cleaved the side chains from the core protein, promotes functional recovery after spinal cord injury (Bradbury et al., 2002).

Another major class of regeneration inhibitors is the myelin-associated inhibitors which are mainly found in the CNS but not in the PNS. One of the best characterized myelin-associated inhibitors is Nogo (GrandPre et al., 2000). Nogo inhibits neurite outgrowth *in vitro* (Prinjha et al., 2000), and restricts axonal sprouting *in vivo* (Kim et al., 2003b). Forced expression of Nogo in

Schwann cells, which do not normally express it, delays axonal re-extension in PNS injury (Kim et al., 2003a). Genetic deletion of Nogo improves regeneration after spinal cord injury (Simonen et al., 2003). Antibodies that neutralize Nogo also promote axonal regeneration and functional recovery in CNS injuries (Wiessner et al., 2003; Seymour et al., 2005), and one such antibody has reached clinical trial (Zorner and Schwab, 2010).

On the contrary, studies showed that elimination of Nogo is not sufficient to induce extensive axon regeneration (Zheng et al., 2003), and genetic deletion of other myelin-associated inhibitors fails to increase axon regeneration (Lee et al., 2010), which suggests either the existence of other inhibitory factors or that the removal of the inhibitory environment alone is insufficient to support regrowth of injured axons. For example, knockdown of retinoblastoma protein, a tumor suppressor protein, increases axonal regeneration and functional recovery (Christie et al., 2014). In addition, increasing the intrinsic growth ability of injured DRG by axotomy to the peripheral branch before (Neumann and Woolf, 1999), at the same time as (Neumann et al., 2005), or after (Ylera et al., 2009) axotomy to the central branch, greatly enhances the regeneration of the central branch. This indicates that the failure of axonal regeneration in the CNS is not solely due to the existence of inhibitory environments, but also due to the lack of intrinsic growth ability.

1.1.3 Intrinsic growth ability

1.1.3.1 Up-regulation of regeneration-associated genes

Injury to PNS neurons leads to the up-regulation of several regeneration-associated genes (RAGs), which plays a direct role in nerve regeneration. These include transcription factors such as activating transcription factor 3 (ATF3) (Tsujino et al., 2000), c-Jun (Raivich et al., 2004), signal transducer and activator of transcription 3 (STAT3) (Schwaiger et al., 2000), and SRY-box containing gene 11 (Sox11) (Jankowski et al., 2009); and growth associated proteins such as growth associated protein 43 (GAP43) and CAP23 (Bomze et al., 2001).

These RAGs are of importance in regulating nerve regeneration. Forced expression of GAP43 promotes neurite outgrowth (Seijffers et al., 2007); Sox11(Jankowski et al., 2009) and c-Jun (Ruff et al., 2012) are required for axonal regeneration; and deletion of STAT3 in DRG neurons impairs the regeneration of peripheral DRG branches (Bareyre et al., 2011). However, in injured CNS neurons, the up-regulation of RAGs requires injury proximal to the cell body

(Doster et al., 1991) and does not happen or only transiently happens if axons are injured at greater distances from the cell bodies (Fernandes et al., 1999; Liu et al., 2011) the latter correlating with reduced regenerative propensity for these axons (Richardson and Verge, 1986).

Not only is the synthesis of RAGs required for regeneration, but where the protein synthesis takes place is also important. For example, only axonally synthesized GAP43, but not cell body-synthesized GAP43, increases axonal growth (Donnelly et al., 2013).

1.1.3.2 Axonal protein synthesis

The discoveries that blocking general or specific protein synthesis selectively in axons inhibits regeneration (Verma et al., 2005), and that there is an association of decreased axonal protein synthesis with reduced regeneration ability in mature neurons (Jung et al., 2012), support a hypothesis that axonal protein synthesis is required in nerve regeneration.

1.1.3.2.1 Evidence for axonal protein synthesis

Axons were once believed to not have the ability to synthesize proteins, as early studies showed that axoplasm contained no detectable ribosomal RNA (Lasek et al., 1973). However, this interpretation was later challenged by evidence from more sensitive biochemical and microscopic methods showing the presence of ribosomal RNA (Rapallino et al., 1988), mRNAs (Giuditta et al., 1986), and ribosomal proteins (Tcherkezian et al., 2010; Walker et al., 2012) in axons. More convincing evidence supporting axonal protein synthesis came from experiments that showed endogenous (Eng et al., 1999) and exogenous (Van Minnen et al., 1997) mRNA can be translated in axons without somal input.

Even though protein synthesis occurs in axons, there was a failure to detect the endoplasmic reticulum (ER) and Golgi apparatus in early ultrastructure studies (Yamada et al., 1971; Bunge, 1973) raising the question about whether axons have the ability to process proteins. However, isolated axons do have the capacity to traffic axonally-synthesized proteins to the plasma membrane (Merianda et al., 2009) suggesting the existence of functional equivalents of the ER and Golgi apparatus in the axons, with additional studies revealing ER- and Golgi-associated proteins within the axons (Jung et al., 2012; Gonzalez and Couve, 2014).

Local synthesis of proteins allows axons to quickly respond to the changing environment before the arrival of soma-derived proteins. Indeed, even in the absence of neuronal cell bodies,

axons can respond to guidance cues (Campbell and Holt, 2001; Ming et al., 2002) and correctly grow toward their targets (Harris et al., 1987), indicating that axonal protein synthesis plays functional roles in regulating axon growth.

1.1.3.2.2 Function of axonal protein synthesis in axon regeneration

In vivo nerve injury results in increased axonal protein synthesis (Zheng et al., 2001; Verma et al., 2005) and enhanced regeneration *in vitro* (Smith and Skene, 1997; Verma et al., 2005). Conversely, reducing axonal protein synthesis by protein synthesis inhibitors (Verma et al., 2005) or by blocking the axonal localization of mRNAs (Donnelly et al., 2011) inhibits axon regeneration after nerve injury. These findings indicate that the ability of axons to regenerate is associated with their ability to locally synthesize proteins. Indeed, olfactory receptor neurons, one of the few structures in the CNS that naturally regenerate axons (Costanzo, 1991), have proteins locally synthesized in their axons (Dubacq et al., 2009).

Over 2,000 mRNAs have been identified in embryonic and adult peripheral axons (Gumy et al., 2011). Many of them have been shown to be locally translated and to regulate axon elongation, branching and regeneration as well as synapse formation and cell survival (Deglincerti and Jaffrey, 2012; Jung et al., 2012). It is interesting that axonal protein synthesis itself is regulated by proteins that are synthesized in the axons. Eukaryotic translation initiation factors eIF2B2 and eIF4G2 are locally synthesized in axons, which when blocked, inhibits general local protein synthesis and axon growth (Kar et al., 2013). The axon growth pattern is also regulated by local protein synthesis. Increasing axonally synthesized β-actin results in highly branched axons, while increasing axonally synthesized GAP43 results in long axons with few branches, the latter consistent with that observed during regeneration (Donnelly et al., 2013).

Mammalian target of rapamycin (mTOR), a protein that regulates global protein synthesis activity (Laplante and Sabatini, 2009), also regulates local protein synthesis in axons (Campbell and Holt, 2001). Blocking mTOR activity diminishes regeneration *in vitro* (Verma et al., 2005), while increasing mTOR activity has been shown to promote regeneration *in vivo* (Christie et al., 2010). Unlike peripheral axons, injury to CNS axons results in down-regulation in global protein synthesis activity that can be prevented by genetic deletion of the negative regulators of mTOR. By increasing mTOR activity, the injured CNS neurons can regenerate axons (Park et al., 2008), although it is not clear whether axonal or general protein synthesis plays a more direct role in

this effect. Thus, this differential capacity for protein synthesis in the injured PNS versus CNS may be causally linked to their ability to regenerate axons.

1.1.3.3 Retrograde transport of injury signals

Besides functioning in the axons, axonally synthesized proteins can be retrogradely transported back to the cell bodies to deliver the injury signals and regulate a cell body response that is supportive for nerve regeneration. Retrograde transport is mediated by an interaction between cargo proteins and dynein, a motor protein that converts chemical potential energy stored in adenosine triphosphate (ATP) into the kinetic energy of movement (Schnapp and Reese, 1989) along microtubules. Two major retrograde transport dynein interacting protein complexes have been identified: c-Jun amino-terminal kinase (JNK)-interacting protein (JIP) and importins (Rishal and Fainzilber, 2014).

1.1.3.3.1 JIP and associated proteins

JNK is one of the three family members of mitogen-activated protein kinases (MAPKs), with the other two being p38 MAPKs and extracellular signal-regulated kinases (ERKs) [reviewed in (Raman et al., 2007)], that has been shown to be required for successful axonal regeneration (Ruff et al., 2012). JIPs are a group of proteins that interact with activated JNK and bind to JNK cascade kinases. Sciatic nerve injury induces axonal activation of JNK, allowing activated JNK and JIP3 to then be retrogradely transported. This transport is mediated by an injury-enhanced interaction between JIP3 and dynactin (Cavalli et al., 2005), an essential component for dynein activity (Gill et al., 1991). The retrograde transport of JNK also requires the direct interaction between JIP3 and dynein, and this interaction potentially allows JIP3 to carry other retrograde cargos (Drerup and Nechiporuk, 2013), including dual leucine zipper kinase (DLK).

DLK, a MAPK kinase kinase (MAPKKK) that can activate JNK, regulates axonal regeneration by improving the stability of mRNA that is required for local protein synthesis (Yan et al., 2009), and regulates injury responses by JIP3 (Klinedinst et al., 2013). DLK knockout impairs injury-induced enhanced axonal regeneration by blocking the retrograde transport of JIP3 and phosphorylated STAT3 (Shin et al., 2012), the latter being activated after PNS injury and retrogradely transported by importins (Ben-Yaakov et al., 2012).

1.1.3.3.2 Importins and associated proteins

Importins are a group of proteins that regulate nucleocytoplasmic protein transport. They bind to the cargo proteins through a nuclear localization signal (NLS), a recognition motif in the cargo proteins, and then transport them from cytoplasm or axoplasm to the nucleus. Importins have two isoforms, importin α which directly binds to the NLS with low affinity, and importin β which binds to importin α to increase its binding affinity to the NLS [review by (Goldfarb et al., 2004)], helping cargo proteins to be retrogradely transported by dynein. The fact that axonal administration of synthetic NLS peptide can inhibit regenerative outgrowth by competitively blocking retrograde transport of injury signals (Hanz et al., 2003) supports an involvement of importins in retrograde transport within axons, with several different forms of importin α being found to associate with dynein in naïve and injured axons (Hanz et al., 2003). Pathology-dependent creation of the high affinity NLS binding complex is accomplished by the fact that only the mRNA for importin β is found in the axon, with its translated protein being absent in naïve axons. Local translation of axonal importin β mRNA is triggered by axonal injury (Hanz et al., 2003), suggesting that the retrograde transport of injury signals is regulated by axonal protein synthesis. Subsequent experiments demonstrated that axonal knockout of importin β attenuates the cell body transcriptional response to nerve injury, and thereby delays regeneration (Perry et al., 2012).

Several NLS-containing proteins have been identified to be transported through the importin-dynein system to regulate different neuronal activities. Cyclic adenosine monophosphate (cAMP) response element-binding protein 1 (CREB1) is translated in the axons in response to nerve growth factor (NGF), and retrogradely transported to promote neuronal survival (Cox et al., 2008); CREB2 is retrogradely transported after the stimuli inducing long-term depression (a process that decreases the efficiency of synapses) (Lai et al., 2008); and Nuclear factor kappa-light-chain-enhancer of activated B cells (NF-κB) is transported via dynein in response to glutamatergic signals (activated by glutamine binding to its receptor) (Wellmann et al., 2001; Mikenberg et al., 2007). Proteins lacking NLSs were also found to be transported through dynein. Intermediate filament protein vimentin is locally translated in injured sensory axons (Perlson et al., 2005). Vimentin directly binds to importin β and phosphorylated/activated ERK, which does not have NLS, thus allowing ERK to be retrogradely transported through

importins after nerve injury (Perlson et al., 2005). One substrate of ERK is Jacob which is transported to nucleus to regulate cell survival and synaptic plasticity (Karpova et al., 2013).

In injured peripheral neurons, retrograde signals produced at the site of injury or from cells associated with the nerve bind to receptors on the axons and are transported back to the cell body as signalling endosomes ultimately activating transcription of genes believed essential for survival and regeneration (Michaelevski et al., 2010). Alternatively, the absence of retrograde signals normally derived from target tissues that the injured axon is now disconnected from can also trigger alterations in gene expression [reviewed in (Verge et al., 1996; Harrington and Ginty, 2013)]. Some of the injury-associated retrograde signals include transcription factors already localized in the nerve and activated by the injury and/or axonally synthesized in response to the injury. As such, transcription factors are important candidates for retrograde transport cargo proteins. Studies using proteomics and microarrays have identified 39 transcription factors as potential retrograde injury signal candidates (Michaelevski et al., 2010), and have verified this to be the case for STAT3 (Ben-Yaakov et al., 2012). Phosphorylation of STAT3 was found to occur in injured sciatic nerve, with this response extending back to the soma after injury, suggesting that the activated STAT3 acts as a retrograde signal (Lee et al., 2004). Further study revealed that axonal STAT3 is locally translated and activated in response to injury, and is then retrogradely transported through importins to regulate neuronal survival (Ben-Yaakov et al., 2012).

Since retrograde signals play an important role in altering neuronal response to injury, the formation of the retrograde transport complex must be tightly regulated. Indeed, the classical nuclear transport machinery is also found to be functional in the axons (Yudin et al., 2008). The ability of importins to transport their cargo is regulated by Ras-related nuclear protein (Ran), which cycles between a GDP-bound form (RanGDP) in the cytoplasm and a GTP-bound form (RanGTP) in the nucleus. The binding of RanGTP to importins in the nucleus prevents the interaction between importin α and importin β, causing the release of the cargo protein. The RanGTP-importins complex then translocates to the cytoplasm, where Ran binding protein (RanBP) dissociates the complex allowing RanGTP to be converted to RanGDP. RanGTP was found in naïve sciatic nerve axons, where it binds to importin α and dynein preventing retrograde transport from happening (Yudin et al., 2008). RanBP, which is only axonally translated after

injury, promotes RanGTP dissociation from importins, thereby allowing binding of importins to dynein and cargo proteins to form a retrograde transport complex. In support of such a role, blocking the activity of RanBP in injured axons has been shown to reduce the cell body response to injury (Yudin et al., 2008; Yudin and Fainzilber, 2009).

While nerve injury is linked to dramatic increases in protein synthesis at both the axon and soma level, only properly folded proteins are transported from the endoplasmic reticulum (ER) to their destination, while misfolded or unfolded proteins are targeted for refolding or degradation. The accumulation of unfolded proteins in the ER triggers several signal pathways, collectively known as unfolded protein response (UPR).

1.2 Unfolded protein response

In eukaryotic cells, secreted, plasma membrane and organelle proteins fold and mature in the lumen of endoplasmic reticulum (ER) before they can be delivered to their destination as correctly functioning proteins. After being synthesized in the ribosome, unfolded polypeptide chains enter the ER. The amount of newly synthesized polypeptide entering the ER rapidly changes in response to the cell growth state and environmental conditions. To ensure correct protein folding under different loads, cells change the ability of protein folding according to the requirement. This balance is achieved through several signalling pathways that sense the protein folding status in the ER and convey this information to the other components of the cell. Collectively, these signal pathways are referred to as the unfolded protein response (UPR) [reviewed in (Ron and Walter, 2007)].

The imbalance between the unfolded protein in the ER and the cellular protein folding capacity ultimately causes ER stress. The UPR helps cells to cope with this stress and regain balance by increasing the capacity of ER to correctly fold the unfolded proteins and reduce protein synthesis and translocation to the ER [reviewed in (Walter and Ron, 2011)]. However, if cells fail to re-establish homeostasis, then the UPR triggers apoptosis to protect organisms from the toxicity caused by accumulated unfolded proteins.

1.2.1 UPR pathways

Three different, but interactive, pathways have been identified to regulate the UPR. Each pathway utilises a different ER stress transducer and forms a distinct arm of the UPR. The three

signal transducers are inositol-requiring protein-1 (IRE1), protein kinase RNA-like ER kinase (PERK), and activating transcription factor 6 (ATF6).

1.2.1.1 IRE1

IRE1 is the first identified ER stress transducer (Cox et al., 1993) and is the most conserved and the only UPR pathway in lower eukaryotes (Mori, 2009). IRE1, a type 1 ER-resident transmembrane protein, has a cytoplasmic domain containing a kinase module and an endoribonuclease (RNase) domain, and an ER lumenal domain which binds to a molecular chaperone protein, glucose-regulated protein 78 (GRP78). In yeast, IRE1 is activated by the direct binding of unfolded proteins to its ER lumenal domain (Gardner and Walter, 2011). In mammalian cells, the activation of IRE1 depends on dissociation of GRP78 rather than direct interaction with unfolded proteins (Zhou et al., 2006; Oikawa et al., 2009).

Upon receiving the activation signal, IRE1 oligomerizes allowing the kinase domain to undergo trans-autophosphorylation (Li et al., 2010). Instead of generating a conventional cascade of sequential kinase activity (Papa et al., 2003), the phosphorylation of IRE1 triggers its RNase activity, resulting in the endonucleolytic cleavage of X-box binding protein 1 (XBP1) mRNA (Calfon et al., 2002), and endonucleolytic decay of a specific subset of mRNAs (Hollien and Weissman, 2006; Han et al., 2009). The latter reduces the flow of newly synthesized polypeptides into the stressed ER.

Both the precursor and the spliced XBP1 mRNA are translated in metazoans (Yoshida et al., 2006), but their encoded proteins have different functions due to the splicing-mediated reading frame shift. The spliced form of XBP1 (XBP1s) functions as an activator of the UPR and is translated from the spliced mRNA, and this translation increases when IRE1 is activated (Calfon et al., 2002). In contrast, the translation of the unspliced form of XBP1 (XBP1u) from the precursor XBP1 mRNA increases when IRE1 is inactivated and this unspliced form functions as an inhibitor of the UPR (Yoshida et al., 2006). XBP1u binds to XBP1s, and the complex is rapidly degraded. Thus, XBP1u is a negative feedback regulator of XBP1s, terminating the transcription of target genes of XBP1s during the recovery phase of ER stress (Yoshida et al., 2006).

XBP1s is a basic leucine zipper (bZIP) transcription factor that regulates target gene expression via their ER stress response element (ERSE) (Yoshida et al., 1998) and UPR element (UPRE) (Cox and Walter, 1996). XBP1s regulates phospholipid biosynthesis and ER biogenesis (Sriburi et al., 2004), and also increases expression of UPR-related genes (Lee et al., 2003). These genes include SRP54 which helps the entry of newly synthesized polypeptides into the ER (Rapiejko and Gilmore, 1997); ERdj4 and EDEM which facilitate the degradation of misfolded proteins (Hosokawa et al., 2001; Lai et al., 2012); and protein disulfide isomerase which catalyzes protein folding.

1.2.1.2 PERK

Similar to IRE1, PERK is a type I ER transmembrane protein. It has an ER lumenal stress-sensing domain that is functionally interchangeable with the lumenal domain of IRE1 (Bertolotti et al., 2000) and a cytoplasmic domain containing protein kinase activity (Harding et al., 1999). The activity of PERK is also triggered by the dissociation of GRP78 from its lumenal domain (Bertolotti et al., 2000), which leads to oligomerization of PERK and trans-autophosphorylation of its kinase domain. Activated PERK phosphorylates eukaryotic translation initiation factor 2 (eIF2) (Harding et al., 1999), an essential factor in initiating protein translation. Phosphorylation of eIF2 inhibits general protein translation at the initiation stage, thereby reducing the flux of protein entering the already stressed ER.

During the shutoff of global protein synthesis, certain proteins are still being translated in order to help the stressed cell regain homeostasis. One of those proteins is ATF4, a bZIP transcription factor, whose mRNA contains small open reading frames in the 5'-untranslated region, allowing translation to occur even when eIF2 is phosphorylated (Lu et al., 2004). ATF4 regulates gene expression by binding to CCAAT-enhancer binding protein-activating transcription factor response elements (CARE) (Fawcett et al., 1999). Two key target genes driven by ATF4 are CCAAT/enhancer-binding protein homologous protein (CHOP) (Fawcett et al., 1999) and the growth arrest and DNA damage-inducible protein 34 (GADD34) (Ma and Hendershot, 2003).

CHOP is a transcription factor that promotes the transcription of apoptosis-associated genes [reviewed in (Sano and Reed, 2013)]. Thus, while the PERK pathway protects cells against ER stress by reducing protein synthesis, it also produces signals leading to apoptosis.

GADD34 binds to type I protein phosphatase (PP1) (Connor et al., 2001) and induces dephosphorylation of eIF2 (Novoa et al., 2001), allowing protein synthesis to recover (Ma and Hendershot, 2003) and therefore serving as negative feedback regulator of PERK pathway.

1.2.1.3 ATF6

The third ER stress transducer ATF6 is a type II ER transmembrane protein. ATF6 has an ER lumenal domain that interacts with GRP78 (Haze et al., 1999) and a cytoplasmic domain that contains a bZIP motif (Hai et al., 1989). Under ER stress conditions, ATF6 dissociates from GRP78, unmasking Golgi localization signals that facilitate its translocation from the ER to the Golgi apparatus (Shen et al., 2002) through coat protein II (COPII) transport vesicles (Schindler and Schekman, 2009). This translocation is also regulated by the glycosylation status (Hong et al., 2004) and the disulfide bonds status (Nadanaka et al., 2007) of ATF6. After arrival in the Golgi, ATF6 is cleaved by site-1 protease (S1P) and site-2 protease (S2P), which releases its N-terminal cytoplasmic domain (Ye et al., 2000) that eventually moves into the nucleus to function as a bZIP transcription factor.

ATF6 regulates target gene expression by binding to an ERSE (Yoshida et al., 2000). The key target genes driven by ATF6 are UPR-related genes, including GRP78 (a molecular chaperone), Derlin-3 (an ER-associated degradation system-associated protein) (Adachi et al., 2008), CHOP and XBP1 (Yoshida et al., 2000). ATF6 is also involved in the regulation of ER biogenesis and phospholipid biosynthesis (Bommiasamy et al., 2009; Maiuolo et al., 2011).

Several other proteins that have structure similar to ATF6 have been identified. These ER-transmembrane, bZIP transcription factors include Luman/CREB3 (Lu et al., 1997), OASIS/CREB3L1 (Honma et al., 1999), CREB3L2 (Storlazzi et al., 2003), CREB3L4 (Nagamori et al., 2005) and CREBH (Zhang et al., 2006). These ATF6-like proteins appear to regulate the UPR in specific organs and tissues as they differ in respect to activating stimuli, tissue distribution and response element binding [reviewed in (Asada et al., 2011)].

1.2.1.4 Crosstalk between UPR pathways

While IRE1, PERK and ATF6 function individually, these three pathways of the UPR communicate with each other in ER-stressed cells. IRE1 and PERK crosstalk with each other through their downstream targets XBP1 and eIF2, respectively. XBP1 up-regulation is an

important event in the UPR. However, in PERK knockout cells, XBP1 is not up-regulated under ER stress (Calfon et al., 2002) due to the lack of eIF2 phosphorylation (Huang et al., 2010). Further studies demonstrate that the mechanism behind the XBP1 up-regulation is via an eIF2 phosphorylation stabilization of the mRNA of XBP1 (Majumder et al., 2012).

As mentioned above, IRE1 regulates the UPR through splicing the mRNA of XBP1. The fact that the transcription of XBP1 can be driven by ATF6 (Yoshida et al., 2001) links IRE1 and ATF6 pathways. Indeed, in *Caenorhabditis elegans*, deletion of either *ire-1* or *xbp-1* is synthetically lethal with deletion of *atf-6* (Shen et al., 2005), indicating a functional redundancy between the IRE1 and ATF6 pathways. Although the bZIP transcription factors XBP1s and ATF6 regulate distinct sets of UPR-related genes, they can form heterodimers to promote the transcription of genes involved in ER-associated protein degradation (Yamamoto et al., 2007).

ER stress induces the cleavage of ATF6 to generate the active N-terminal fragment of ATF6. However, in PERK knockout cells, ATF6 activation is not sustained under ER stress and as a consequence its target gene, GRP78 remains expressed at a lower level (Adachi et al., 2008). This indicates the existence of crosstalk between PERK and ATF6 pathways. Indeed, the PERK pathway regulates the activity of ATF6 and its target genes by facilitating ATF6 synthesis, as well as its transport from the ER to the Golgi (Teske et al., 2011), the latter being a crucial step in ATF6 activation.

1.2.2 UPR and cholesterol

Besides transcriptionally and translationally regulating proteins that function in coping with ER stress, the UPR also contributes to cellular lipid homeostasis and formation of ER membranes. This is supported by observations that the UPR can be activated by phospholipid depletion (Cox et al., 1997) and membrane lipid saturation (Volmer et al., 2013). As well as induction of the UPR up-regulates many rate-limiting enzymes in lipid biogenesis (Travers et al., 2000) indicating that the UPR participates in lipid metabolism. The expansion of the ER membrane is another key event in the cellular response to accumulated unfolded proteins. This generation of new ER membrane requires UPR activity and lipid biosynthesis (Schuck et al., 2009). The levels of membrane phospholipids and the volume of the ER are increased when XBP1 is overexpressed (Sriburi et al., 2004). Intriguingly, sterol regulatory element-binding proteins (SREBPs), transcription factors that sense sterol sufficiency and regulate sterol

biosynthesis, are controlled by the UPR [reviewed in (Colgan et al., 2011)] and share the same activating machinery with the UPR (Ye et al., 2000).

1.2.2.1 SREBP and cholesterol

Cholesterol, which regulates membrane fluidity and permeability, is an essential structural component of the cell membrane. However, excess cholesterol is toxic to the cells [reviewed in (Maxfield and Tabas, 2005)]. Therefore its cellular levels are tightly regulated. Exogenous cholesterol is absorbed by cells through the interaction between low-density lipoprotein (LDL) receptor and LDL which is associated with cholesterol. Endocytosis of the LDL receptor bound to LDL brings cholesterol into the cells. Besides obtaining cholesterol exogenously, cells also have the ability to synthesis cholesterol endogenously. The cholesterol biosynthetic pathway requires several enzymes that are regulated by SREBPs, including HMG-CoA reductase (Wang et al., 1994), a rate-limiting enzyme of cholesterol synthesis.

SREBPs are ER-associated transcription factor precursors. In the presence of cholesterol, SREBPs are associated with SREBP cleavage activating protein (SCAP) (Hua et al., 1996a) and localized to the ER membrane through the interaction between SCAP and ER resident protein insulin-induced gene (INSIG) (Yabe et al., 2002; Yang et al., 2002). Decreased cholesterol levels triggers the dissociation of INSIG and SCAP (Yang et al., 2002), allowing the SREBP and SCAP complex to be transported to the Golgi apparatus (Nohturfft et al., 2000) through COPII vesicles (Espenshade et al., 2002). Upon arrival at the Golgi, SREBP undergoes proteolytic cleavage by S1P and S2P (Wang et al., 1994; Hua et al., 1996b; Sakai et al., 1996), and the cytoplasmic portion of SREBP is released and transported to the nucleus to function as transcription factor.

SREBP regulates target gene expression by binding to the sterol regulatory element. The two key target genes involved in cholesterol metabolism are LDL receptor (Yokoyama et al., 1993), which mediates cellular cholesterol uptake, and HMG-CoA reductase (Wang et al., 1994), which is the rate-controlling enzyme in the cholesterol synthesis pathway. SREBP also regulates the expression of PCSK9 (Jeong et al., 2008), which promotes the internalization and degradation of LDL receptor (Seidah et al., 2006); therefore, serving as a negative feedback regulator in cholesterol metabolism.

Three isoforms of SREBPs, SREBP-1a, SREBP-1c (Yokoyama et al., 1993), and SREBP-2 (Hua et al., 1993), have been identified. STEBP-1a and 1c are produced from a single gene through alternative translation start sites (Hua et al., 1995), while SREBP-2 is produced from a separate gene (Miserez et al., 1997). Forced expression of SREBP-1a increases the expression of genes involved in cholesterol, fatty acid, triglycerides, and phospholipids synthesis (Shimano et al., 1996; Horton et al., 2003). SREBP-1c, which is less active than isoform 1a, induces expression of lipogenesis (Shimano et al., 1997) and glycolysis (Foretz et al., 1999) genes. SREBP-2 differs in that it appears to more selectively activate genes involved in cholesterol synthesis, althoufgh moderate induction of fatty acid synthesis genes has been observed in SREBP-2 overexpression mice (Horton et al., 1998).

1.2.2.2 UPR and SREBP activation

The observations that SREBP and ATF6 share the same proteolytic mechanism (regulated intramembrane proteolysis) and ER to Golgi transport machinery suggest that a correlation exists between the UPR and SREBP. Indeed, increased UPR causes the activation of SREBP and accumulation of cholesterol (Werstuck et al., 2001). Elevated cholesterol level also activates the UPR and induces apoptosis through the activation of CHOP, a target of ATF6 (Feng et al., 2003).

The UPR regulates the SREBP activity through several mechanisms. General protein synthesis is suppressed by eIF2 phosphorylation under ER stress, which reduces the expression of INSIG (Bobrovnikova-Marjon et al., 2008). Decreased INSIG allows SREBP to be released from the ER and to be activated (Lee and Ye, 2004; Bobrovnikova-Marjon et al., 2008). On the other hand, forced expression of GRP78 inhibits ER stress-induced SREBP activity (Werstuck et al., 2001) through the interaction between these two proteins (Kammoun et al., 2009).

While the UPR shows broad influences on protein and lipid homeostasis, the discovery of a number of ATF6-like proteins, including Luman/CREB3, may help us understand the mechanisms by which the UPR is activated by different stimuli in specific tissues.

1.3 Luman

Luman (also known as CREB3 or LZIP, hereafter referred to as Luman) was first identified through its association with the host cell factor (HCF, a protein involved in regulation

of herpes simplex virus infection cell cycle) (Freiman and Herr, 1997; Lu et al., 1997). Luman is a cyclic AMP response element (CRE)-binding protein and belongs to the bZIP transcription factor superfamily. The functions of Luman that have been described to date include regulation of the UPR, dendritic cell maturation and cell migration (see below).

1.3.1 Structure and activity regulation

Luman has a similar structure to ATF6, one of the three ER stress transducers. It has an ER transmembrane domain that allows binding to the ER, a bZIP domain allowing DNA binding, and a transcription activation domain. The transcription activation domain contains three elements: two LxxLL motifs, which are present in many transcription factors and cofactors mediating protein-protein interactions, and one HCF-binding motif (Luciano and Wilson, 2000). An additional amino acid sequence adjacent to the N-terminal end of the bZIP domain is conserved in other ATF6-like, bZIP transcription factors, including OASIS/CREB3L1, CREB3L2, CREB3L4 and CREBH. But this sequence is not found in typical bZIP transcription factors, including ATF6 [reviewed in (Asada et al., 2011)]. The ER lumenal domain of Luman contains an S1P cleavage sequence and a partial S2P cleavage sequence (Raggo et al., 2002), indicating it is processed by regulated intramembrane proteolysis. However, the ER lumenal domain of Luman shows little homology to that of ATF6, suggesting different mechanisms in sensing stress signals and transport from the ER to the Golgi.

The inactive form of Luman binds to the ER. After receiving activation signals, Luman translocates to the Golgi where it is cleaved by S1P and an unidentified protease. The proteolytic cleavage releases the cytoplasmic N-terminal portion of Luman with all the known regulatory domains, that eventually moves into the nucleus to function as a transcription factor (Raggo et al., 2002). Luman regulates transcriptional activity through binding to the cAMP response element, UPRE and ERSE II in the promoter region of target genes. Luman recruitment factor (Audas et al., 2008) and Jun activation domain-binding protein 1 (DenBoer et al., 2013) are two proteins that negatively regulate the activity of Luman by promoting its degradation, consistent with active transcription factors being usually quickly degraded after their functions are accomplished.

1.3.2 Function

The observation that forced expression of Luman protects cells against ER stress-induced apoptosis (Liang et al., 2006) indicates a role for Luman in regulating the UPR. Indeed, Luman

promotes the transcription of two UPR-related genes, ER degradation-enhancing alpha-mannosidase (EDEM) (DenBoer et al., 2005), which contains UPRE in its promoter region, and homocysteine-induced endoplasmic reticulum protein (HERP) (Liang et al., 2006), which contains ERSE II in its promoter region. Both EDEM (Hosokawa et al., 2001) and HERP (Kim et al., 2008) are involved in the ER-associated protein degradation pathway, which suggests that Luman regulates the UPR by facilitating the degradation of misfolded proteins.

Through networking with other proteins, the functions of Luman extend beyond regulating the UPR. Luman participates in cell migration through interacting with different chemokine receptors. It regulates monocyte migration by binding to CCR1 (Ko et al., 2004), enhancing the activity of NF-κB (Jang et al., 2007), and increasing the expression of CCR1 and CCR2 (Sung et al., 2008). Luman also regulates the migration of breast cancer cells by promoting the expression of CXCR4 (Kim et al., 2010). In addition, the interaction between Luman and DC-specific transmembrane protein is involved in dendritic cell maturation (Eleveld-Trancikova et al., 2010), and interplay between Luman and ADP ribosylation factor 4 mediates cellular response to Golgi stress (Reiling et al., 2013).

Despite the various reported functions of Luman, little is known about its role in the nervous system other than that it is expressed by sensory neurons and is involved in reactivation of the herpes simplex virus (HSV), a process that normally occurs in response to environmental stresses (Lu and Misra, 2000). In preliminary studies by our labs, expression of Luman in DRG neurons was found to be regulated by axonal injury and also co-localized with importin β1 in the injured axons (Hasmatali et al., 2011 Society for Neuroscience Abstract 438.1) suggesting a potential role in retrograde signaling. Such a role is further supported by the fact that the Luman transcript was isolated, but not validated, in a transcriptome analysis of injured sensory axons (Gumy et al., 2011). Thus, I hypothesized that axonal Luman is an ER-localized transcription factor that transduces injury stress signals from remote axonal locations back to the neuronal cell body where it serves to regulate expression of regeneration-associated transcripts. Understanding the role that Luman plays in regulating a cell body response supportive of peripheral nerve regeneration is the main goal of this thesis and elucidation of this role was achieved by addressing the objectives below.

1.4 Thesis objectives

Objective 1: clone and characterize the rat Luman gene so that the function of Luman can be studied in a rat model;

Objective 2: to characterize the role of axonally-derived Luman in the response to peripheral nerve injury and determine its potential role in regulation of axonal regeneration;

Objective 3: to elucidate the mechanism by which Luman regulates axonal regeneration.

2 Material and methods

2.1 Animals, surgical procedure, and tissue preparation

All animal procedures were conducted in accordance with the Canadian Council on Animal Care and approved by the University of Saskatchewan Animal Research Ethics Board. Adult male Wistar rats (Charles River Laboratories) weighing ~250 grams were housed at room temperature on a 12-h light-dark cycle and had free access to food and water.

2.1.1 Sciatic nerve crush injury

The animals were anesthetised with 2 % Isoflurane. Animals were given pre- and post-operative analgesics subcutaneously (Buprenorphine 0.05 mg/kg). Approximately 5 mm of the sciatic nerve was exposed at the mid-thigh level, followed by crush injury using a fully closed smooth-jaw ultra-fine hemostat (0.6 mm tip) for 10 sec.

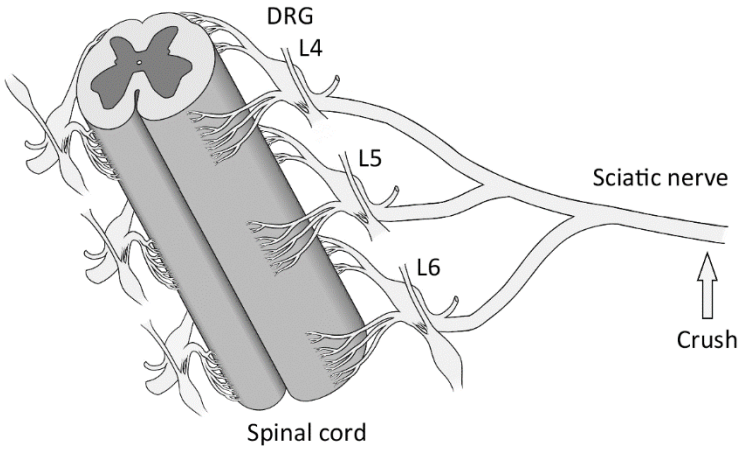

Figure 2.1.1 Sciatic nerve injury model

2.1.2 Perfusion

Deeply anesthetised rats (Sodium Pentobarbital, 70 mg/kg) were perfused via the aorta with cold PBS and 4 % paraformaldehyde. Right and left L4, 5, 6 DRGs or sciatic nerve segments were dissected, postfixed and cryoprotected in 20 % sucrose in PBS overnight. Paired experimental and control tissues were mounted in the same cryomold, covered with OCT

compound (Tissue-Tek) and frozen in isopentane at -80 °C. Transverse serial sections were cut at 8 μm on a cryostat (Microm) and collected on ProbeOn Plus slides (Fisher Scientific).

2.2 Cell culture, transfection, and enzymatic assay

2.2.1 Cell lines

Vero cells or HEK 293 cells were cultured in Dulbecco's Modified Eagle Medium (DMEM) supplemented with 10 % newborn calf serum or 10 % fetal bovine serum, 100 unit/ml penicillin and 100 mg/ml streptomycin at 37 °C in humidified air with 5 % CO_2. One day prior to transfection, Vero cells were seeded into six-well plates at a concentration of 5×10^5/well. One μg of pcDNA3.1, pcLuman, pcRatLuman, or pcGFP-Lu-RFP was cotransfected with 100 ng of pCAT3BATF6 by using Lipofectamine 2000 (Life Technologies). Chloramphenicol acetyltransferase (CAT) activity was measured 24 h post transfection, using the CAT Enzyme-linked immunosorbent assay (ELISA) kit (Roche).

2.2.2 Adult DRG culture

Rat DRG were treated with 0.25 % collagenase (1 h, 37 °C) and dissociated with 2.5 % trypsin (30 min, 37 °C) before plating on laminin (1 μg/mL) and poly-D-lysine-coated (25 μg/mL) coverslips at 10^4 cells per well in a 6-well plate (BD Biosciences) in DMEM supplemented with 10 ng/ml of 2.5S NGF (Cedarlane Labs). Cytosine β-D-arabinofuranoside (Ara-C, 10 μM) was added to inhibit proliferation of non-neuronal cells.

In select experiments MG-132 (Sigma, 5 μM) and chloroquine (Sigma, 100 μM) were added to inhibit protein degradation; cycloheximide (Sigma, 10 μg/mL) to inhibit translation; or colchicine (Sigma, 10 μg/mL) to inhibit microtubule polymerization. NLS peptide (Enzo, AAVALLPAVLLALLAPVQRKRQKLMP, 50 μg/ml) was added to compete with Luman for binding to the importin transport complex. Mismatch NLS peptides (Enzo, AAVALLPAVLLALLAPVQRNGQKLMP, 50 μg/ml) served as control.

To study the effect of lowered Luman expression, some DRG cultures were transfected with Luman siRNA (Integrated DNA Technologies) or negative control nontargeting siRNA using Lipofectamine RNAiMAX Reagent (Life Technologies). Luman knockdown efficiency was assessed by Western blot.

To monitor changes in cholesterol biosynthesis in cultured neurons, total and free cellular cholesterol mass was determined using an enzymatic fluorometric assay, employing the Amplex Red Cholesterol assay kit (Life Technologies).

2.3 Culture methods for isolation of axons

2.3.1 Transwell insert

Isolation of DRG axons was as previously described (Zheng et al., 2001) with the minor modification, of using transwell insert membranes with 3 μm. Dissociated DRG neurons were plated onto a tissue culture insert containing a polyethylene tetraphthalate (PET) membrane with 3 μm pores (BD Biosciences) that had been coated with poly-L-lysine and laminin. To isolate axons, the top membrane surface was scraped with a cotton-tipped applicator (Q-tips). For isolation of cell bodies, the surface underneath the membrane was scraped.

2.3.2 Compartmented explant culture

DRGs were cut into 4-5 smaller pieces and explant cultures were grown in compartmented culture chambers [adapted from (Vogelaar et al., 2009)] whereby individual DRG explants can extend axons into isolated right or left compartments, allowing for the differential treatment of the neurites under control or experimental conditions. DRG explants (15–20 per well) were plated in a row on top of scratches made with a pin rake (Tyler Research Corporation) in 6-well plates coated with poly-D-lysine (25 μg/mL) and laminin (1 μg/mL) in DMEM supplemented with 50 ng/mL NGF. The volume of medium was kept low for the first day to better hold the explants to the culture surface via surface tension. After 1 day *in vitro* (DIV), a compartmented insert cut from 1 mm thick medical grade silicon sheet (Rubber Sheet Roll) was placed into the dish creating leak proof compartments. Ara-C (10 μM) was added to abolish cell proliferation. The cultures were maintained for 7 days, with Ara-C treatment every other day.

2.4 Gene expression analysis

2.4.1 Nucleic acid sequence

2.4.1.1 Primers for qRT-PCR

Table 2.1 shows the oligonucleotide sequence (Integrated DNA Technologies) of primers used in qRT-PCR assay.

Table 2.1 Primers for qRT-PCR

Gene	Upstream primers
	Downstream primers
18S rRNA	TCCTTTGGTCGCTCGCTCCT
	TGCTGCCTTCCTTGGATGTG
β-actin	CCGTAAAGACCTCTATGCCAACA
	CGGACTCATCGTACTCCTGCT
Calnexin	TTTGGGTGGTCTACATTC
	CTTCTTCGTCCTTCACAT
CHOP	TGGAAGCCTGGTATGAGGAC
	TGCCACTTTCCTCTCGTTCT
γ-actin	ACACTGCGTTTCTTTCCG
	AATGCCGTGCTCAATAGG
GAPDH	GGTGCTGAGTATGTCGTGGAGTC
	GTGGATGCAGGGATGATGTTCT
GRP78	GGCTTGGATAAGAGGGAAGG
	GGTAGAACGGAACAGGTCCA
Insig1	ACAGTGGGAAACATAGGAC
	TGAACGCATCTTTAGGAG
Insig2	AGCAACCGTTGTCACCCA
	TCCCATCGTTATGCCTCC
Luman	TGTGCCCGCTGAGTATGTTG
	AGAAGGTCGGAGCCTGAGAA
Mbtps2	GTCCCGTTACTAATGTGC
	CAAACTTGAGTGGCTTCA
SREBP1	CGCTACCGTTCCTCTATCA
	CTCCTCCACTGCCACAAG

Gene	Upstream primers
	Downstream primers
Ubxn4	GGAACGGTGCTTTATCCA
	ATCTTGAGTCCGCAGTCG
XBP1	TCAGACTACGTGCACCTCTGC
	TAAGGAACTGGGTCCTTCT
XBP1 spliced	TCTGCTGAGTCCGCAGCAGG
	TAAGGAACTGGGTCCTTCT

2.4.1.2 Primers for cloning rat Luman

Upstream: GAGTTTCTATCCATAAATATTCCAA

Downstream: CTGAGGACACCCCATATCCTCACAC

2.4.1.3 Probe sequences used for in situ hybridization:

CHOP: CTCTTCAGCAAGCTGTGCCACTTTCCTCTCATTCTCCTGCTCCTTCTC

GRP78: GTATCCTCTTCACCAGTTGGGGGAGGGCCTCCACTTCCATAGAGTTTG

Luman: CAATTCTTGCACGGAGTTCTCGGAAGGCGACAGCTCCAAGTCCAGGGG

2.4.1.4 siRNA sequence for Luman knockdown

CGACUGGGAGGUAGAGGAUUUAC

2.4.2 Cloning rat Luman coding sequence

tBLASTn analysis with the amino acid sequence of mouse Luman amino acid sequence (NCBI Reference Sequence: NP_038525.2) was performed against the rat genome sequence. A potential rat mRNA (TL0ABA47YN07 mRNA sequence, GenBank: FQ219084.1) was identified that codes for rat Luman. Total RNA was extracted from adult Wistar rat DRG using the RNeasy Kit (Qiagen) and converted to cDNA using the QuantiTect Rev. Transcription Kit (Qiagen). cDNA was amplified with a thermal cycler (DNA Engine) by 30 cycles of PCR (30 s at 94°C, 60 s at 55°C, and 90 s at 72°C). The PCR product was TOPO cloned into pCR2.1-TOPO (Life Technologies) to form pCRLuman and the nucleotide sequence of the insert was determined.

2.4.3 Plasmid

The construction of pcLuman (Lu et al., 1997), a plasmid expressing human Luman in mammalian cells, and the CAT reporter plasmid pCAT3BATF6 (Misra et al., 2005), with the coding sequences for chloramphenicol acetyl transferase (CAT) following five copies of the UPRE (unfolded protein response element)-containing oligonucleotide, have been previously described.

A plasmid that expresses rat Luman in mammalian cells, pcRatLuman, was constructed by transferring the coding sequence of rat Luman from pCRLuman to pcDNA3.1 (Life Technologies) at the EcoRI site. The insert orientation was checked by digestion with KpnI.

The coding sequences for enhanced green fluorescent protein (GFP) and red fluorescent protein (RFP) were fused in frame to the 5' terminus and 3' terminus of the rat Luman gene, respectively, by using In-Fusion HD Cloning Plus (Clontech). The fused gene was cloned into pcDNA3.1 to generate pcGFP-Lu-RFP.

2.4.4 Adenovirus preparation

The open reading frame of the GFP-Luman-RFP fused protein was inserted into the Adeno-X Viral DNA vector as per the manufacturer's instruction (Clontech). Adenovirus, named Ad/GFP-Lu-RFP, was grown and purified using the Adeno-X Expression System (Clontech). For *in vitro* infection, neurons were infected with 100 multiplicity of infection (MOI) 48 h prior to axotomy. For *in vivo* infection, 15 μL of Ad/GFP-Lu-RFP (2×10^{11} PFU/mL; N=4) or control Adeno-LacZ (expressing E. coli beta-galactosidase; 2×10^{11} PFU/mL; N=2) was injected intrathecally via a sterile silicon catheter inserted at the lumbar sacral junction such that the tip of the catheter delivering the vector was at the L5 DRG level. Rats were left 1 week in order to transduce the sensory neurons before 48 h sciatic nerve crush injury at the midthigh level.

2.4.5 Real-Time Quantitative Reverse Transcription PCR (qRT-PCR) analysis

Total RNA was isolated using the RNeasy Kit (Qiagen). The quality of RNA was analyzed by electrophoresis using the Agilent 2100 bioanalyzer (Agilent Technologies). One μg of total RNA with RNA integrity number (RIN) > 9 was converted to cDNA using the QuantiTect Rev. Transcription Kit (Qiagen). cDNAs were amplified with a RT-PCR machine (Stratagene). The levels of housekeeping genes GAPDH, β-actin, and 18S rRNA were used as

internal control to verify the qRT-PCR reaction. A non-template control was included in each set of reactions.

2.4.6 In Situ hybridization histochemistry

Oligonucleotide probe complementary to and selective for Luman, GRP78, and CHOP mRNA were synthesized (Integrated DNA technologies). The probes were labeled at the 3'-terminus with α-[35S] dATP (PerkinElmer) using terminal deoxynucleotidyl-transferase (Life Technologies), and purified through QIAquick nucleotide removal kit (Qiagen).

The sections were hybridized at 43°C for 18 h before processing for radioautography by coating in NTB nuclear track emulsion (Kodak), and exposed for 14 days before developing in D-19 (Kodak) and viewing under darkfield and brightfield conditions.

The specificity of hybridization signal for the probes were confirmed using serial sections hybridized with radio-labeled probe, radio-labeled probe with a 1000-fold excess of unlabeled probe (which effectively competed all specific binding of labeled probe), or labeled probe with a 1000-fold excess of another, dissimilar unlabeled probe of the same length and similar GC content (which did not alter the hybridization signal pattern observed using the labelled probe alone).

2.4.7 qRT-PCR array

Unfolded protein response qRT-PCR arrays were purchased (SABiosciences). The array contained primers for 84 gene transcripts involved in the UPR. The array also contained controls for genomic DNA contamination and reverse transcriptase efficiency. The results were analyzed by using a SABiosciences online resource RT2 profiler. To confirm the results of the qRT-PCR array, primers were designed for genes down-regulated for more than 2 fold.

2.5 Protein expression analysis

2.5.1 Antibodies

2.5.1.1 Primary antibodies

Table 2.2 lists the primary antibodies used in Western blot and Immunofluorescence.

Table 2.2 Primary antibodies employed

Target	Host species	Western blot dilution	Immunofluorescence dilution	Source
β III-tubulin	Mouse/Rabbit	1:1,000	1:1,000	Millipore
Calnexin	Rabbit	1:1,000	1:50	CST
CHOP	Mouse	1:1,000	1:250	CST
GAPDH	Mouse	1:2,000		Novus Biologicals
GRP78	Rabbit	1:1,000	1:200	CST
importin α	Mouse	1:1,000		Sigma
importin β	Mouse	1:1,000	1:200	Thermo Scientific
IRE1	Rabbit	1:1,000		CST
Lamin B	Goat	1:200		Santa Cruz
Luman	Rabbit	1:400	1:400	Misra's lab
PDI	Rabbit	1:1,000		CST
PERK	Rabbit	1:1,000		CST

2.5.1.2 Secondary antibodies

Table 2.3 lists the secondary antibodies used in Western blot and Immunofluorescence.

Table 2.3 Secondary antibodies

Target	Host species	Conjugate	Dilution	Source
Goat	Donkey	Alexa Fluor 680	1:10,000	Life Technologies
Mouse	Donkey	DyLight 488	1:1,000	Jackson ImmunoResearch
Mouse	Donkey	DyLight 594	1:1,000	Jackson ImmunoResearch
Mouse	Goat	IRDye 680	1:10,000	LI-COR Biosciences
Mouse	Goat	IRDye 800	1:10,000	LI-COR Biosciences
Rabbit	Donkey	Alexa Fluor 350	1:500	Life Technologies
Rabbit	Goat	DyLight 488	1:1,000	Jackson ImmunoResearch

Target	Host species	Conjugate	Dilution	Source
Rabbit	Goat	Alexa Fluor 555	1:1,000	Jackson ImmunoResearch
Rabbit	Goat	IRDye 680	1:10,000	LI-COR Biosciences
Rabbit	Goat	IRDye 800	1:10,000	LI-COR Biosciences

2.5.2 Immunofluorescence cytochemistry

Dissociated DRG neurons were grown on coverslips for 24-72 h, and fixed in 4 % paraformaldehyde for 20 min, followed by permeabilization with 0.1 % Triton X-100 in PBS at room temperature for 30 min. The cells were then blocked with 2 % goat serum, 2 % horse serum and 1 % BSA for 30 min, prior to incubation with primary antibodies overnight at 4 °C. Cells were then incubated with secondary antibodies for 1 h at room temperature. Coverslips were then mounted onto glass slides with an anti-fade reagent with DAPI (Prolong Gold; Life Technologies) and subject to fluorescence microscopic analysis.

2.5.3 Immunofluorescence histochemistry

Sections were blocked with SEA BLOCK blocking buffer (Thermo Scientific) for 1 h at room temperature. Tissues were incubated with primary antibodies overnight at 4 °C. Sections were then washed, incubated with secondary antibodies for 1 h at room temperature. Slides were coverslipped with anti-fade reagent (Prolong Gold; Life Technologies).

2.5.4 Analysis and quantification of immunostaining signal

Images were captured under identical parameters for control and experimental conditions also processed at the same time. Images were quantified for average fluorescence signal using Northern Eclipse software (Empix Imaging).

2.5.5 Western blot analysis

Proteins were extracted with RIPA buffer containing protease inhibitors cocktail. Twenty μg of protein were electrophoresed on a SDS polyacrylamide gel, and then transferred onto a polyvinylidene fluoride membrane (Bio-rad). Membranes were blocked with blocking buffer (LI-COR Biosciences) at room temperature for 1 h. Membranes were then incubated with primary antibodies overnight at 4 °C, followed by incubation with secondary antibodies for 1 h at room temperature. Proteins were visualized by the Odyssey Infrared Imaging System (LI-COR

Biosciences). Lamin B was used as a loading control. For quantification, the density of each band on the immunoblot was estimated by densitometry and normalized to the density of the loading control band in the sample.

2.5.6 Immunoprecipitation

Antibodies were cross-linked to Dynabeads protein A (Invitrogen Dynal AS). Cell lysates were precleared with IgG Dynabeads protein A for 30 min at 4 °C before incubation with specific antibody-linked Dynabeads overnight at 4 °C. The immunoprecipitated Dynabead complexes were washed three times with RIPA buffer. Proteins were eluted by boiling in protein loading buffer prior to Western blot analysis.

2.6 Statistical analyses

All statistical analyses were performed with Prism (GraphPad Software). Differences between means were assessed by one-way analysis of variance (ANOVA) with post hoc Tukey's analysis. All values in the figures are expressed as means ± SEM (standard error of the mean) with differences in the mean values considered to be significant at $p<0.05$.

3 Results

3.1 Cloning and characterization of rat Luman

The coding sequences for the Luman gene have been reported for human (Lu et al., 1997), mouse (Burbelo and Kozak, 1998), and pig (Qi et al., 2009). But, when a previously reported rat sequence for Luman (GenBank: BC062241.1) was examined, I discovered that it was truncated, coding only a portion of the cytoplasmic domain. The truncated rat sequence lacked important functional domains including the nuclear localization signal, the bZIP domain that mediates DNA binding, the transmembrane domains and the ER luminal domain found in the mouse and human equivalents. I amplified by PCR the full Luman coding nucleotide sequence from transcripts from rat DRG tissue, cloned the sequence, and characterized its expression and distribution in a variety of rat tissues (Ying et al., 2014).

3.1.1 Cloning of rat Luman cDNA

Using a PCR-based approach I recovered cDNA for a putative transcript for Luman from rat DRG and determined its nucleotide sequence (Figure 3.1.1). The 1164 nucleotide sequence codes for a 387 amino acid protein, 233 amino acids longer than the predicted rat sequence in the Genbank database (GenBank: BC062241.1). The derived amino acid sequence contains a potential bipartite nuclear localization signal (NLS) and a basic leucine zipper (bZIP) region. When aligned to mouse Luman (NP_038525.2) and human Luman (NP_006359.3), rat Luman displays 85 % and 66 % amino acid identity, respectively (Figure 3.1.2). In addition, all of the important functional domains including the bipartite nuclear localization signal, leucine zipper region, HCF-binding domain and transmembrane domain are conserved with most of the amino acid substitutions being conservative. These data suggest that the cloned cDNA represents an orthologue of the mouse and human Luman.

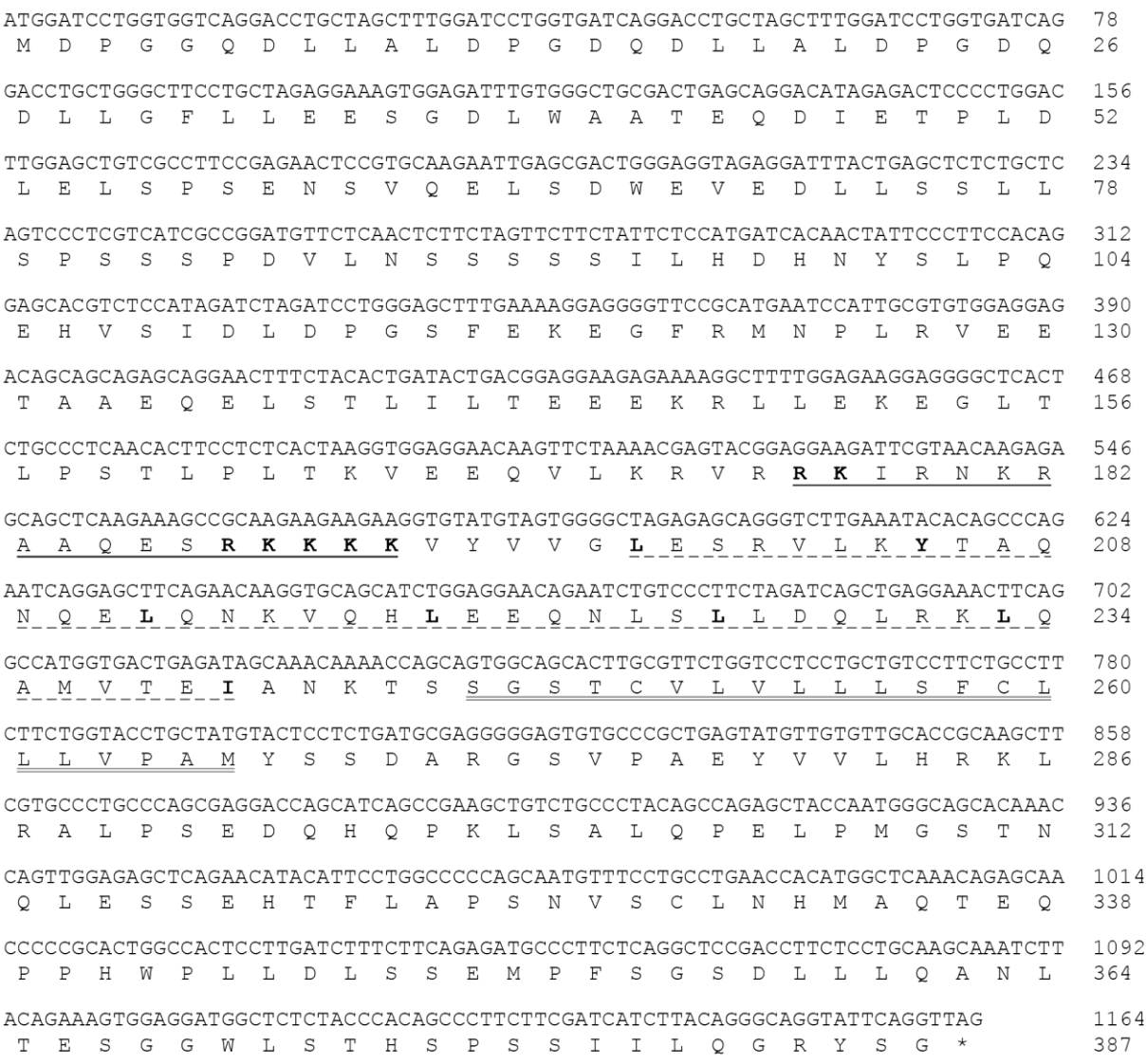

Figure 3.1.1 cDNA and putative amino acid sequences of rat Luman

The nucleotide sequence of the identified cDNA encodes a protein of 387 amino acids with a predicted molecular mass of 42.9 kDa. This sequence contains a predicted bipartite nuclear localization signal (underlined with basic amino acids shown in bold); a leucine zipper region (underlined with a dashed line with leucines shown in bold) with a tyrosine substitution at the second and an isoleucine substitution at the seventh leucine heptad positions; and the predicted transmembrane domain (underlined with a double line).

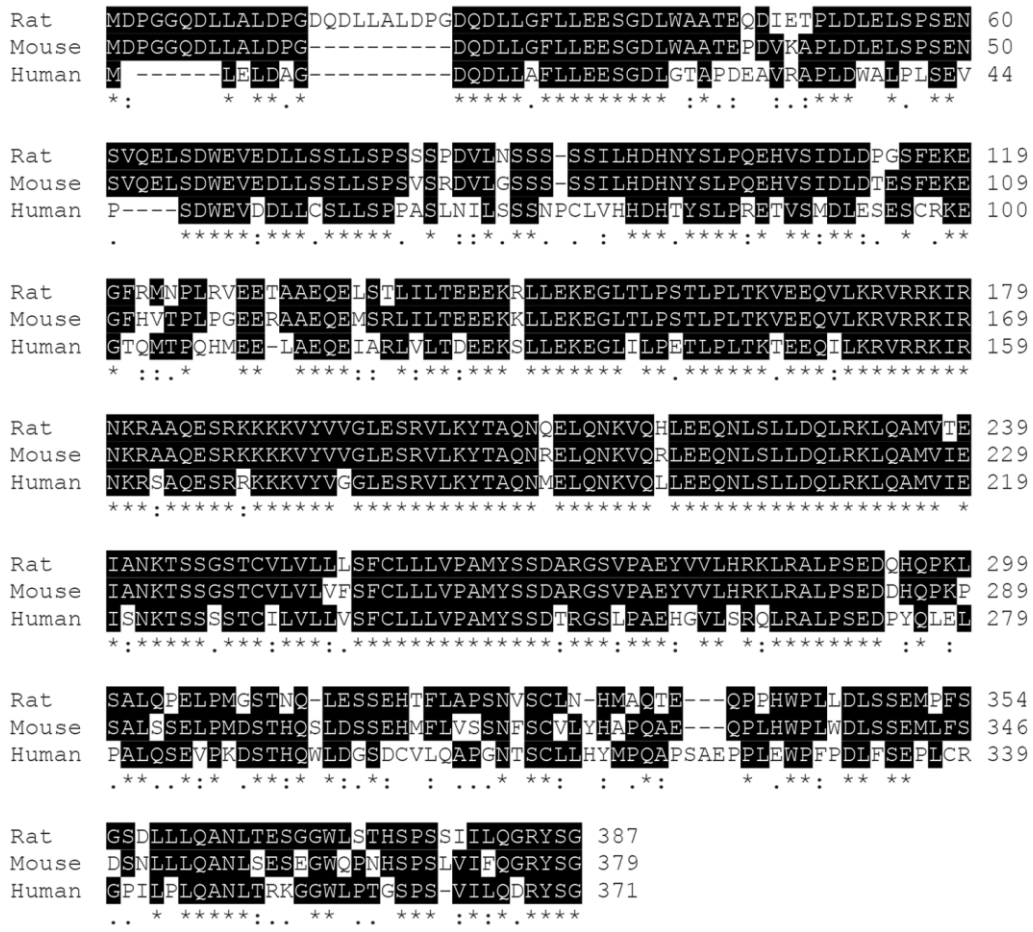

Figure 3.1.2 Amino acid sequence alignment of rat, mouse, and human Luman

Amino acids in shaded boxes indicated by asterisks "*****" represent fully conserved residues; colons "**:**" indicate conservation between groups of strongly similar properties, and periods "**.**" indicate conservation between groups of weakly similar properties.

3.1.2 Rat Luman activates transcription from UPRE consensus sequences

I next assessed whether the rat Luman sequence encodes a functional protein capable of activating transcription from the unfolded protein response element (UPRE) in a manner similar to human Luman (Liang et al., 2006). Luman constructs (pcLuman or pcRatLuman) or control plasmid and pCAT3BATF6, a CAT reporter plasmid with the coding sequences of CAT following five copies of the UPRE, were cotransfected into Vero cells. Figure 3.1.3A reveals that both human and rat Luman can activate the UPRE reporter and appear to drive similar levels of CAT expression (> 20 times above the control plasmid/background level).

3.1.3 Tissue distribution of rat Luman mRNA

The relative levels of Luman transcripts were assessed in various tissues of the nervous system as well as other organs. RNA was extracted from cortex, cerebellum, hippocampus, DRG, sciatic nerve, liver, spleen, stomach, heart, lung, kidney, and intestine. Figure 3.1.3B shows high integrity and quality of isolated RNA. Luman transcript levels in these tissues, relative to 18S RNA, were assessed by qRT-PCR. 18S RNA was selected as the normalizer as its levels, in contrast to other "house-keeping" genes such as GAPDH and β-actin, were consistent in the various tissues examined. Figure 3.1.3C shows that with the exception of liver, Luman RNA was more abundant in various nervous tissues (cortex, cerebellum, hippocampus, DRG and nerves) than in non-nervous tissue (spleen, lung, heart, kidney and intestine).

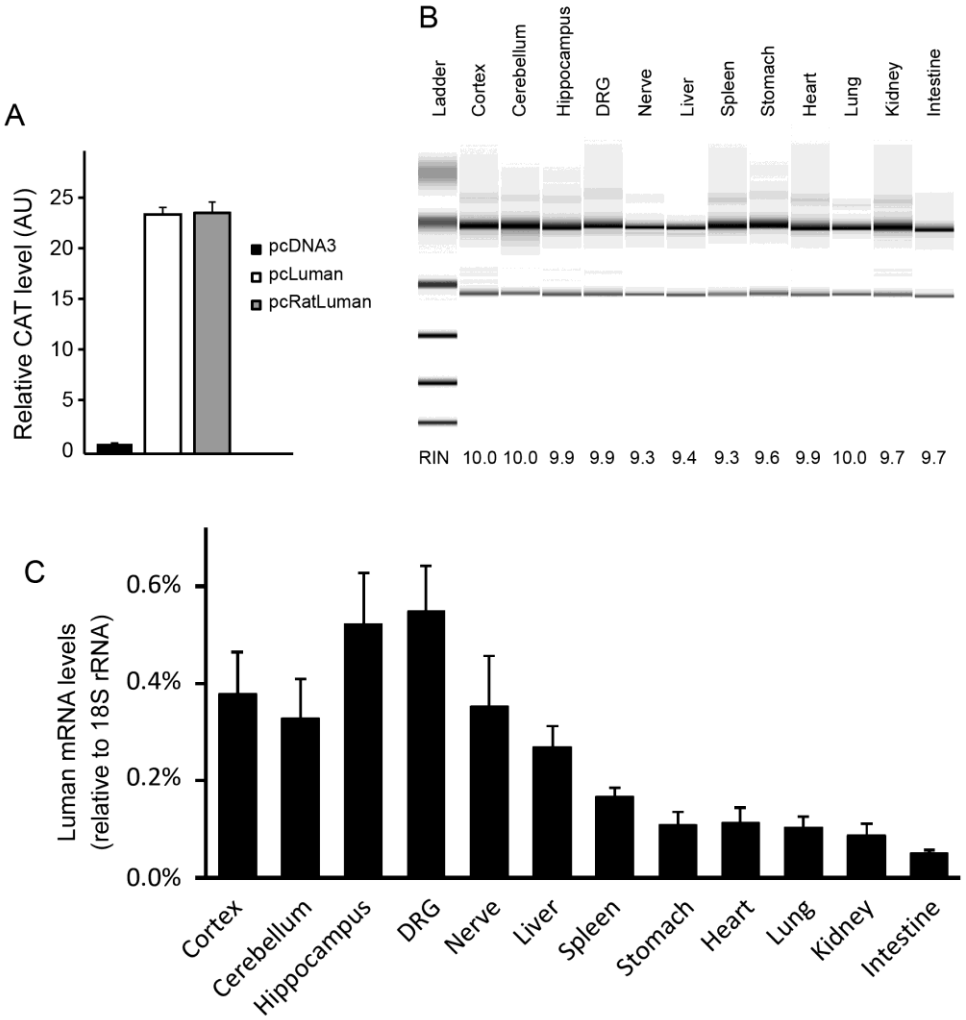

Figure 3.1.3 Rat Luman activates transcription and its mRNA is widely expressed

(A) Human and rat Luman are equipotent at activating CAT reporter gene expression via the unfolded protein response element. pcDNA3.1, pcLuman or pcRatLuman was contransfected with CAT reporter plasmid pCAT3BATF6 into Vero cells. CAT protein level measured by ELISA, 24 h post-transfection. (B) Total RNA extracted from rat tissues was analyzed with Agilent bioanalyzer. A representative simulated electrophoresis gel is shown with the average RNA integrity number (RIN) shown at the bottom. (C) Mean (±SEM) levels of Luman mRNA relative to 18S rRNA levels from tissues as indicated. Note Luman mRNA is most highly expressed in nervous system tissues. N=3.

I next localized Luman mRNA transcripts in DRG, hippocampus, and liver by *in situ* hybridization. Transcripts for Luman mRNA were detected in the cytoplasm of neurons and satellite glial cells in the DRG sections (Figure 3.1.4A, B) and in the cytoplasm of hepatocytes in liver sections (Figure 3.1.4C, D). The transcripts were mainly expressed in the pyramidal cell layer of CA1 and CA3, and the granular cell layer of the dentate gyrus in the hippocampal region in the brain (Figure 3.1.4E, F). The hybridization signal over the tissue was specific as it could be effectively competed away with an excess of cold probe (Figure 3.1.5).

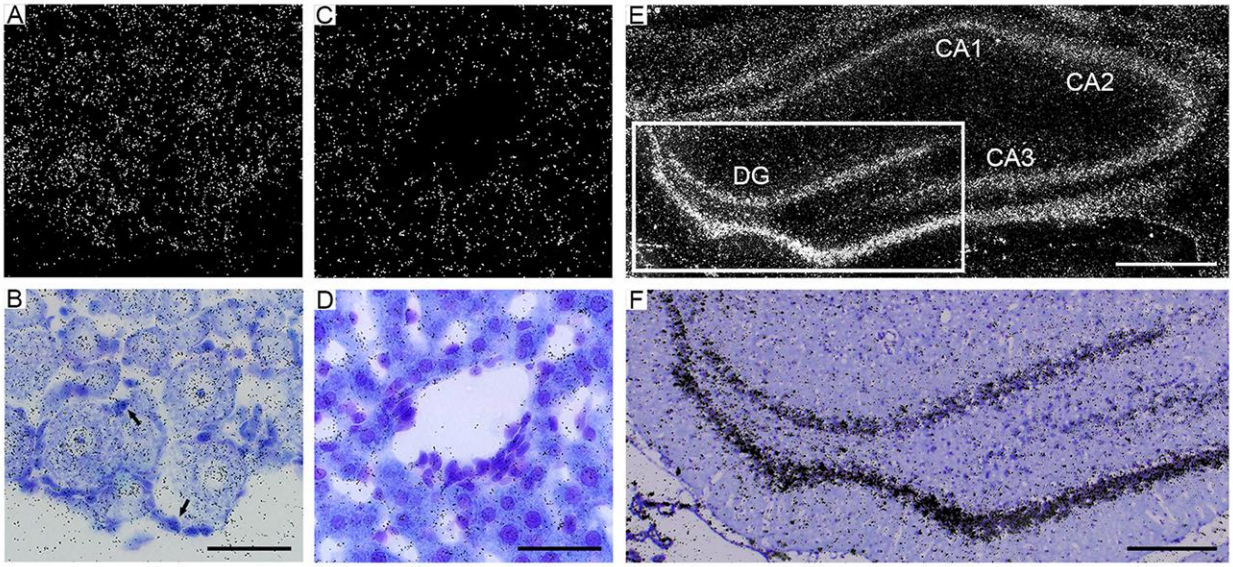

Figure 3.1.4 Luman mRNA localization in DRG, liver, and hippocampus

Dark-field photomicrographs of rat DRG (A), liver (C) and hippocampus (E) sections processed for radioactive *in situ* hybridization to detect Luman mRNA. Brightfield photomicrographs of the same fields of rat DRG (B), liver (D) and insert box of hippocampus (E) reveals that all cells appear to have some basal level of Luman expression. (A

and B) DRG neurons are positive for Luman expression while arrows indicate representative satellite glial cells with positive hybridization signal. Scale bar: 50 μm. (C and D) Hybridization signal localizes to hepatocyte cytoplasm. Scale bar: 50 μm. (E and F) Luman mRNA transcripts in CA1-CA3 pyramidal cell layers and the granule cell layer of the dentate gyrus (DG). Region within the white box in E (Scale bar: 500 μm) is shown at a higher magnification in F (Scale bar: 250 μm).

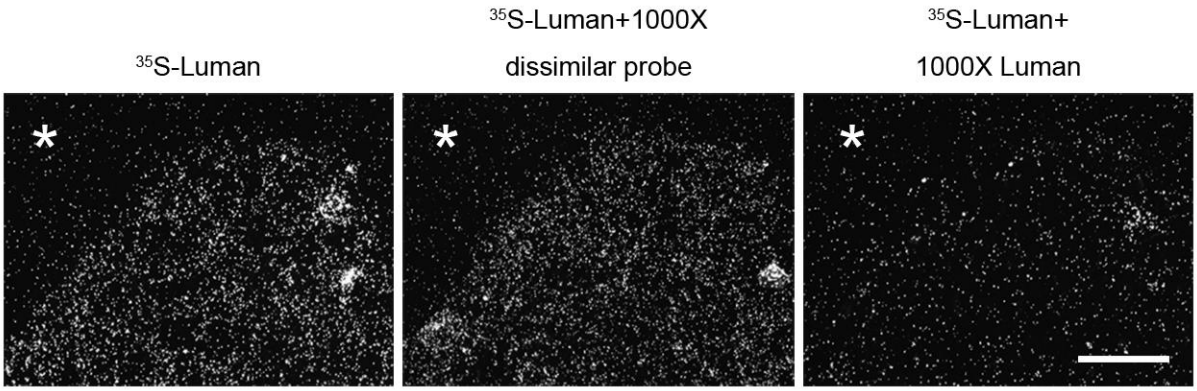

Figure 3.1.5 In situ hybridization specificity control for Luman probe

Serial L4 DRG sections were hybridized with radio-labeled probe (^{35}S-Luman), labeled probe with a 1000-fold excess of another dissimilar unlabeled probe (^{35}S-Luman+1000X dissimilar probe), or radio-labeled probe with a 1000-fold excess of unlabeled probe (^{35}S-Luman+1000X Luman). Note: the excess dissimilar probe did not alter the hybridization signal pattern, while the excess unlabeled Luman probe effectively competed all specific binding leaving only background levels over tissue and non-tissue regions of the slide. Scale bar: 100 μm; * indicates non-tissue regions.

3.2 Importin-mediated retrograde transport of Luman promotes neurite out growth in injured sensory neurons

A complex series of cellular and molecular events participate in reprogramming sensory neurons as they transition to a regenerating state following peripheral nerve injury (Lieberman, 1974; Abe and Cavalli, 2008; Gumy et al., 2010; Ben-Yaakov et al., 2012). Injury discharge and rapid ion-fluxes initiate this transition, with loss of target-derived signals and receipt of retrograde signals from the site of injury following (Gunstream et al., 1995; Murphy et al., 1999; Michaelevski et al., 2010; Jung et al., 2012). These include injury-induced activation of intra-

axonal transcription factors and their local synthesis (Lindwall and Kanje, 2005; Ben-Yaakov et al., 2012). Multiple axonal transcription factor transcripts have been identified in the injured nerve suggesting that many may serve as retrograde regeneration signals linking axonal injury to nuclear activities. However, only a role for axonal STAT3 in neuronal survival of injured sensory neurons has thus far been demostrated (Ben-Yaakov et al., 2012).

Luman localizes to both the somal and axonal ER of DRG neurons and its transcript was previously identified, but not validated, in transcriptome analysis of injured sensory axons (Gumy et al., 2011). Based on the facts that Luman transcripts are highly expressed in DRGs and nerves (Figure 3.1.3) and that Luman contains the NLS sequence (Figure 3.1.1), I hypothesized that axonal Luman, as an ER-localized transcription factor, may serve to transduce injury stress signals from remote axonal locations back to the cell body.

3.2.1 Luman mRNA localizes to adult sensory neuron axons

Transcriptome analysis of adult sensory axons led to the identification of mRNA transcripts for several transcription factors including Luman (Gumy et al., 2011). To validate the axonal localization of Luman mRNA, the transwell culture insert approach for isolating axons and obtaining pure axonal isolates was employed (Figure 3.2.1A). Dissociated DRG neurons from naïve animals cultured on the top surface of membrane inserts can extend their neurites through the membrane pores, thereafter growing on the lower membrane surface. A pure axonal sample for analysis was obtained by carefully scraping away cultured cell components from either the top or bottom surfaces of the insert membrane. Immunofluorescence staining of the scraped membranes for the neuronal marker β–III tubulin coupled with nuclear DAPI staining (Figure 3.2.1B) revealed that all cell bodies could be removed from the upper surface of the membrane without peeling away axons extending to the lower membrane surface. To assess the purity of the lower membrane axonal preparations, protein extracts from the upper (cell bodies and proximal axons/neurites) and the lower (distal axons) surfaces of the membrane inserts were prepared and analysed by Western blot. The nuclear envelope protein Lamin B was detected only in upper membrane samples, while the microtubule protein β-III tubulin was detected in samples from both sides of the membrane (Figure 3.2.1C), confirming the presence of axons and a lack of neuronal and nonneuronal cell bodies on the lower membrane surface.

To examine for the presence of axonal Luman mRNA, upper or lower membrane mRNAs were extracted and used for reverse transcription. RT-PCR revealed that both Luman and β-actin mRNAs could be amplified from the lower membrane axonal preparations, the latter being a confirmed axonal mRNA (Zheng et al., 2001). The purity of the axonal mRNA preparation was confirmed by the absence of a signal for γ-actin, a previously identified mRNA excluded from the axonal compartment, but present in the neuronal cell bodies (Figure 3.2.1D) (Zheng et al., 2001). Taken together, these data indicate that Luman mRNA localizes to axons of DRG neurons.

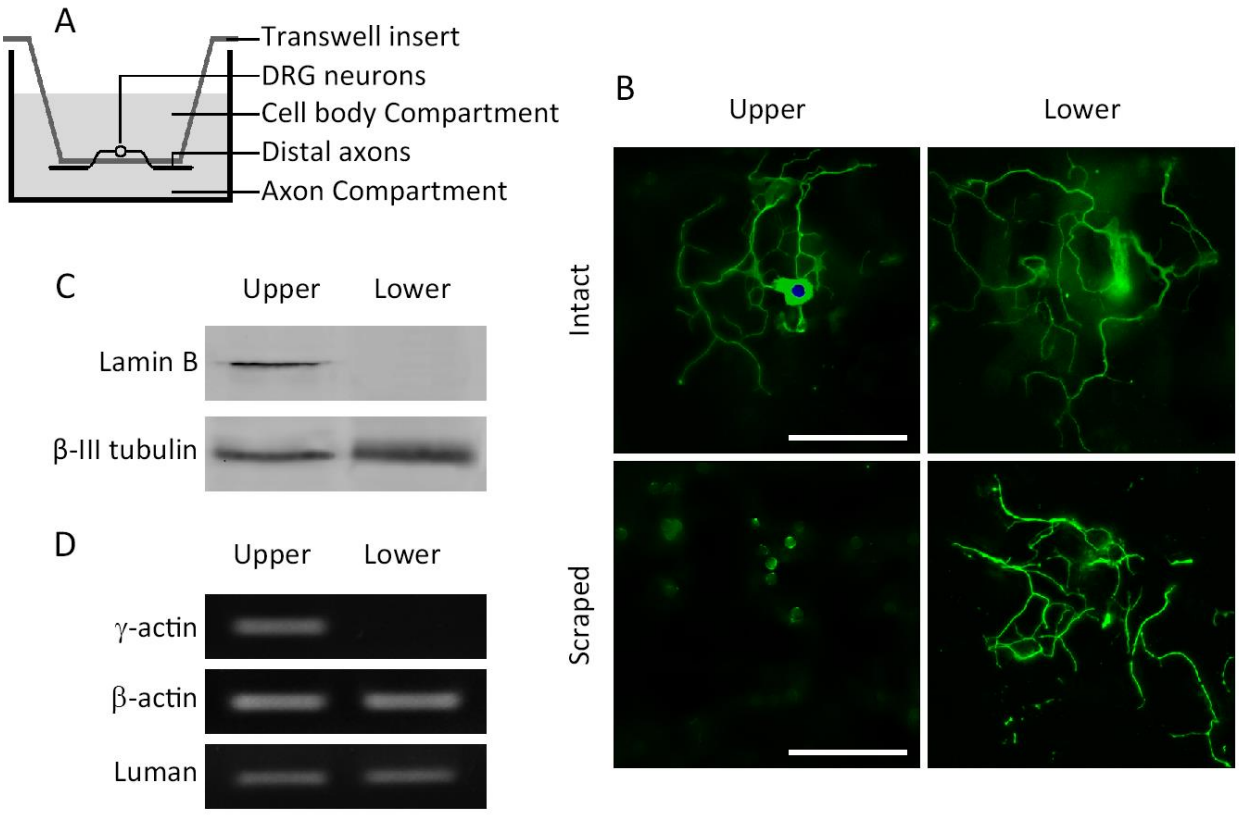

Figure 3.2.1 Luman mRNA is localized to axons

(A) Schematic representation of transwell cell culture insert employed. Dissociated naïve DRG neurons are seeded on top of the porous membrane (3 μm pores). Axons grow through the membrane pores such that distal axons are localized on the lower surface of the membrane. (B) DRG neurons plated onto a transwell insert 24 h prior to processing for immunofluorescence to detect β-III tubulin (green) with DAPI-stained nuclei (blue). Lower membrane images acquired directly below the upper membrane focal plane reveal no detectable nuclear DAPI signal along the lower membrane surface. To isolate axons, the upper membrane was scraped, removing all cellular elements from the upper membrane surface, while axons that had traversed the membrane remain adhered to the lower surface of the membrane. Scale bars, 100 μm. (C) Western blot analysis of proteins extracted from

neurite/axonal (Lower) and cell body and proximal axons (Upper) preparations of DRG neurons cultured for 24 h revealed no detectable nuclear envelope Lamin B protein in neurite/axonal (Lower) samples, while β-III tubulin is detected in both compartments. (D) RNA extracted from neurite/axonal (Lower) and cell body (Upper) preparations from DRG neurons cultured as in (B) was analyzed by RT-PCR. No signal for the neuronal cell body restricted γ-actin was detected in the axonal prep (Upper), but β-actin and Luman mRNAs were both detected in the isolated axons (Lower).

3.2.2 Luman in synthesized in axons in response to nerve injury

The presence of Luman mRNA (Figure 3.2.1D) and protein synthesis machinery (Merianda et al., 2009) in axons support the hypothesis that Luman could be locally synthesized in injured axons. To examine this, L4, L5 and L6 DRG neurons were injury-conditioned with a sciatic nerve crush injury 24 h prior to being isolated and cultured on transwell inserts. After 48 h in culture, distal axons were severed from the cell bodies to exclude anterograde transport of cell body-synthesized Luman to the axon. Desomatized sensory axons remain metabolically active and capable of continued protein synthesis (Zheng et al., 2001). Thus, *de novo* Luman protein synthesis was assessed in desomatized axons by immunofluorescence microscopy, which revealed that axonal Luman protein levels increased in the absence of cell bodies over the 6 h period examined (Figure 3.2.2A and C). To confirm that the increased axonal Luman level represented newly synthesized protein, the isolated axons were treated with the protein synthesis inhibitor cycloheximide (10 μg/mL) for the 6 h *de novo* protein synthesis period, which effectively inhibited the increase in axonal Luman (Figure 3.2.2A and C).

Desomatization does not appear to serve as the signal regulating continued axonal Luman synthesis, as axonal Luman levels associated with naïve neurons do not increase following desomatization *in vitro* (Figure 3.2.2B and C). These data instead indicate that Luman is synthesized *de novo* in axons in response to molecular events triggered by pre-culture nerve injury.

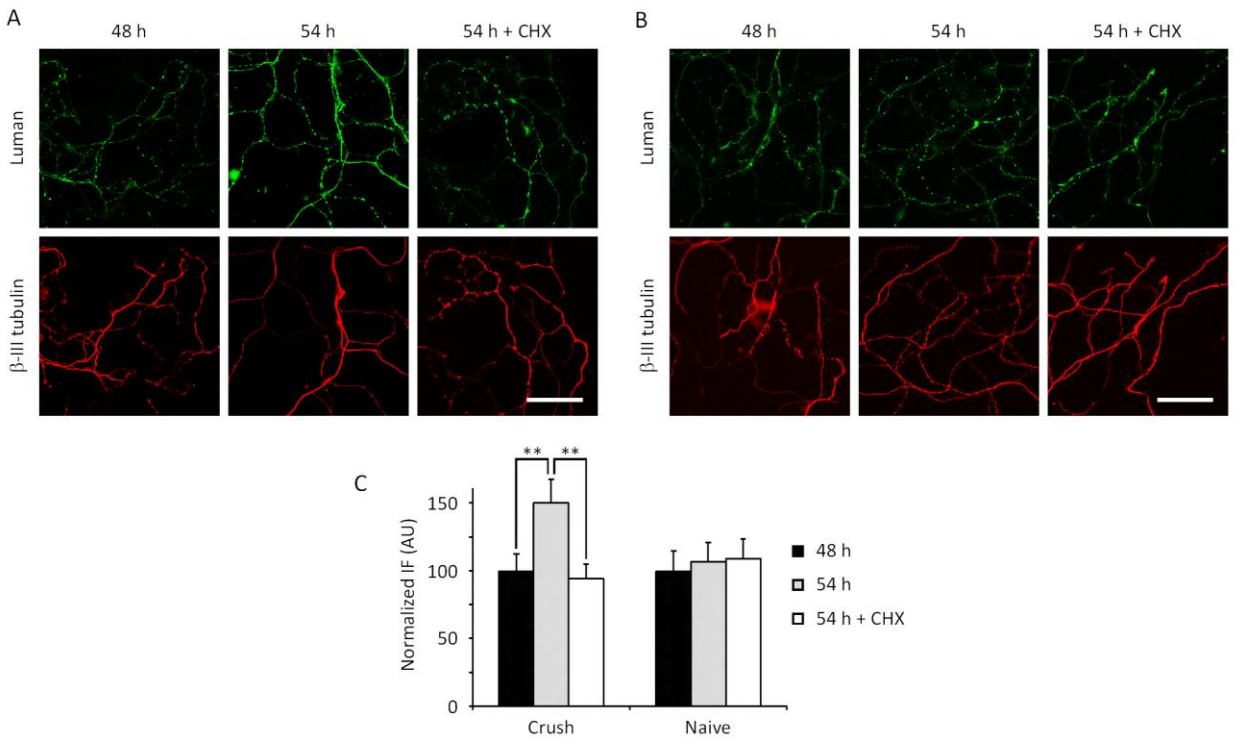

Figure 3.2.2 Luman is locally translated in axons of pre-injured neurons

(A) Dissociated 24 h injury-conditioned neuronal cultures from associated L4, 5, 6 DRG. After 48 h *in vitro*, upper membranes (cell bodies and proximal axons) were scraped, and the lower components (desomatized neurites) continued to be cultured ± 10 μg/mL the translation inhibitor cycloheximide (CHX) for 6 h. Alterations in Luman protein levels were assessed by immunofluorescence (green) of axons identified with anti-β-III tubulin (red). Scale bars, 50 μm. (B) Same experiments as in (A), but DRGs were not pre-injured. (C) Quantification of results in A and B. Application of CHX prevented the increase in Luman immunofluorescence normally observed in the desomatized injury-conditioned axons, demonstrating that the increase in Luman levels requires ongoing protein synthesis (mean ± SEM; N = 40; **p<0.01).

3.2.3 Luman is removed from axons in a proteasome-independent manner following nerve injury

Luman is an ER-resident bZIP transcription factor that can be rapidly activated by regulated intramembrane proteolysis resulting in the translocation of the cleaved/activated N-terminal cytoplasmic portion back to the nucleus (Lu and Misra, 2000; Raggo et al., 2002). In DRG cultures from naïve animals, I find Luman localizes to both neuronal somata and associated neurites. The neurite/axonal localization of Luman is largely restricted to punctae colocalizing

with the ER membrane marker calnexin (Figure 3.2.3A). This distribution pattern however, changes with peripheral nerve injury. The punctate axonal distribution of Luman observed in naïve neurons had largely disappeared in the 1 d injury-conditioned neurons (Figure 3.2.3B). To examine whether this was due to degradation of Luman protein, the experiments were repeated in the presence of the proteasome inhibitor MG-132, but this did not prevent the disappearance of axonal Luman in the injury-conditioned neurons (Figure 3.2.3B). Further, temporal Western blot analysis of *in vivo* nerve crush experiments revealed that the levels of cleaved/activated Luman gradually decreased over time in sciatic nerve protein samples from 10 mm segments just proximal to the crush site, but then correspondingly increased in samples from the L4, 5, 6 DRGs contributing to these injured nerves (Figure 3.2.3C). Together, this evidence suggests that the disappearance of axonal Luman is likely due to retrograde transport from axon to soma. But it is also plausible that the protein might have been degraded by a process not inhibited by MG-132.

To assess whether Luman is removed from axons of injury-conditioned neurons by retrograde transport versus protein degradation and to eliminate the potential contributions of Schwann and satellite cell-derived Luman in interpretation of the results, the transwell insert culture approach was employed to obtain pure axonal isolates. Temporal analysis of alterations in Luman protein levels in isolated axon samples from injury-conditioned neurons cultured in the presence or the absence of the proteasome inhibitor MG-132 was performed and then compared to Luman axonal protein levels in cultures derived from naïve sensory neurons at the various time points examined (Figure 3.2.3D). Axonal Luman immunofluorescence signal detected on the lower membranes of injury-conditioned cultures ± proteasome inhibition revealed that proteasome inhibition did not alter the Luman levels detected in the injured axons at all time points examined. Luman levels in injured axons were always significantly less then levels from naïve neuronal cultures. By 2 DIV (3 d after *in vivo* injury) axonal Luman protein levels were maximally decreased to 25 % that of naïve axons/neurites at the same time point (Figure 3.2.3D). However, this change appeared transient as levels of Luman protein detected in the axons increased approaching that of the naïve culture levels by 3 DIV (4 d post sciatic nerve conditioning injury; Figure 3.2.3D). Because the reductions in axonal Luman levels in the injury-conditioned cultures were not altered by proteasome inhibition, this indicates a proteasome-independent pathway for Luman removal from axons, likely one of retrograde transport. It

should also be noted that the axonal Luman levels did not change significantly in the naïve group over the time course of the experiment (Figure 3.2.3).

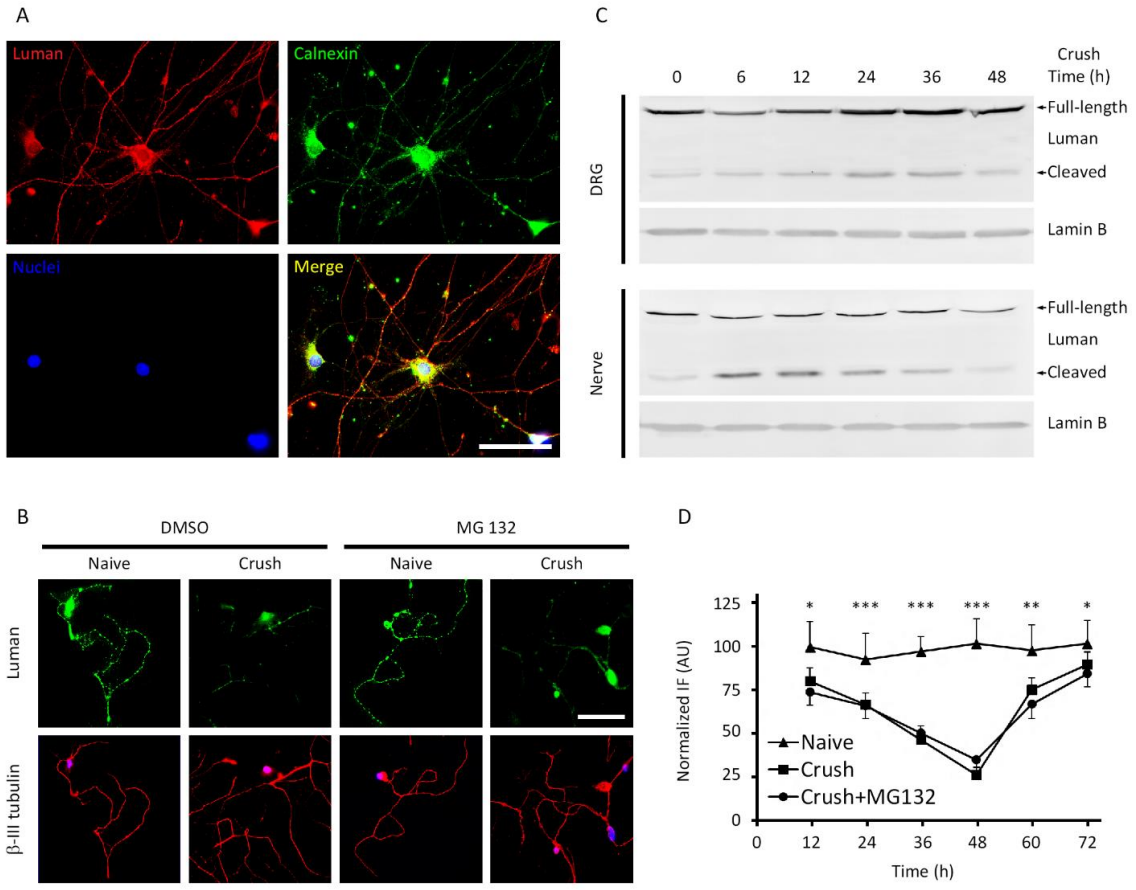

Figure 3.2.3 Luman localizes to the ER and is removed from DRG axons in a proteasome-independent manner in response to nerve injury

(A) Dissociated naïve DRG neurons cultured for 24 h then processed for immunofluorescence to detect Luman (red) and the ER component Calnexin (green) with DAPI-stained nuclei (blue). Merged figure shows that Luman colocalizes with Calnexin and appears as discrete punctae along the axons/neurites. (B) Dissociated DRG neurons that were injury-conditioned for 24 h prior to culturing for 24 h, and processing for immunofluorescence to detect Luman (green) and β-III tubulin (red) with nuclei visualized by DAPI staining (blue). Note: axon localized Luman has largely disappeared from the pre-injured axons relative to naïve control axons. This change is not inhibited by proteasome inhibitor MG-132 nor altered in the presence of its diluent DMSO. (C) Representative Western blot temporal analysis of proteins extracted from sciatic nerve injured DRGs and associated 10 mm segments of sciatic nerves just proximal to the injury site detect Luman at times post-injury as indicated, with Lamin B serving as the loading control. Levels of the cleaved/activated cytoplasmic N-terminal of Luman (lower bands) transiently increase then decrease in injured nerves, while gradually increasing in a reciprocal manner in DRGs, suggesting the gradual loss of Luman in the nerves is due to retrograde transport back to the neuronal cell bodies in the DRG. (D) Naïve or

24 h injury-conditioned DRG neurons were dissociated and seeded onto tissue culture inserts with or without MG-132 and fixed at the time points indicated. Luman in axons were analyzed by assessing changes in the levels of axonal immunofluorescence (mean ± SEM; N=40) as normalized to naïve controls at 12 h culture time point. Note that the decrease in axonal Luman levels is transient and that at all time points examined there is significantly less Luman detected in both experimental groups as compared to naïve controls. The lack of a significant difference between crush and crush+MG-132 groups indicates that Luman disappears from axons via a proteasome-independent pathway (*$p<0.05$; **$p<0.01$; ***$p<0.001$). Scale bars = 100 μm.

3.2.4 The importin system is activated by nerve injury

Axonal proteins containing NLS are retrogradely transported to the soma and nucleus by importins (Hanz et al., 2003). To confirm the influence of nerve injury on the levels of importins in the sciatic nerve injury model, I analyzed the levels of importin α and importin β. In protein samples derived from sciatic nerve segments proximal to injury, both importin α and importin β are significantly increased after nerve injury (Figure 3.2.4A and B). Cellular alterations in the levels of importin β and Luman in DRG neurons were also examined on L4 DRG from naïve and sciatic nerve crushed rats. Figure 3.2.4C shows that the levels of Luman and importin β increased only in the injury-conditioned neurons, with the most notable increase being observed in the nuclei where both markers co-localized. These data indicate that the importin system is activated by sciatic nerve crush injury in agreement with previous studies (Hanz et al., 2003) and provide anatomical evidence that Luman may be one of the cargo proteins.

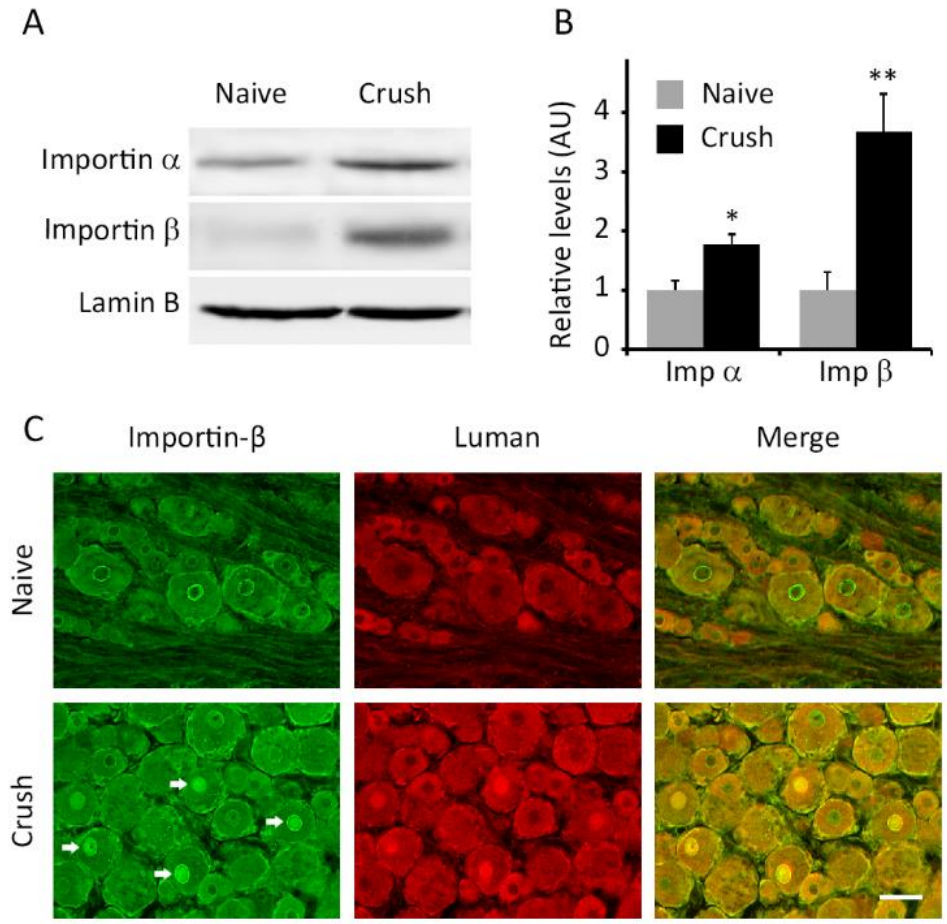

Figure 3.2.4 Nerve injury activation of the importin system

(A) Representative Western blot analysis of Importin α and β in proteins extracted from 10 mm nerve segments just proximal to a 24 h sciatic nerve crush site with Lamin B as the loading control. (B) Quantification of results obtained in (A). Expression of Importin α and β are significantly increased in response to nerve injury (mean ± SEM; *p< 0.05; **p<0.01; N=3). (C) L4 DRG sections from naïve or 24 h injury-conditioned animals processed for immunofluorescence to detect Importin β (green), and Luman (red), reveal that 24 h after nerve injury, neuronal nuclei with increased Importin β staining (examples indicated with arrows) also show increased nuclear Luman signal, but there is no nuclear Luman detected in sections from naïve animals. Scale bar, 50 μm.

3.2.5 Retrograde transport of Luman following nerve injury is mediated by importin α

The presence of a bipartite NLS in Luman (Figure 3.2.5A) identifies it as a potential cargo protein of importin α. To determine the interaction between Luman and importin α, immunoprecipitation experiments were performed using protein samples from L4, 5, 6 DRG neuronal cultures from naïve or injury-conditioned animals. Using anti-importin α, importin α and associated proteins were immunoprecipitated and the resulting samples were probed for Luman. A 40 kDa Luman band was immunoprecipitated along with importin α in samples from sciatic nerve injured animals, but not from naïve animals (Figure 3.2.5B). 40 kDa Luman is the expected size of the proteolysis cleaved/activated N-terminal cytoplasmic domain of Luman, which contains all its identified functional domains, including its activation domain, basic region and leucine zipper and has been shown to translocate to the nucleus (Lu et al., 1997; Lu et al., 1998; Raggo et al., 2002); To determine whether the NLS is critical to the interaction between Luman and importin α, I used a membrane-permeable peptide that contains the NLS sequence found within the NF-κB p50 subunit (Lin et al., 1995) which has been shown to be able to block nuclear transport of NF-κB, AP-1, NFAT and STAT1 (Torgerson et al., 1998) and also that of CREB2 (Lai et al., 2008) by antagonizing their interaction with importin α. Incubation with excess NLS peptide significantly abolished the interaction between Luman and importin α, compared with untreated cultures or with cultures incubated with peptides in which the NLS sequence was mutated (mNLS) so that it no longer binds to importin α (Figure 3.2.5B). These findings support the hypothesis that Luman interacts with importin α via its NLS.

To more directly test whether the cleaved/activated cytoplasmic domain of Luman is retrogradely transported from axon to soma after nerve injury, I blocked the polymerization of microtubules which play a crucial role in retrograde transport of importin-associated cargo (Hanz et al., 2003). In the pure axonal samples, the reduction/disappearance of the cytoplasmic domain of Luman from the injury-conditioned axons was unaffected by addition of the proteasome inhibitor MG-132 and lysosome inhibitor chloroquine, indicating once again that this process occurs via a proteasome/protein degradation-independent pathway. However, application of colchicine, which inhibits the polymerization of microtubules prevented microtubule-dependent

transport of Luman and eliminated the normally observed reduction in axonally localized cleaved/cytoplasmic domain of Luman following nerve injury (Figure 3.2.5C and D).

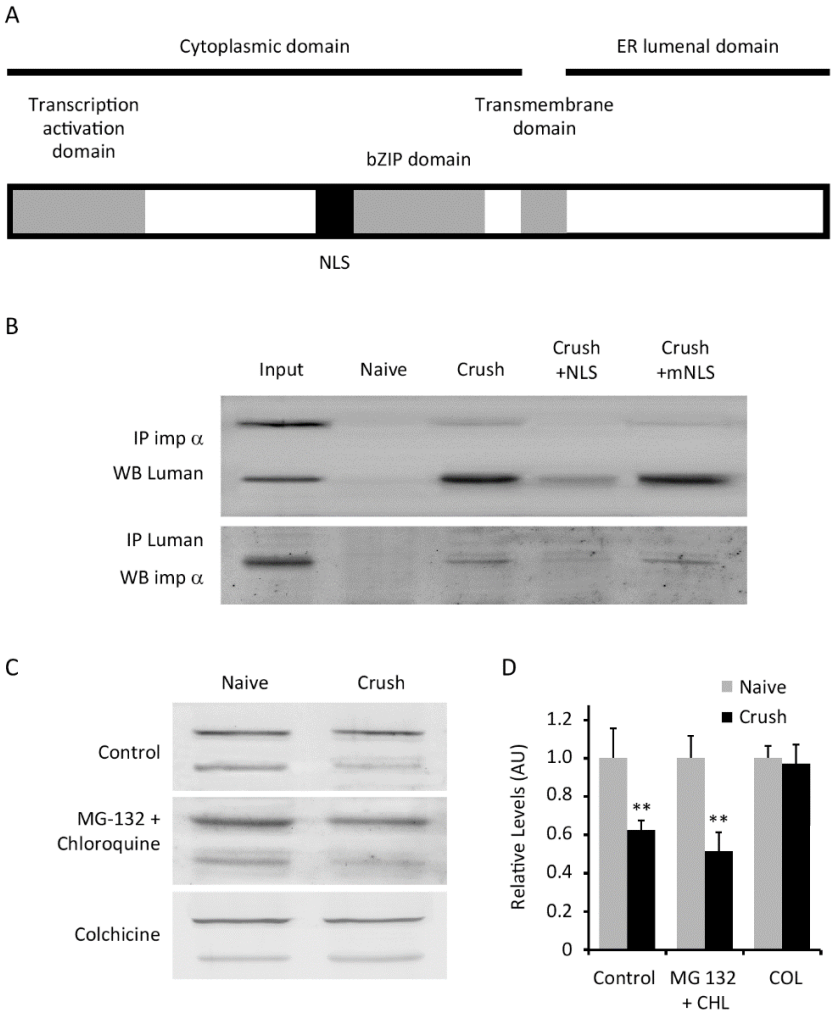

Figure 3.2.5 Importin-α interacts with Luman in injured neurons

(A) Schematic representation of the structure of Luman. NLS predicts site of interaction of Luman with importin α. (B) The interaction between Luman and importin α was analyzed by immunoprecipitation (IP) followed by Western blot. Association of the cleaved cytoplasmic domain of Luman (lower band) with importin α is detected in rat DRG neurons subjected to a 24 h sciatic nerve injury, but not from naïve rats. The interaction is abolished in neurons treated with an NLS competitor peptide (Crush + NLS) but not in neurons treated with control mutant NLS (Crush + mNLS). Input lane represents control sample from injury-conditioned DRGs prior to IP. (C) 24 h injury-conditioned DRG neurons were cultured for 48 h on tissue culture inserts in the presence or absence of MG-132 + chloroquine or colchicine, followed by isolation of axons and detection of axonal Luman levels by Western blot. Note that relative to naïve control, injury conditioned axons have less Luman, especially evident for the

cleaved/activated cytoplasmic domain form (lower band). This decrease is unaffected by inhibition of protein degradation (MG-132+chloroquine), but is prevented in the presence of the retrograde transport inhibitor colchicine. (D) Quantification of the Luman cleaved/activated cytoplasmic domain levels (lower band) observed in C (mean ± SEM; **p<0.01; N=3). Note: Axonal levels of cleaved Luman cytoplasmic domain decrease significantly after nerve injury with or without protein degradation inhibitors MG-132 and chloroquine, but this is prevented by colchicine inhibition of microtubule polymerization, implying that the removal of Luman from axons is a microtubule-dependent process.

In response to cellular stressors, such as nerve injury in the present study, Luman is cleaved/activated by regulated intramembrane proteolysis releasing an N-terminal fragment for translocation back to the nucleus (Raggo et al., 2002) This fragment is visualized as the lower molecular weight form of Luman on Western blots (Figure 3.2.5B). To more precisely examine retrograde trafficking of the activated Luman N-terminal fragment, an adenoviral vector Ad/GFP-Lu-RFP was created in which a GFP tag was fused to the cytoplasmic N-terminus that contains all the functional domains of the protein, while a RFP tag was fused to the C-terminus of rat Luman which remains bound to the membrane. Ad/GFP-Lu-RFP enabled sufficient expression of GFP-Luman-RFP fusion protein in cultured DRG neurons (Figure 3.2.6A). In infected neurons the addition of these tags did not appear to alter the localization of this protein nor it functional properties. The GFP-Luman-RFP fusion protein activated transcription from the UPRE in a manner similar to wild type Luman (Figure 3.2.6B), and it localized to the ER in both the cell bodies and neurites/axons (Figure 3.2.6C and D) consistent with that observed for wild type Luman (Figure 3.2.3A).

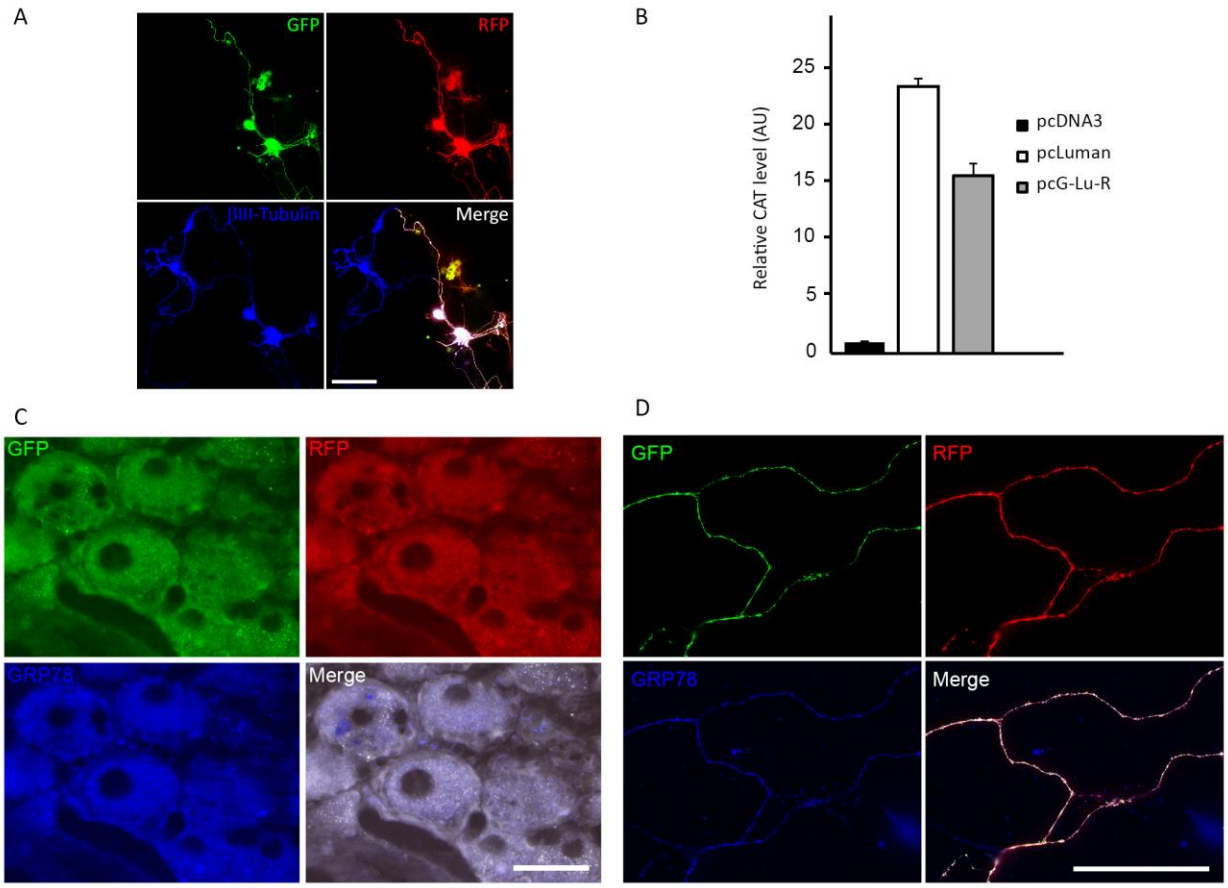

Figure 3.2.6 Ad/GFP-Lu-RFP delivers functional GFP-Luman-RFP into neurons that localizes to the ER

(A) DRG neuron cultures were infected with Ad/GFP-Lu-RFP at a MOI of 100 and neurons were visualized by β III tubulin immunostaining (blue). Scale bar: 100 μm. (B) Luman (pcRatLuman) and GFP-Luman-RFP fusion protein (pcGFP-Lu-RFP) can activate CAT reporter gene expression but the control plasmid does not (pcDNA3.1). (C and D) DRG sections from animals infected *in vivo* (C) and *in vitro* (D). Colocalization of GFP-Luman-RFP fusion protein and ER protein GRP-78. Merged images reveal that GFP-Luman-RFP fusion protein localizes to the ER both *in vivo* and *in vitro*. Scale bar: 50 μm.

Exposure of dissociated DRG cultures to this construct at 100 MOI for 48 h was sufficient to transduce the neurons such that both RFP and GFP tags were visible and perfectly colocalized in the soma and neurites (Figure 3.2.7A, 0 h). To investigate whether axonal injury results in Luman cleavage/activation and translocation to the nucleus *in vitro,* an axonal scratch injury was made with a pin rake, and neurites immediately adjacent (proximal) to the injury site and their cell bodies were imaged with time-lapse microscopy for 24 h. The injury resulted in the

disappearance of GFP from the distal most tips of axons just proximal to the injury site and a corresponding accumulation of GFP in the nucleus, with no discernible change in the distribution of RFP (Figure 3.2.7A, C, and D). This is consistent with the cleavage/activation of the N-terminal cytoplasmic portion of Luman while the C-terminus remains membrane bound. The disappearance of GFP in the axon and the accumulation of GFP in the nucleus was significantly blocked by a competitor NLS peptide, suggesting importin-dependent transport of GFP-Luman from the axon (Figure 3.2.7B, C, and D).

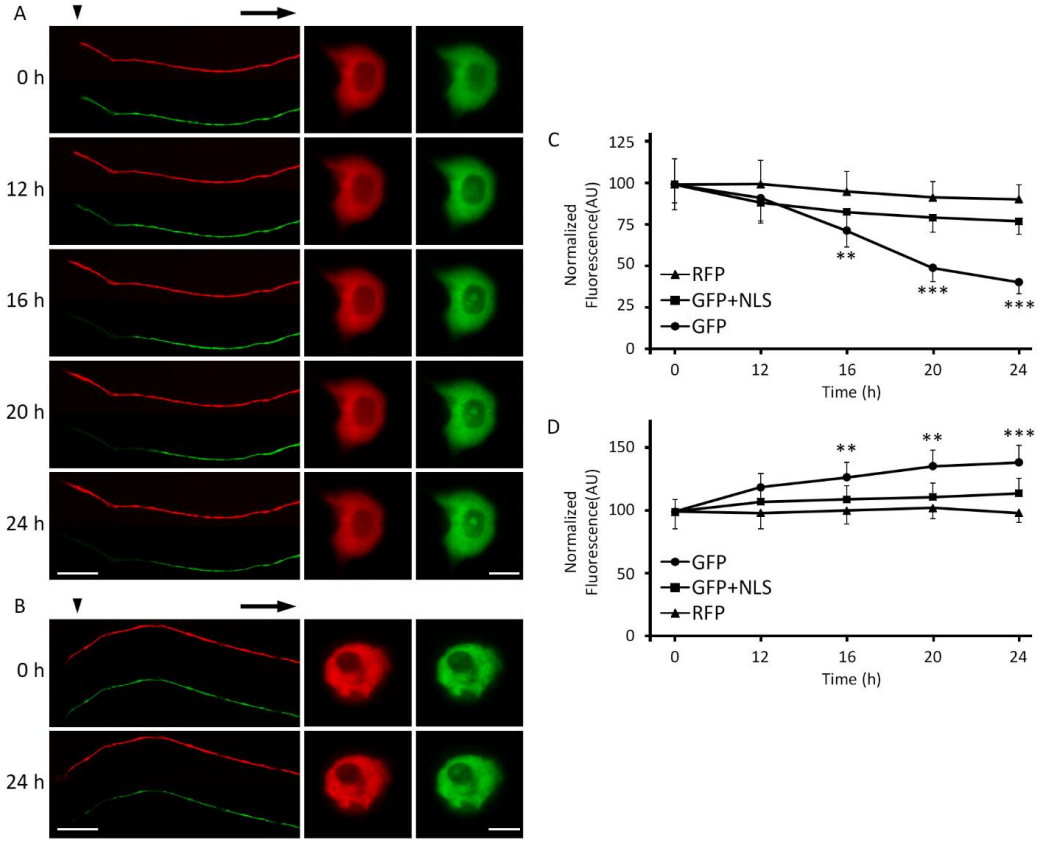

Figure 3.2.7 *in vitro* retrograde transport of GFP/RFP dual tagged Luman

(A) Dissociated DRG cultures were infected Ad/GFP-Lu-RFP for 48 h. An *in vitro* scratch injury was made at 0 h and a temporal analysis of alterations in disappearance of the cleaved/activated GFP-tagged N-terminus (green) was monitored at the 5 time points indicated. Note that the RFP-tagged C terminus of Luman (red) remains unchanged and presumably membrane associated. Movement of GFP-tagged cleaved/activated N-terminal fragment of Luman was analyzed in the axon and cell body at the times indicated in the figure. Arrowheads indicate the injury site and arrows indicate the retrograde transport direction. Scale bar axon: 50 μm, scale bar cell body: 20 μm. (B) Same

experiments as in (A), but NLS peptide was added 24 h before the *in vitro* injury. Note the greatly diminished loss of Luman N-terminus GFP from the axon tip just proximal to the nerve injury site even 24 h post-lesion. Scale bar axon: 50 μm, scale bar cell body: 20 μm. (C) Quantification of the intensity of axonal GFP and RFP in (A) and axonal GFP in (B). (D) Quantification of the intensity of nuclear GFP and RFP in (A) and nuclear GFP in (B). The relatively stable levels of RFP, decreased levels of GFP in the axon and increased levels of GFP in the nuclei support that the N terminus of Luman (fused with GFP) is retrogradely transported from axons to nuclei after axonal injury, and this is inhibited in NLS-treated neurons. (N=10).

To determine if retrograde transport of Luman also occurs *in vivo*, the sciatic nerve was crush injured for 24 h and then ligated proximal to the injury site for another 24 h followed by processing for Luman immunohistochemistry. The presence of intense immunostaining (Figure 3.2.8A) distal to the ligation site is consistent with Luman being in transit in a retrograde direction from the initial crush injury site, as is the decrease in signal observed in the portion of the nerve proximal to the ligation. The intense Luman staining was only observed in the crush and ligated nerves, but not ligation only nerves, suggesting that retrograde transport from the initial crush injury site is activated by injury.

The Ad/GFP-Lu/RFP was also used to track the movement of cleaved/activated Luman *in vivo*. Ad/GFP-Lu-RFP was injected intrathecally at the L5 DRG level and left for 7 d. Intrathecal injection has been shown to result in higher neuronal transduction efficiency than sciatic nerve injection (Towne et al., 2009). Expression of the viral construct in both DRGs and sciatic nerve was confirmed in sections from 7 d infected rats (Figure 3.2.6C and 3.2.8C). The right sciatic nerve was then crushed, and right and left sciatic nerves and L5 DRGs were dissected 48 h after the injury. In the intact nerve and DRG, GFP and RFP colocalized, and were not found in the neuronal nuclei (Figure 3.2.8C). On the injured side, the marked loss of GFP, but not RFP in the nerve proximal to injury and the accumulation of GFP in the nuclei of the DRG (Figure 3.2.8B) confirms that the N terminus of Luman was retrogradely transported to the nuclei after nerve injury *in vivo*.

Together, the data indicate that the injury-associated loss of Luman from axons is due to importin-mediated retrograde transport back to the nucleus.

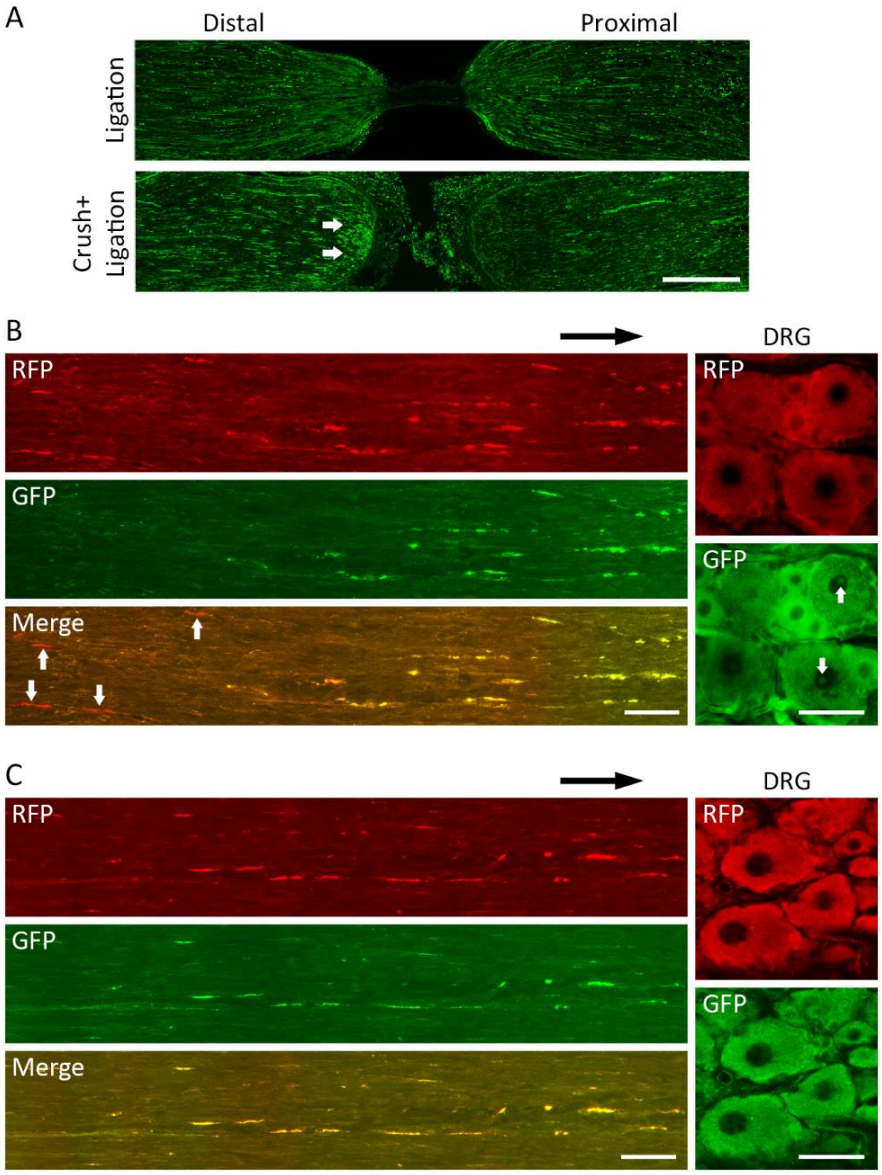

Figure 3.2.8 *in vivo* retrograde transport of Luman after nerve injury

(A) Upper panel, sciatic nerve was ligated at mid-thigh level for 24 h (Ligation). Lower panel, sciatic nerve was crush injured for 24 h, then ligated proximal to the injury site for an additional 24 h (Crush + Ligation). The distribution of endogenous Luman was visualized by immunohistochemistry. An accumulation of Luman on the distal side of the ligation is most evident in the crush + ligation nerve (arrows) consistent with retrograde transport from the initial crush injury site. There is also a paucity of staining on the proximal side of the ligation, also consistent with retrograde transport centrally from ligation site. Scale bar, 50 μm. N=3. (B and C) Ad/GFP-Lu-RFP was intrathecally injected at the L5 DRG level and left for 7 d prior to unilateral 48 h crush injury of the sciatic

nerve. Nerve sections were taken 1 mm proximal to injury site with the retrograde transport direction indicated by black arrows. Sections of injured (B) and intact (C) sciatic nerves and corresponding L5 DRGs were prepared. The localization of GFP (fused to the N terminus of Luman) and RFP (fused to the C terminus of Luman) were analyzed. GFP and RFP are colocalized in the uninjured nerves, and are not observed in the uninjured DRG nuclei (C). The cleavage/activation and apparent retrograde transport of the N terminus of Luman (GFP) after nerve injury results in reduced colocalization of GFP and RFP in the injured nerve most evident in the region of nerve closest to the injury site (B, arrows, nerve), and examples of the appearance of GFP in the nuclei of injured sensory neurons are shown (B, arrows, DRG). Scale bars: 100 μm (nerve); 50 μm (DRG). N=4.

3.2.6 Axonal knockdown of Luman inhibits axonal outgrowth in injury-conditioned DRG neurons

Luman has been shown to participate in regulation of cell migration of osteogenic sarcoma cells that involves intricate cytoskeletal rearrangements (Ko et al., 2004). Because of this I speculated that axonal injury-activated Luman may serve to promote axon outgrowth in injured sensory neurons. Thus, I analyzed the neurite outgrowth of cultured DRG neurons where Luman expression was knocked down by transfecting the cultures with Luman selective siRNA. siRNA can be efficiently transfected into cultured DRG neurons (Figure 3.2.9A), and Luman siRNA transfection significantly decreased the Luman expression at both the mRNA (Figure 3.2.9B) and protein (Figure 3.2.9C and D) levels.

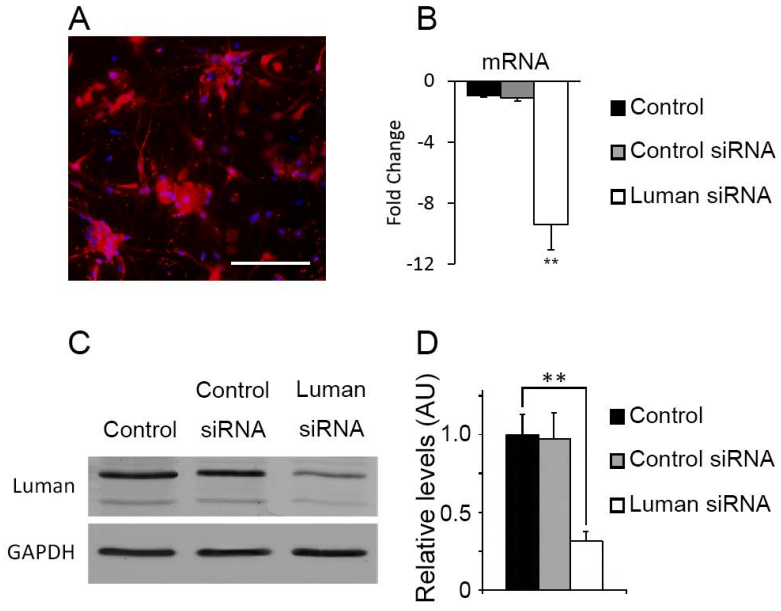

Figure 3.2.9 Luman siRNA knocks down Luman expression in DRG neurons

(A) Transfection efficiency test of siRNA. DRG neurons were transfected at a final concentration of 10 nM with the TYE 563 DS Transfection Control duplex, and imaged 24 h post-transfection (Red: labelled siRNA; blue: nuclei). Most cells can be transfected with labelled siRNA. (B) The mRNA levels of Luman in neurons cultured in experimental conditions as indicated. (C) Expression level of Luman was analyzed by Western blot from protein samples of cultured DRG neurons transfected with control nontargeting siRNA (Control siRNA) or rat Luman-specific siRNA (Luman siRNA) 48 h previously. A representative blot is shown. (D) Quantification of Luman levels detected in Western blots from 3 separate experiments as in (C). Note: Luman siRNA significantly decreases the level of Luman detected (**$p<0.01$).

DRG neurons cultured from 24 h sciatic nerve injury-conditioned or naïve rats were transfected with control siRNA or Luman siRNA. Forty-eight h after transfection, neurites were visualized by β-III tubulin immunostaining. Total neurite outgrowth and branching were analyzed with representative neurons shown in Figure 3.2.10A. Injury-conditioned DRG neurons have longer and less branched neurites relative to naïve neurons. While knockdown of Luman significantly decreased the total neurite length of the pre-injured DRG neurons, it had no discernible impact on branching and had no effect on either parameter for the naïve neurons (Figure 3.2.10B and C).

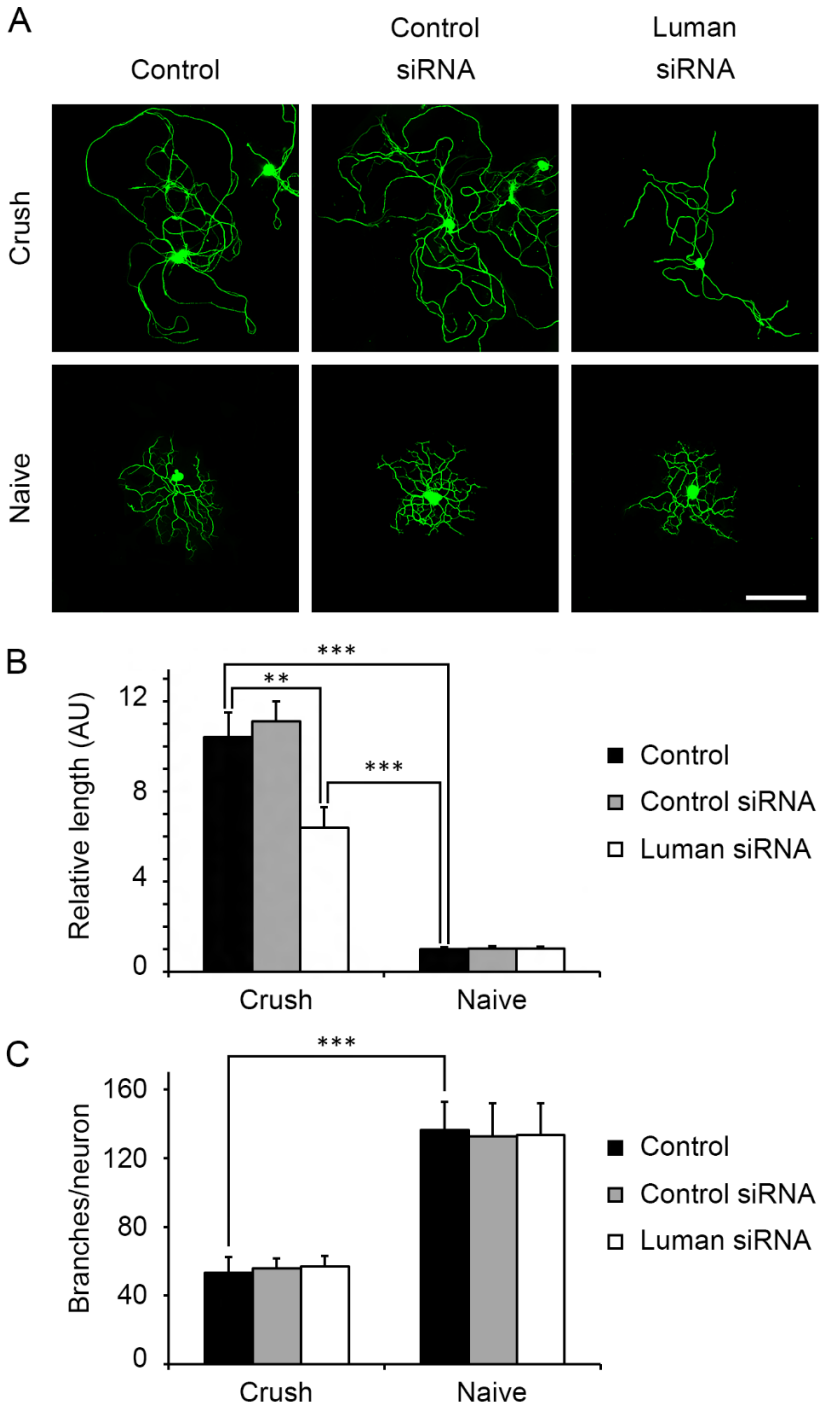

Figure 3.2.10 Knockdown of Luman inhibits axonal outgrowth in pre-injured DRG neurons.

(A) Naïve DRG neurons or 24 h injury-conditioned neurons (Crush) were assayed *in vitro* for 48 h in the presence of medium alone (Control), or transfected with nontargeting siRNA (Control siRNA) or Luman selective siRNA (Luman siRNA) for 48 h followed by β-III tubulin (green) immunofluorescence. Note that pre-injured DRG neurons

have longer but less branched neurites as compared to naïve controls with substantially less neurite outgrowth in cultures transfected with Luman siRNA. Scale bar, 200 μm. (B) Quantification of total neurite length in A (mean ± SEM; **p<0.01; ***p<0.001; N=250). Luman siRNA treatment significantly impaired axonal outgrowth from injury-conditioned neurons, but did not discernibly impact the outgrowth of DRG neurons from naïve rats. (C) Quantification of axon branches/neuron in A (mean ± SEM; ***p<0.001; N=50). The number of axon branches (end points/neuron) is significantly decreased after sciatic nerve injury, but knockdown of Luman did not impact the number of axon branches in either injury conditioned or naïve neurons.

To better mimic the *in vivo* situation *in vitro,* and to more selectively knockdown axonal Luman expression, I cultured injury-conditioned DRG mini explants in compartmented chambers. The DRG explant cultures preserve relationships among neurons, Schwann cells and satellite glial cells that are lost in dissociated cultures. These cell relationships may play an important role in sensory neuron regeneration *in vivo* (Allodi et al., 2012; Zochodne, 2012). Compartmented culture allows selective application of Luman siRNA only to the distal axonal compartment (Figure 3.2.11A). Compartmented inserts formed three sealed compartments. Brilliant Blue G dye added to the central compartment showed no diffusion underneath the barrier (Figure 3.2.11B), and retrograde tracers applied to the side compartments labelled neurons with neurites extending to the corresponding compartments (Figure 3.2.11C). Axonal specific Luman knockdown was shown in figure 3.2.11 D and E, where only the region of neurites exposed to the siRNA were transfected (Figure 3.2.11D), and the expression of Luman was impacted only in the compartment exposed to the Luman siRNA (Figure 3.2.11E).

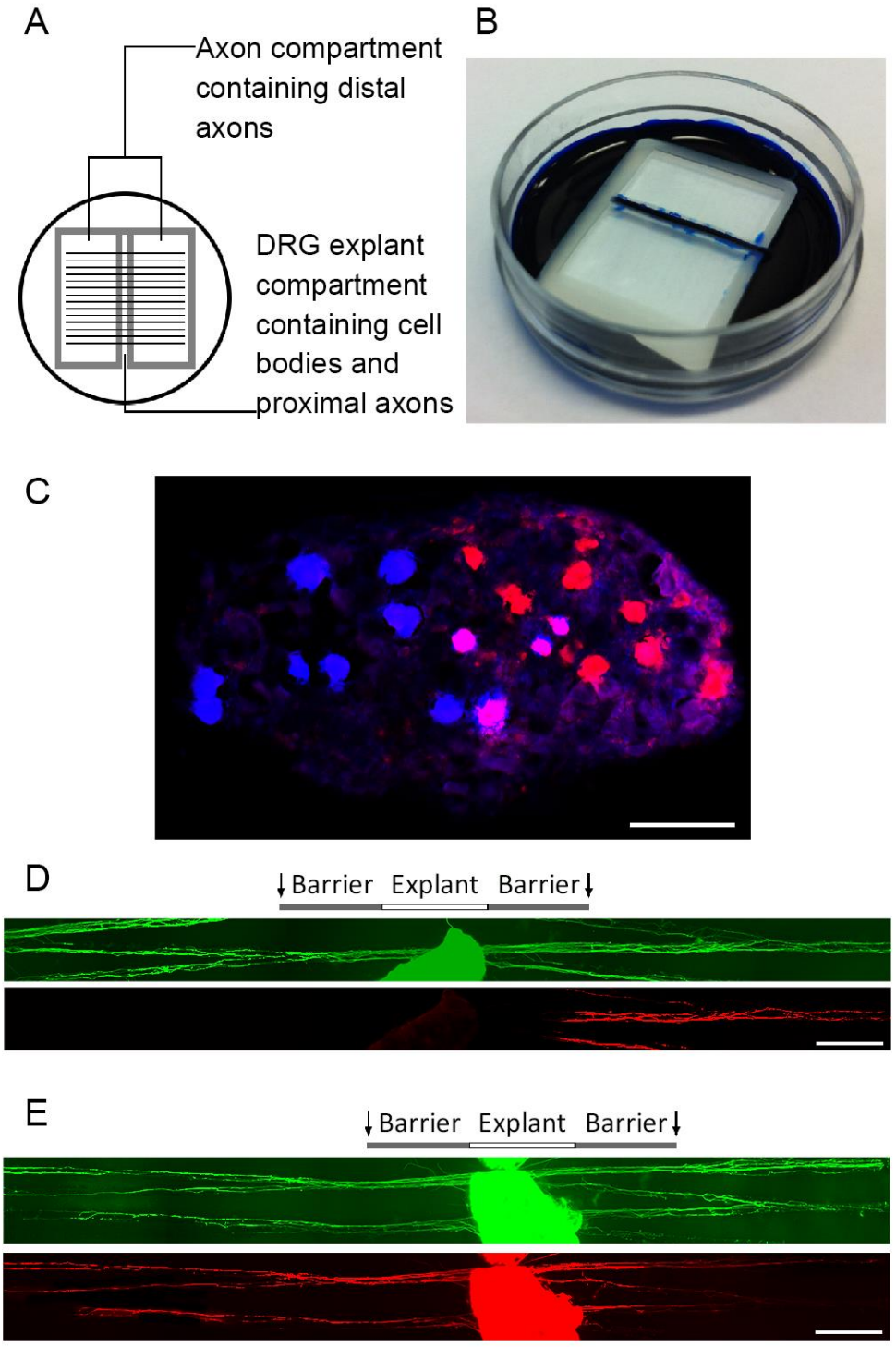

Figure 3.2.11 Axon-specific Luman knockdown

(A) Schematic representation of compartmented cell culture dishes created by scratching the surface with a pin rake and placing a compartmented insert cut from 1 mm silicon on top of the scratches 1 d after DRG explants are seeded in the middle chamber. Axons from DRG explants grow under the silicon barrier, but all neuronal and noneuronal

cells are prevented from entering the axon compartments. (B) Solutions are compartmentally restricted, with Brilliant Blue G added to the central compartment and external to the compartments showing virtually no diffusion underneath the barrier over 24 h. (C) Section of a DRG explant whose neurites extended to the left and right compartments were treated with fluorogold (blue) and fluororuby (red), respectively. (D) Representative fluorescence photomicrograph montages of axonal outgrowth detected with β-III tubulin immunofluorescence (green) from DRG explants. Explant compartment and silicon barrier regions (grey) are indicated. Right axon compartments were transfected with TYE 563 DS Transfection Control duplex (red). (E) Representative fluorescence photomicrograph montages of axonal outgrowth detected with β-III tubulin immunofluorescence (green) and Luman immunofluorescence (red) from DRG explants. Explant compartment and silicon barrier regions (grey) are indicated. Left axon compartments were transfected with negative control nontargeting siRNA, while right axon compartments were transfected with Luman siRNA. Scale bar, 1 mm.

Injury-conditioned DRG explants were transfected with control siRNA in the left axon compartment and rat Luman selective siRNA in the right axon compartment (Figure 3.2.12A). Control cultures compare culture medium alone in the right compartment to control siRNA in the left (Figure 3.2.12B). Seven days after the transfection, cultures were fixed and neurites were visualized with anti-β-III tubulin. The length of the 10 longest neurites/explant (left and right compartments) were measured with representative cultures shown in Figure 3.2.12A and B. Neurites/axons grown under normal culture conditions (Figure 3.2.12B right chamber) and control siRNA conditions (Figure 3.2.12A and B left chambers) are longer than axons transfected with Luman siRNA (Figure 3.2.12A, right chamber). Axonal knockdown of Luman significantly decreased the neurite length of injured DRG explants (Figure 3.2.12C). Collectively, these data support the hypothesis that axonal Luman translation is required for optimal neurite outgrowth after peripheral nerve injury.

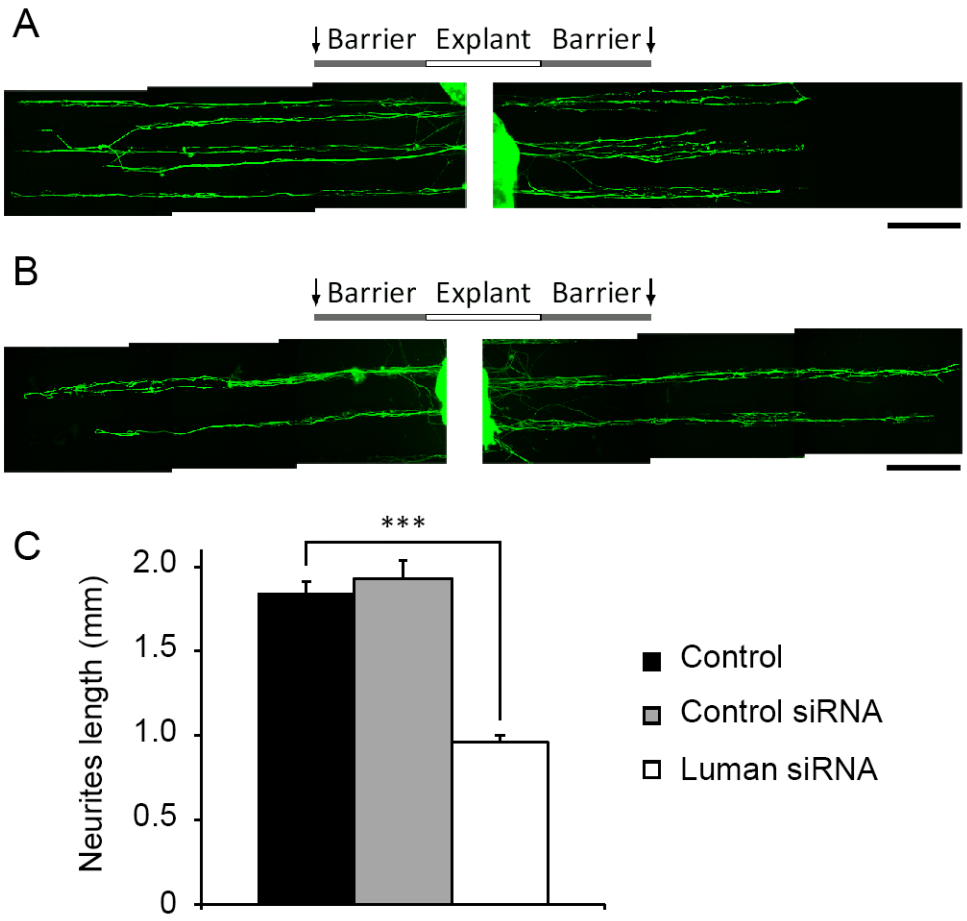

Figure 3.2.12 Subcellular axonal knockdown of Luman inhibits axonal outgrowth in injury-conditioned DRG neurons.

(A) Representative fluorescence photomicrograph montages of axonal outgrowth detected with β-III tubulin immunofluorescence (green) from L4, 5, 6 DRG explants that were 24 h sciatic nerve injury-conditioned prior to culturing. Explant compartment and silicon barrier regions (grey) are indicated. Left axon compartments were transfected with negative control nontargeting siRNA, while right axon compartments were transfected with Luman siRNA for 7 d. Note: axon outgrowth is significantly shorter for axons treated with Luman siRNA as compared to those in the nontargeting control siRNA compartment. (B) Montages showing outgrowth from explants as in (A) but cultured under control conditions: normal medium (right compartment) or transfected with negative control nontargeting siRNA (left compartment) for 7 days with no discernible difference observed between control treatments. Scale bar, 1 mm. (C) Quantification of the 10 longest neurite/axon lengths from each DRG explant into right and left compartments; N = 60 (normal medium); 130 (control siRNA) or 70 (Luman siRNA) neurites/axons measured in A and B (mean ± SEM; ***$p<0.001$). Note: Knockdown of Luman in the axon compartment significantly decreased the length of neurites/axons from injury-conditioned DRG explants.

3.3 The UPR is a major mechanism by which Luman regulates injury-induced neurite outgrowth

During regenerative axon growth in the PNS complex pathophysiologic changes, including increased synthesis of RNA, protein, and lipids, occur at the levels of the injured axon and the cell body (Flores et al., 2000). The increased protein synthesis in the axon (Jung et al., 2012) and the cell body (Burnett and Zager, 2004) plays a crucial role in nerve regeneration. Normally the accumulation of misfolded and unfolded proteins during protein synthesis triggers the UPR. The activation of UPR has been observed in many neurodegenerative diseases (Doyle et al., 2011). It is also involved in axon injury-induced retinal ganglion cell death (Hu et al., 2012) and Schwann cell survival after injury (Mantuano et al., 2011), but little is known about the function of UPR in regulating peripheral nerve regeneration. Thus, I decided to assess the UPR in axotomized DRG neurons and study the role of UPR in regulating PNS regeneration.

3.3.1 Sciatic nerve crush injury triggers the UPR in DRGs

To determine whether the increased protein synthesis during nerve regeneration induces the UPR in sensory neurons, I tested the levels of expression of several UPR-related genes in DRGs after sciatic nerve crush injury. ER resident chaperone GRP78 is expressed early in the UPR, as the dissociation of GRP78 and ER stress transducers activates the UPR pathways (Ron and Walter, 2007). CHOP, which has generally been used as an UPR marker (Samali et al., 2010), was found to be up-regulated by optic nerve injury (Hu et al., 2012). Through the use of the mRNA isolated from DRGs, quantitative real-time PCR (qRT-PCR) analysis showed increased expression of GRP78 mRNA and CHOP mRNA in axotomized DRGs (Figure 3.3.1A), which was further confirmed by both in situ hybridization and immunohistochemical analysis in L4 DRG sections (Figure 3.3.1B and C). PERK and IRE1, the transducers of UPR (Cox et al., 1993; Harding et al., 2000), Calnexin, a chaperone protein characterized by assisting protein folding and quality control (Ou et al., 1993), and protein disulfide isomerase (PDI), an enzyme that catalyzes disulfide formation and protein folding (Wilkinson and Gilbert, 2004) were also increased by axotomy in DRGs (Figure 3.3.1D). XBP-1 splicing has been considered as another marker of the UPR (Calfon et al., 2002). I examined whether the splicing product of XBP-1 could be detected in DRGs after sciatic nerve injury. qRT-PCR showed significant increased

spliced XBP-1in the DRGs obtained one day after sciatic nerve crush injury (Figure 3.3.1A). These results demosntrate that 1 d sciatic nerve injury triggers the UPR in axotomized DRGs.

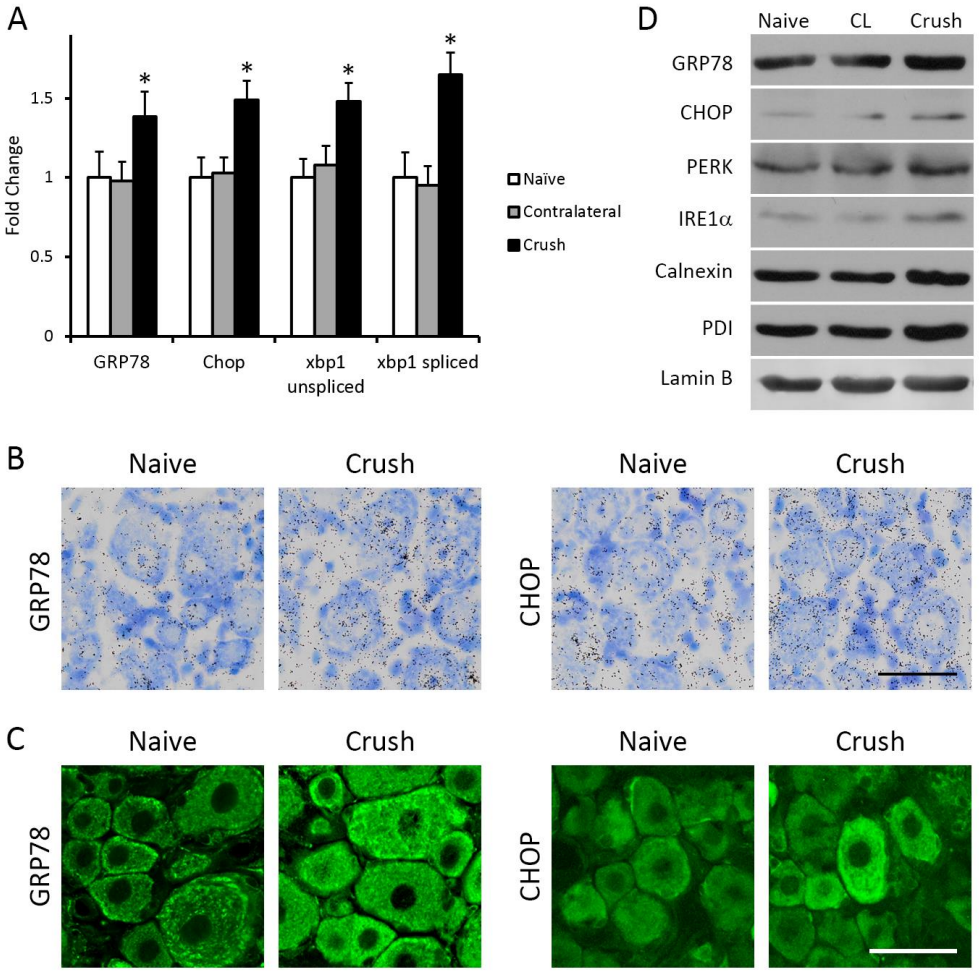

Figure 3.3.1 One day sciatic nerve crush injury induces the UPR in adult DRG

(A) Relative changes in mRNA levels of GRP78, CHOP, unspliced Xbp-1, and spliced Xbp-1 in DRGs from naïve and 1 d sciatic nerve crush injury animals normalized to naïve controls (means ± SEM; N=6; * $p<0.01$). (B) *In situ* hybridization shows the expression of GRP78 and CHOP in the L4 DRG under conditions as indicated. Scale bar, 100 μm. (C) Immunohistochemical analysis of GRP78 and CHOP immunoreactivity in DRG sections from experimental conditions as indicated. Scale bar, 100 μm. (D) Immunoblot analysis of DRG protein samples from experimental conditions as indicated. Lamin B was employed as a loading control. CL, contralateral uninjured DRG. Note: All the UPR markers examined have increased levels of mRNA and protein expression in response to injury relative to the naïve state.

3.3.2 Luman is activated in response to sciatic nerve crush injury

The induction of the UPR in DRG in response to sciatic nerve crush injury and the ability of Luman to regulate aspects of the UPR in other cell types, made me speculate that Luman likely regulates the peripheral nerve injury-associated UPR. To examine this, I first verified that the sciatic nerve crush injury model employed in these UPR studies induced expression and activation of Luman in the DRG. qRT-PCR analysis showed increased expression of Luman in 1 d axotomized DRGs (Figure 3.3.2A), further confirmed by both Western blot and immunohistochemical analysis (Figure 3.3.2B and C). Luman is activated by regulated intramembrane proteolysis, which results in the amino-terminal portion of Luman being released from the ER and entering the nucleus to serve as a transcription factor (Raggo et al., 2002). Figure 3.3.2B shows that the crush injury not only increased the level of full length Luman, but also increased cleaved/activated Luman. Nuclear localization of Luman was also observed in the axotomized DRGs (Figure 3.3.2C). Therefore, these results indicate that Luman is activated and its expression is elevated in response to 1 d sciatic nerve crush injury.

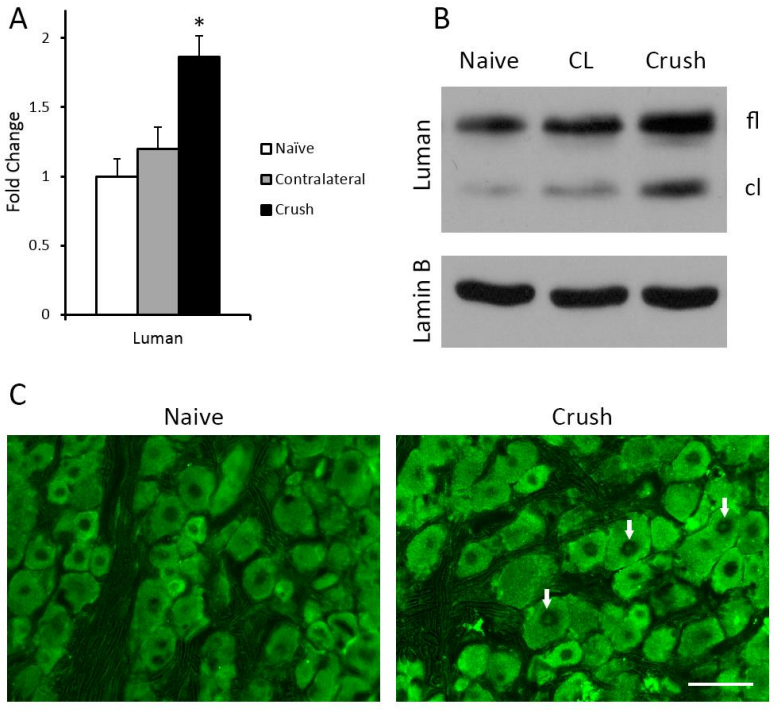

Figure 3.3.2 Sciatic nerve injury activates Luman in DRG

(A) Quantification of expression of Luman mRNA in DRG detected by qRT-PCR. 18 S rRNA was used as the endogenous control (means ± SEM; N=6; * $p<0.01$). (B) Immunoblot analysis of DRG protein samples from experimental conditions as indicated. Upper band, full-length Luman (fl); lower band, cleaved Luman (cl). Lamin B was employed as a loading control. CL, contralateral uninjured DRG. (C) Immunohistochemical analysis of Luman immunoreactivity in DRG sections from experimental conditions as indicated. Nuclear localization of Luman is indicated by arrows. Scale bar, 100 μm. Note: The mRNA and protein (both full-length and the cleaved/activated forms) levels of Luman increased in response to sciatic nerve injury.

3.3.3 Knockdown of Luman decreases the injury-induced UPR

To study the role of Luman in regulating the sciatic nerve injury-triggered UPR, I used qRT-PCR arrays designed to assess expression of genes related to the UPR to determine if knockdown of endogenous Luman altered the response. I compared RNA purified from dissociated 1 d injury-conditioned DRG neurons transfected with Luman-specific siRNA, or nontargeting control siRNA, for an additional 2 d. Figure 3.3.3A reveals that many UPR-related genes are down-regulated in the Luman knockdown neurons. To confirm these results I designed primers to amplify the genes that were down-regulated more than twofold, as well as GRP78, CHOP, XBP1, and spliced XPB1. qRT-PCR using these primers confirmed the results of the array (Figure 3.3.3B and C). Among the eight genes that were down-regulated more than twofold, Insig1, Insig2, Srebf1, and Mbtps2 are known to be involved in the regulation of cholesterol. Ubxn4 promotes ER-associated protein degradation and Canx facilitates protein folding and quality control.

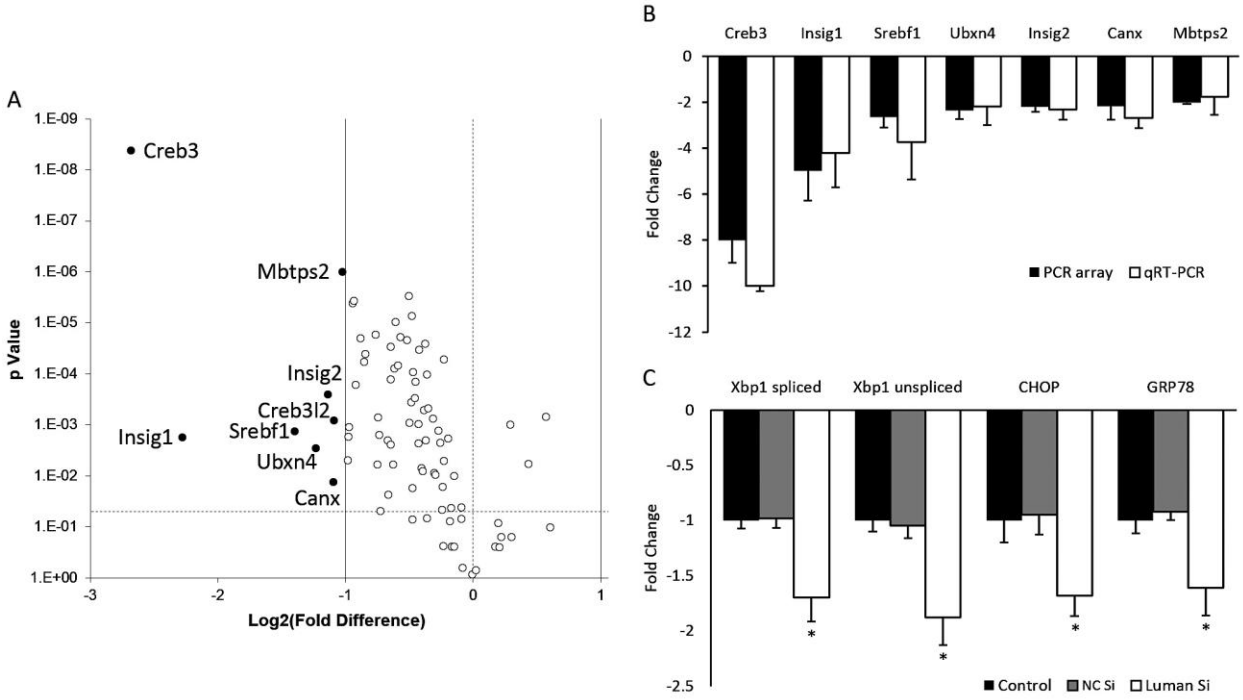

Figure 3.3.3 Knockdown of neuronal Luman decreases the injury-induced UPR

(A) Volcano plots from data derived from qRT-PCR arrays designed to monitor transcripts of genes associated with the UPR. The horizontal axis represents log2 fold differences between 1 d injury-conditioned DRG neurons transfected with scrambled non-targeting siRNA and Luman- specific siRNA. The vertical axis represents P values. The horizontal dashed line represents a P value of 0.05. Transcripts that were down-regulated more than 2-fold (vertical lines) and had a P value <0.05 were considered significant and are indicated by solid spots with gene designations. (B) A comparison of data from the qRT-PCR array with data from qRT-PCR experiments using primers designed in-house. Insig1 - insulin-induced gene 1, Srebf1 - Sterol regulatory element-binding transcription factor 1, Ubxn4 - UBX domain-containing protein 4, Insig2 - insulin-induced gene 2, Canx - Calnexin, Mbtp2 - Membrane-bound transcription factor site-2 protease. (C) Relative changes in mRNA levels of spliced Xbp-1, unspliced Xbp-1, CHOP and GRP78 in injury-conditioned DRG neurons transfected with scrambled siRNA and Luman-specific siRNA. Means ± SEM; N=6; * p<0.01.

3.3.4 Rescue of axon/neurite outgrowth in Luman knockdown neurons by supplemented cholesterol *in vitro*

The qRT-PCR results revealed that 4 genes involved in the regulation of cholesterol were down-regulated after Luman knockdown (Figure 3.3.3). Because cholesterol is an essential

structural component of cell membranes, I speculated that the Luman knockdown neurons were not making enough cholesterol to support the regenerative membrane growth induced by the 1 d sciatic nerve crush injury. Figure 3.3.4A shows that free and total cholesterol levels in injury-conditioned sensory neurons were significantly decreased by 34 ± 7 % and 33 ± 5 %, respectively after Luman knockdown. To investigate whether the decreased cholesterol levels were causally linked to the shortened neurite outgrowth observed in response to Luman siRNA, Luman knockdown neurons from injury-conditioned DRGs were analysed *in vitro* in the presence and absence of cholesterol supplementation. In the absence of supplemented cholesterol, Luman knockdown neurons formed axons/neurites that were 48 ± 6 % shorter. Cholesterol supplementation had only a minor impact on control siRNA transfected neurons, but was significantly effective in the Luman siRNA treated neurons partially rescuing their intrinsic ability to extend axons/neurites such that they were now 74 ± 9 % that of control neurons after 2 DIV (Figure 3.3.4B and C). These data also suggest that 1 d axotomized DRG neurons must produce all the cholesterol required for the extension of axons/neurites, as cholesterol supplementation did not increase total axon/neurite length (Figure 3.3.4 B and C). In Luman knockdown neurons, the lower levels of endogenous cholesterol production are apparently not sufficient to support the increased membrane growth caused by axotomy, which can be partially rescued by cholesterol supplementation.

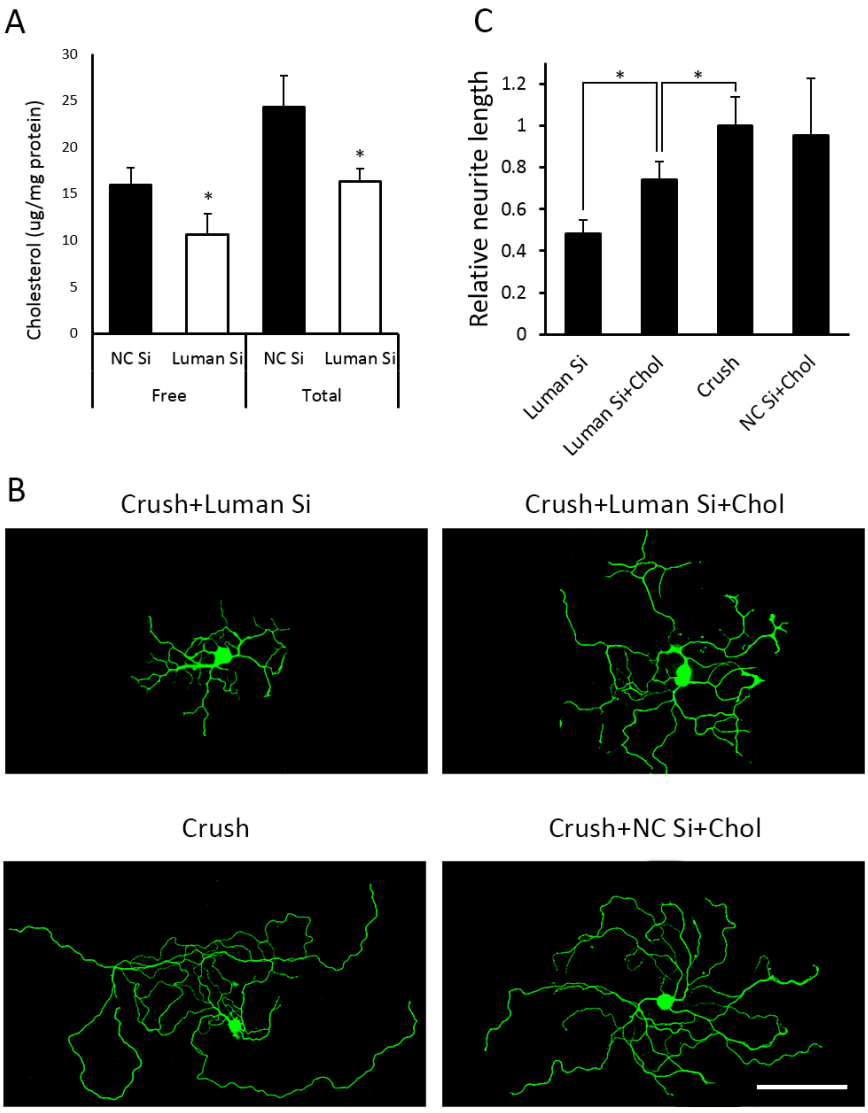

Figure 3.3.4 Cholesterol dependency of neurite outgrowth

(A) Cholesterol levels in cultured DRG neurons transfected with scrambled siRNA and Luman-specific siRNA. Knockdown of Luman decreased the free and total cholesterol levels (N=4). (B) Representative 24 h injury-conditioned DRG neurons (Crush) assayed *in vitro* for 48 h in the presence of medium alone (Crush), transfected with control siRNA and 2 μg/mL cholesterol (Crush + NC Si + Chol), transfected with Luman-specific siRNA (Crush + Luman Si), or transfected with Luman-specific siRNA and 2 μg/mL cholesterol (Crush + Luman Si + Chol) followed by neurite detection with β-III tubulin immunofluorescence. Scale bar, 200 μm. (C) Quantification of total neurite length in B (N=150). Knockdown of Luman decreased the neurite outgrowth. Cholesterol supplementation partially rescued the neurite outgrowth in Luman knockdown neurons, but did not impact the pre-injured neurons. Means ± SEM; * $p<0.01$.

3.3.5 Rescue of axon/neurite outgrowth in Luman knockdown neurons by a UPR inducer

Because cholesterol supplementation does not fully rescue the axon/neurite outgrowth reduction caused by Luman siRNA treatment (Figure 3.3.4), I next investigated whether other UPR-related genes down-regulated by Luman knockdown (Figure 3.3.3) may also contribute to the observed shortened axon/neurite outgrowth in a manner independent of cholesterol. Thus, tunicamycin, a UPR inducer previously shown to not activate Luman (Liang et al., 2006), was employed to increase the UPR level. Luman knockdown decreased Canx, Ubxn4, GRP78, CHOP, XBP1, and spliced XBP1 levels by 1.6 ± 0.25 fold to 4.2 ± 1.5 fold. In an attempt to increase those genes back to their normal injury-associated levels, different concentrations of tunicamycin were tested to determine whether any of them increased levels of the UPR markers in the Luman knockdown neurons, without an impact on the reduced levels of Luman or cholesterol. Figure 3.3.5A shows that when tunicamycin was used at 2 ng/mL, the levels of the aforementioned UPR-associated genes were increased by 1.4 ± 0.5 fold to 3.1 ± 0.4 fold. Notably, this concentration did not have a discernible influence on the levels of Luman or cholesterol (Figure 3.3.5B and C). I then analyzed axon/neurite outgrowth in Luman knockdown neurons from axotomized DRGs *in vitro* in the presence and absence of 2 ng/mL tunicamycin. While tunicamycin treatment had only minor impact on control siRNA transfected neurons, it partially rescued the axon length in Luman knockdown neurons after 2 DIV such that it was now 69 ± 9 % of that observed in control injury-conditioned neurons (Figure 3.3.5D and E).

The Luman knockdown dependent decrease in axon/neurite outgrowth was partially rescued when cholesterol and tunicamycin were used alone. Since tunicamycin treatment did not alter the level of cholesterol (Figure 3.3.5C), cholesterol and tunicamycin may play different roles in the regulation of neurite outgrowth in axotomized DRG neurons. Figure 3.3.5E shows that when cholesterol and tunicamycin were used together, the axons/neurites grew significantly longer than that of when they were used individually, reaching 83 ± 10 % of that of control injury-conditioned only neurons.

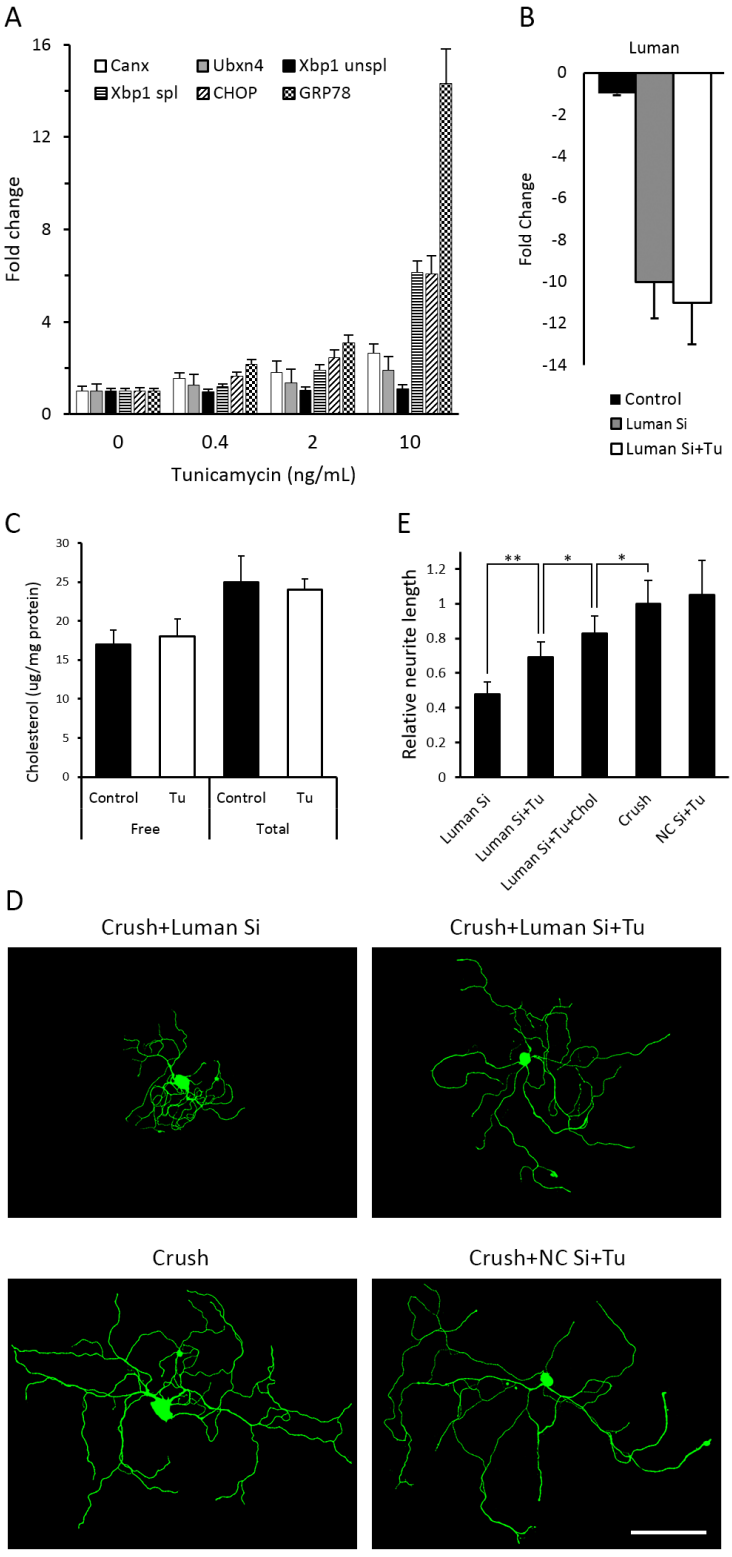

Figure 3.3.5 Tunicamycin rescues axon/neurite outgrowth in Luman knockdown neurons

(A) mRNA levels of Canx, Ubxn4, XBP1, spliced XBP1, CHOP, and GRP78 in DRG neurons cultured in indicated concentration of tunicamycin. (B) mRNA levels of Luman in DRG neurons cultured in experimental conditions as indicated. (C) Free and total cholesterol levels in DRG neurons cultured in the absence or presence of 2 ng/mL tunicamycin (N=4). (D) Representative 24 h injury-conditioned DRG neurons (Crush) assayed *in vitro* for 48 h in the presence of medium alone (Crush), or transfected with either control siRNA and 2 ng/mL tunicamycin (Crush + NC Si + Tu), Luman-specific siRNA (Crush + Luman Si), or Luman-specific siRNA and 2 ng/mL tunicamycin (Crush + Luman Si + Tu) followed by axon/neurite detection with β-III tubulin immunofluorescence. Scale bar, 200 μm. (E) Quantification of total axon/neurite length in D, as well as 24 h injury-conditioned DRG neurons cultured in the presence of Luman-specific siRNA, tunicamycin and cholesterol for 48 h (Luman Si + Tu + Chol). (N=150). Note: tunicamycin treatment partially rescued the decrease in neurite outgrowth in Luman knockdown neurons, but did not impact the pre-injured neurons. Means ± SEM; * $p<0.05$, ** $p<0.01$.

4 Discussion

Luman is an ER-localized bZIP transcription factor that has been reported to regulate the UPR, cell migration, dendritic cell maturation, and secretory capacity. In this study, I cloned the rat Luman coding sequence and analyzed its expression and distribution in a variety of rat tissues. I further showed that, in response to peripheral nerve injury, Luman serves as an important axonally-derived retrograde injury signal that serves to regulate axon/neurite outgrowth through its regulation of the UPR pathway and cholesterol biosynthesis.

4.1 Luman is highly expressed in nervous system

Section 3.1 describes the isolation of a full-length coding sequence and the derivation of the predicted amino acid sequence for rat Luman. This rat sequence is comprised of 387 amino acids (Figure 3.1.1), 233 amino acid residues longer than the rat Luman sequence currently reported in the Genbank database (GenBank: BC062241.1). This latter sequence corresponds to only 154 amino acids of the amino-terminus of the protein. The rat Luman isolated in this study, when aligned to derived mouse and human amino acid sequences for Luman displays 85 % and 66 % identity, respectively (Figure 3.1.2). Further, unlike the currently reported sequence, this new sequence has all of the known functional domains conserved, and encodes a protein capable of activating transcription from the UPRE in a manner equivalent to human Luman (Figure 3.3.3A).

Luman is distinguished from other members of the CREB family as being a member of a subfamily of membrane-associated bZIP transcription factors that in mammals includes CREB3 and CREBL1-L4 [reviewed in (Chan et al., 2011)]. Another feature of this CREB subfamily is that these transcription factors are activated by regulated intramembrane proteolysis, which liberates the N-terminal active fragment from the membrane, thereby allowing it to translocate to the nucleus where it has been shown to modulate transcriptional activity. But, the exact nature of the physiological signals that mediate activation of Luman *in vivo* remain elusive.

The broad expression of rat Luman that I found across all tissues examined, is consistent with that reported for human Luman (Lu et al., 1997) and implicates it in potentially diverse or alternatively, common cellular physiological functions. The highest levels of expression occurred in liver and nervous system tissue. In the liver, transcripts were found in the cytoplasm of

hepatocytes. It is well known that hepatocytes are rich in endoplasmic reticulum (ER), which is the site of the synthesis and modification of a large number of secreted proteins. This high level of secretory function makes the liver particularly susceptible to ER stress (Ji et al., 2011), where Luman may play a role as an ER stress transducer (DenBoer et al., 2005; Liang et al., 2006). More recently, expression of Luman has been shown to be amongst a group of intracellular signalling cascade genes that are up-regulated during liver regeneration and are believed to subserve roles in that process (Xu et al., 2009).

Consistent with the up-regulation in Luman in response to liver tissue regeneration, I observe heightened expression following axonal injury in rat primary sensory neurons (Figure 3.2.4C and 3.3.2). In addition, the higher levels of Luman found in all nervous system tissue examined, may be linked to the important secretory function of both neurons and nonneuronal glial cells that creates a higher demand for protein production (Jha et al., 2013). In support of this, the Luman-like transcription factors are capable of activating the secretory pathway by enhancing the expression of secretory pathway genes (Fox et al., 2010), with the *drosophila* equivalent CREB-H and each of the 5 human CREB3 factors also showing linkage to this pathway (Barbosa et al., 2013). Finally at a cellular level, I found that there were high levels of expression in the region of the hippocampus involved in learning and memory consolidation, a highly plastic part of the brain. It is interesting to note that the mRNA expression pattern of one of Luman's target genes HERP (Liang et al., 2006; Truettner et al., 2009), in the hippocampal region that I examined, mirrors that which I observed for Luman. As with Luman, HERP expression is regulated by cellular stress events. More specifically, in the hippocampus, HERP is up-regulated in response to conditions that induce ER stress such as transient ischemia (Truettner et al., 2009) and in neurons it is believed to subserve a neuroprotective role by stabilizing ER Ca^{2+} homeostasis and mitochondrial function (Chan et al., 2004). Whether a similar impact on Luman expression occurs and whether this is causally linked to the observed HERP responses is not known but appears anatomically feasible given the similarities in their expression patterns and their ability to both respond to ER cellular stress events.

The isolation of a full length rat Luman and its robust expression in the rat nervous system provids the tools and rationale for further study of its role in nervous system plasticity involving cellular stress responses.

4.2 Sensing nerve injury at the axonal ER: Luman serves as a retrograde regeneration signal

Retrograde injury signals help the neuron transition to a regenerative state, assisting the neuron in dealing with the increased demand for protein associated with regeneration (Rishal and Fainzilber, 2010; Fainzilber et al., 2011; Jung et al., 2012). Despite proteomics and microarray analyses revealing that there are ~400 signaling networks connecting to 39 transcription factors in the sensory neuron response to axotomy (Michaelevski et al., 2010) and a transcriptome analysis identifying Luman as an intra-axonal transcript (Gumy et al., 2011), there is a paucity of information on the role(s) that axonally localized and synthesized transcription factors subserve beyond neuronal survival as described for CREB and STAT3 (Cox et al., 2008; Ben-Yaakov et al., 2012). My results in section 3.2 provide the first insights into the role of the ER-localized transcription factor Luman as a critical regulator of intrinsic neurite outgrowth in injured sensory neurons. I validated that Luman mRNA localizes to axons (Gumy et al., 2011) and characterized the presence of Luman protein in axons. I revealed that Luman is synthesized in, and removed from, injured axons via retrograde transport back to the cell body in an importin α-dependent, but proteasome-independent manner. Finally, I presented evidence supporting a novel role for this axonally synthesized transcription factor in specific support of the intrinsic elongating form of axonal growth associated with regeneration.

4.2.1 Luman as an axonal ER-associated transducer of injury stress signals

My finding that markers of the ER extend the length of the axon is in agreement with recent findings by others (Stirling et al., 2014) and provides a mechanism whereby injury at any site along this axoplasmic ER may impact ER-associated events. While this could include signals derived proximal to the injury site such as the local activation and synthesis of Luman as described in this study, I cannot exclude that additional signals propagated along the length of the axonal ER may also impact this response (Stirling et al., 2014).

Luman is an ~60 kDa bZIP transcription factor containing an ER-transmembrane domain first that was identified for its potential role in herpes simplex virus reactivation (Lu et al., 1997; Raggo et al., 2002). It is expressed by sensory neurons and retained in the ER (Lu and Misra, 2000), where processing by regulated intramembrane proteolysis releases an ~40 kDa amino

terminal fragment (Raggo et al., 2002) containing all identified functional domains, including its NLS (Lu et al., 1997; Lu et al., 1998). This provides a mechanism whereby neurons can respond to environmental stressors by rapidly activating premade transcription factors.

Nerve injury activates axonally-localized transcription factors and initiates translation of components of their retrograde transport machinery which effects efficient transport back to the nucleus via dynein motors [reviewed in (Jung et al., 2012)]. This machinery includes the protein importin α found throughout neuronal axons, while the mRNA of another core component, importin β, is localized to axons and only translated in response to nerve lesion (Hanz et al., 2003). Once synthesized, axonal importin β associates with importin α creating a high-affinity nuclear localization signal (NLS) binding complex that includes target cargo proteins and that traffics retrogradely via the motor protein dynein (Hanz et al., 2003). The repertoire of validated axonally synthesized transcription factors shown to traffic in this manner is limited to that of STAT3, which mediates neuronal survival following injury (Ben-Yaakov et al., 2012). However, the presence of Luman mRNA and protein in axons in this study (Figure 3.2.1), its injury-induced local synthesis in axons (Figure 3.2.2) and association with importin α in injury-conditioned but not in the naïve state (Figure 3.2.5) identifies Luman as the second transcription factor that can be locally synthesized so that axon autonomous injury/regeneration signals may be generated and appropriately relayed back to the nucleus.

In the naïve state, axonal premade Luman colocalizes with the ER protein calnexin consistent with its aforementioned association with the ER and the presence of an ER functional equivalent in axons (Merianda et al., 2009). How Luman mRNA is transported into the axon is unknown. But it is likely by an interaction of its 3'UTR with a RNA binding protein such as ZBP1, which has been shown to be a necessary and rate limiting step in peripheral nerve regeneration through its ability to target and translationally repress cargo mRNAs such as β-actin until needed (Donnelly et al., 2011).

The rapid appearance of a lower molecular weight form of Luman in the axons at 6 h (the earliest time point examined post sciatic nerve injury) is suggestive of activation by regulated intramembrane proteolysis. This response in the nerve is transient, consistent with a role as a rapid inductive axonal signal. This type of signal transduction requires that the axon-derived molecules must be distinguished from similar molecules located in the cell body. The low basal

level of cleaved Luman in the cell bodies of uninjured DRGs (Figure 3.2.3C) may allow axon-derived Luman to substantially impact Luman-dependent transcriptional activities. Its disappearance from the nerve coincided with an increased appearance in the nuclei of the injured neurons of the corresponding DRG (Figure 3.2.3) along with importin β whose axonal expression was also increased following axotomy (Figure 3.2.4). Further, the observed disappearance of Luman from the injured axons is likely via retrograde transport back to the neuronal cell body and not because of degradation, as inhibitors of degradation had no effect on its disappearance, while disruption of retrograde transport with colchicine effectively prevented it. Notably, these treatments had no discernible effect on the levels of Luman within the axons of short term cultures derived from naïve sensory neurons, consistent with the idea that its disappearance from axotomized axons requires processes or components not activated or synthesized in the naïve state (Figure 3.2.5). Further, even though the naïve neurons are axotomized in the process of being dissected, the rapid dissociation process resulting in complete removal of axons, and likely does not afford sufficient time for the generation and retrograde transport of axonal Luman as an injury signal.

Injury-associated Luman is likely transported as a cargo protein in the importin complex via a NLS/importin α interaction, as this could be specifically competed away with an excess of NLS peptide (Figure 3.2.5 and 3.2.7). The transient nature of Luman up-regulation in injured nerves, its disappearance from the axonal compartment and its subsequent appearance in the neuronal nuclei (Figure 3.2.76 and 3.2.8) were consistent with it being an inductive signal in the cell body response to the injury.

4.2.2 Axonal Luman contributes to axonal growth following injury

The rapid axonal synthesis and subsequent increased nuclear localization of Luman in injured adult sensory neurons suggests that it subserves a transcriptional role associated with the cell body response to axonal injury. Target genes of this transcriptional regulation are currently unknown. However, this form of retrograde signaling does have functional implications with respect to promotion of axonal outgrowth in the injured-conditioned sensory neuron (Figures 3.2.10 and 3.2.12). Previous work has identified retrograde signalling linked to axonal protein synthesis as being vital for optimal axon regeneration in the periphery (Gumy et al., 2010; Liu et al., 2011). Indeed some speculate that the high capacity of peripheral axons to synthesize

proteins in a cell-compartment autonomous way relative to central nervous system axons (Verma et al., 2005; Taylor et al., 2009; Vogelaar et al., 2009) may contribute to their differential propensities for axonal regeneration.

I discerned distinct modes of axon growth for neurons associated with the naïve versus injury-conditioned states (Figure 3.2.10) in agreement with previous studies (Smith and Skene, 1997). Localized translation of the axon-targeted β-actin and GAP43 mRNAs is critical for these distinct modes with roles in axon branching and elongating growth respectively, in sensory neurons (Donnelly et al., 2013). Luman siRNA results revealed a novel mode-specific role for axonal Luman in injury-conditioned neurons in regulation of only the elongating form of axon growth and not branching (Figure 3.2.10). Consistent with the lack of impact on axonal branching Luman knockdown did not alter axonal growth patterns observed for neurons that were naïve prior to assay (Figure 3.2.10).

In conclusion, intra-axonal mRNA translation and retrograde transport of the transcription factor Luman has been shown to mediate an important form of communication between distal axons and the cell bodies in the regulation of axon regrowth in the PNS. Elucidating key transcriptional regulators of intrinsic regenerative axonal growth provides novel targets for enhancing nerve repair.

4.3 Activation of the UPR is required for injury-induced neurite outgrowth

Unlike the CNS, which has limited regeneration ability after injury, the PNS axon regeneration allows functional recovery after peripheral nerve injury (Huebner and Strittmatter, 2009). Although the PNS axons are capable of regeneration and form functional innervations, several factors, including the injury type, delay before re-innervation, and patient's age determine the degree of functional outcome after repair (Scheib and Hoke, 2013), and the overall functional recovery is still disappointing (Johnson et al., 2005). Studying the molecular events behind the PNS regeneration will not only help us to find better treatment options for patients with PNS injury, but also to understand the differences between PNS and CNS regeneration. Complex cellular responses, including calcium influx (Ghosh-Roy et al., 2010), histone acetylation (Finelli et al., 2013), axonal protein synthesis (Ben-Yaakov et al., 2012), and

retrograde (Ben-Yaakov et al., 2012) and anterograde (Misgeld et al., 2007) axonal transport, happen after nerve injury (Mar et al., 2014). In section 3.3, I revealed that the UPR is activated in DRGs after sciatic nerve crush injury, and that this activation is required for injury-induced neurite outgrowth.

The UPR is linked to many neurodegenerative disorders. Activation of the UPR has been observed in Alzheimer's disease (Hoozemans et al., 2005), Parkinson's disease (Hoozemans et al., 2007), and multiple sclerosis (Mhaille et al., 2008). The deletion of CHOP and activation of XBP1 protect retinal ganglion cells from axon injury-induced cell death (Hu et al., 2012), and also promotes Schwann cell survival after injury (Mantuano et al., 2011). The UPR markers that I examined in this study were all increased after nerve injury (Figure 3.3.1), indicating that UPR is activated in axotomized DRG neurons.

Luman has similar structure to the UPR-associated transcription factor ATF6 and similar DNA-binding specificities to another UPR-associated transcription factor, XBP1, and Luman has been previously shown to protect cells against ER stress-induced apoptosis when overexpressed (Liang et al., 2006). This suggests that the elevated levels of activated Luman that I observed in axotomized sensory neurons may be involved in regulation of the UPR. Consistent with a role for Luman in regulation of the UPR in axotomized sensory neurons, I found that the knockdown of Luman decreased the level of the UPR induced in the injury-conditioned neurons (Figure 3.3.3) as well as the observed axon/neurite outgrowth, but had no effect on the axon/neurite outgrowth of naïve neurons in culture (Figure 3.2.10 and 3.2.12), indicating that an increased UPR is a requirement for only enhanced, injury-induced axon regeneration.

To see whether other forms of UPR regulation are implicated in axon/neurite outgrowth, I first manipulated the neuronal expression of Luman with Luman siRNA such that it effected down-regulation of the UPR and then suppressed the effects with the UPR-inducer tunicamycin until the UPR recovered in the Luman knockdown axotomized neurons to a level equivalent to that observed in the control axotomized neurons without any impact on the reduced levels of Luman and cholesterol effected by Luman down-regulation. Although 2 μg/mL tunicamycin treatment can increase the transcription of Luman (Liang et al., 2006), I found that the expression of Luman was not affected by 2 ng/mL tunicamycin (Figure 3.3.5B). This low concentration of tunicamycin was enough to bring the Luman knockdown-induced down-regulation of UPR back

to the levels observed in axotomized control neurons, and also partially rescued the axon/neurite outgrowth in Luman knockdown neurons (Figure 3.3.5), indicating that a certain level of ER stress is beneficial for neurite outgrowth. While this low level of tunicamycin treatment did not impact the Luman siRNA down-regulation of expression of Luman at the mRNA level, one cannot exclude that there may have been an impact of activation of the low levels of Luman protein remaining under these conditions.

Similar to that observed with cholesterol supplementation, when the UPR was elevated above levels normally observed in control axotomized DRG neurons (Figure 3.3.5), it did not alter axon/neurite outgrowth, suggesting that the axotomized neurons are capable of coping with this extra UPR stress and that additional factors involved in the maximal outgrowth attainable were unlikely regulated with the tunicamycin treatment.

The regulation of cholesterol and the UPR have been shown to be linked (Colgan et al., 2011), with the UPR being involved in the activation of SREBPs (Kammoun et al., 2009), transcription factors that regulate sterol biosynthesis. The activation of SREBPs, ATF6, and Luman all requires proteolysis by S1P and S2P (encoded by MBTPS1 and MBTPS2) (Ye et al., 2000; Raggo et al., 2002). Luman knockdown significantly decreased the expression of genes coding for SREBP1 and S2P (Figure 3.3.3) and caused a reduction in cellular cholesterol levels (Figure 3.3.4). Cholesterol is an essential component in membrane structure and signal transduction. In the CNS, defective cholesterol biosynthesis in mature neurons can be completely compensated by cholesterol transfer from astrocytes *in vivo* (Funfschilling et al., 2012). It appears that a similar situation may exist for sensory neurons whereby supplemental cholesterol was able to partially compensate for the reduced cholesterol in axotomized Luman knockdown neurons by increasing the intrinsic ability of these neurons to extend axons/neurites *in vitro* (Figure 3.2.4). However, cholesterol supplementation did not further increase the growth in control siRNA transfected neurons, indicating that normally axotomized DRG neurons are able to endogenously synthesize enough cholesterol to support neurite outgrowth when the UPR is not being compromised by down-regulation of Luman. The observation that cholesterol and tunicamycin treatment only partially rescued neurite outgrowth in Luman knockdown neurons suggests the existence of other mechanisms by which Luman regulates neurite outgrowth in injury conditioned neurons.

Overall, these findings demonstrate for the first time that UPR signaling pathways are activated in axotomized DRG neurons, and that induction of the UPR is linked to injury-induced axon/neurite outgrowth. The exact function of each UPR pathway in nerve regeneration, and whether the up-regulation of UPR promotes the PNS regeneration *in vivo* still need to be investigated.

4.4 A role for the axonal ER in axon injury

Neurons are polarized cells with axons and dendrites extending far from the soma. Considering the extensive lengths of peripheral axons (the sciatic representing the longest), it is not surprising that axons have evolved effective axon-based mechanisms to communicate with the soma, and that certain cellular functions are regulated locally. The continuous network of the ER that runs longitudinally along the axons (Tsukita and Ishikawa, 1976) suggests that the ER plays important roles in regulating axonal homeostasis.

The ER is a highly conserved organelle in eukaryotic cells. It is responsible for the synthesis and folding of membrane and secretory proteins, lipid metabolism, and calcium signaling. Studies have also shown that the ER regulates glucose metabolism (Broadwell and Cataldo, 1984) and protein synthesis and trafficking [reviewed in (Gonzalez and Couve, 2014)] in axons. In sections 3.2 and 3.3, I revealed that the axonal ER functions as an injury signal transducer through the ER-associated transcription factor Luman. Indeed, other ER-associated proteins, especially the ones regulating the UPR, are involved in axon injury (Hu et al., 2012) and neurodegenerative disorders [reviewed in (Doyle et al., 2011)].

In section 3.3, I showed that sciatic nerve injury activated the UPR in the DRGs, which helped the injured axons to regenerate. Similarly, studies have shown that optic nerve injury activates the UPR in the retinal ganglion cells. But instead of promoting regeneration, the activated UPR results in neuronal death (Hu et al., 2012). The conflicting outcomes could be caused by different responses to injury between the PNS and the CNS, or by the different effects of the UPR pathways within these two neuronal subtypes. Although the UPR can be activated by axon injury, how the ER senses injury stress remains unclear. The UPR is triggered by the accumulation of unfolded proteins which is likely to happen during the regeneration stage when protein synthesis is increased. The UPR can also be activated by the treatment of thapsigargin, a chemical ER stress inducer which raises the cytosolic Ca^{2+} concentration. In fact, the Ca^{2+} influx

into the axoplasm is an early event after axon injury, which is required for sealing the axonal ends (Yawo and Kuno, 1985), for local protein synthesis and formation of growth cone [reviewed in (Mar et al., 2014)]. The increased axonal and somal Ca^{2+} concentration may perturb the Ca^{2+} homeostasis, therefore inducing the UPR.

Although increased protein synthesis and Ca^{2+} concentration occur at both the soma and axon levels after axon injury, it is still not known whether the UPR is activated in the injured axons as well as in the cell somas. The observations that axonal application of brain-derived neurotrophic factor caused XBP1 splicing to happen in the axons (Hayashi et al., 2007), and that lysophosphatidic acid treatment increased axonal eIF2 phosphorylation (Vuppalanchi et al., 2012) suggest that the UPR can be activated in the axons. But, further studies need to be done to determine if axon injury actually induces the UPR within the axon locally.

4.5 Conclusions

Research performed in this thesis has greatly extended our understanding of the role of Luman and ER stress in the regenerative capacity of adult sensory neurons. Further, it has also contributed a number of research tools and insights by which to further dissect these signalling pathways in the future. This study isolated the coding sequence of rat Luman and revealed rat Luman transcripts in a variety of rat tissues with the highest levels in nervous system tissue. Adult sensory axons contain Luman mRNA which is locally translated and then transported to the cell body via the importin-mediated retrograde transport system in response to nerve injury. Knockdown of Luman impairs the intrinsic ability of injury-conditioned sensory neurons to extend the regeneration-associated elongating form of neurites. Finally, the UPR is a major mechanism by which Luman regulates injury-induced neurite outgrowth and cholesterol biosynthesis may be a major UPR-dependent process that connects axon injury with enhanced growth potential in DRG neurons.

5 References

Abe N, Cavalli V (2008) Nerve injury signaling. Current opinion in neurobiology 18:276-283.

Adachi Y, Yamamoto K, Okada T, Yoshida H, Harada A, Mori K (2008) ATF6 is a transcription factor specializing in the regulation of quality control proteins in the endoplasmic reticulum. Cell structure and function 33:75-89.

Allodi I, Udina E, Navarro X (2012) Specificity of peripheral nerve regeneration: interactions at the axon level. Prog Neurobiol 98:16-37.

Asada R, Kanemoto S, Kondo S, Saito A, Imaizumi K (2011) The signalling from endoplasmic reticulum-resident bZIP transcription factors involved in diverse cellular physiology. Journal of biochemistry 149:507-518.

Audas TE, Li Y, Liang G, Lu R (2008) A novel protein, Luman/CREB3 recruitment factor, inhibits Luman activation of the unfolded protein response. Mol Cell Biol 28:3952-3966.

Barbosa S, Fasanella G, Carreira S, Llarena M, Fox R, Barreca C, Andrew D, O'Hare P (2013) An orchestrated program regulating secretory pathway genes and cargos by the transmembrane transcription factor CREB-H. Traffic 14:382-398.

Bareyre FM, Garzorz N, Lang C, Misgeld T, Buning H, Kerschensteiner M (2011) In vivo imaging reveals a phase-specific role of STAT3 during central and peripheral nervous system axon regeneration. Proc Natl Acad Sci U S A 108:6282-6287.

Ben-Yaakov K, Dagan SY, Segal-Ruder Y, Shalem O, Vuppalanchi D, Willis DE, Yudin D, Rishal I, Rother F, Bader M, Blesch A, Pilpel Y, Twiss JL, Fainzilber M (2012) Axonal transcription factors signal retrogradely in lesioned peripheral nerve. The EMBO journal 31:1350-1363.

Bertolotti A, Zhang Y, Hendershot LM, Harding HP, Ron D (2000) Dynamic interaction of BiP and ER stress transducers in the unfolded-protein response. Nat Cell Biol 2:326-332.

Bisby MA, Chen S (1990) Delayed wallerian degeneration in sciatic nerves of C57BL/Ola mice is associated with impaired regeneration of sensory axons. Brain Res 530:117-120.

Bobrovnikova-Marjon E, Hatzivassiliou G, Grigoriadou C, Romero M, Cavener DR, Thompson CB, Diehl JA (2008) PERK-dependent regulation of lipogenesis during mouse mammary gland development and adipocyte differentiation. Proc Natl Acad Sci U S A 105:16314-16319.

Bommiasamy H, Back SH, Fagone P, Lee K, Meshinchi S, Vink E, Sriburi R, Frank M, Jackowski S, Kaufman RJ, Brewer JW (2009) ATF6alpha induces XBP1-independent expansion of the endoplasmic reticulum. J Cell Sci 122:1626-1636.

Bomze HM, Bulsara KR, Iskandar BJ, Caroni P, Skene JH (2001) Spinal axon regeneration evoked by replacing two growth cone proteins in adult neurons. Nat Neurosci 4:38-43.

Boyd JG, Gordon T (2003) Neurotrophic factors and their receptors in axonal regeneration and functional recovery after peripheral nerve injury. Mol Neurobiol 27:277-324.

Bradbury EJ, Moon LD, Popat RJ, King VR, Bennett GS, Patel PN, Fawcett JW, McMahon SB (2002) Chondroitinase ABC promotes functional recovery after spinal cord injury. Nature 416:636-640.

Broadwell RD, Cataldo AM (1984) The neuronal endoplasmic reticulum: its cytochemistry and contribution to the endomembrane system. II. Axons and terminals. J Comp Neurol 230:231-248.

Bunge MB (1973) Fine structure of nerve fibers and growth cones of isolated sympathetic neurons in culture. J Cell Biol 56:713-735.

Burbelo PD, Kozak CA (1998) Mapping of the murine LZIP gene (Creb3) to chromosome 4. Genomics 54:357-358.

Burnett MG, Zager EL (2004) Pathophysiology of peripheral nerve injury: a brief review. Neurosurgical focus 16:E1.

Buss A, Brook GA, Kakulas B, Martin D, Franzen R, Schoenen J, Noth J, Schmitt AB (2004) Gradual loss of myelin and formation of an astrocytic scar during Wallerian degeneration in the human spinal cord. Brain 127:34-44.

Calfon M, Zeng H, Urano F, Till JH, Hubbard SR, Harding HP, Clark SG, Ron D (2002) IRE1 couples endoplasmic reticulum load to secretory capacity by processing the XBP-1 mRNA. Nature 415:92-96.

Campbell DS, Holt CE (2001) Chemotropic responses of retinal growth cones mediated by rapid local protein synthesis and degradation. Neuron 32:1013-1026.

Cavalli V, Kujala P, Klumperman J, Goldstein LS (2005) Sunday Driver links axonal transport to damage signaling. J Cell Biol 168:775-787.

Chan CP, Kok KH, Jin DY (2011) CREB3 subfamily transcription factors are not created equal: Recent insights from global analyses and animal models. Cell & bioscience 1:6.

Chan SL, Fu W, Zhang P, Cheng A, Lee J, Kokame K, Mattson MP (2004) Herp stabilizes neuronal Ca2+ homeostasis and mitochondrial function during endoplasmic reticulum stress. J Biol Chem 279:28733-28743.

Christie KJ, Webber CA, Martinez JA, Singh B, Zochodne DW (2010) PTEN inhibition to facilitate intrinsic regenerative outgrowth of adult peripheral axons. J Neurosci 30:9306-9315.

Christie KJ, Krishnan A, Martinez JA, Purdy K, Singh B, Eaton S, Zochodne D (2014) Enhancing adult nerve regeneration through the knockdown of retinoblastoma protein. Nature communications 5:3670.

Colgan SM, Hashimi AA, Austin RC (2011) Endoplasmic reticulum stress and lipid dysregulation. Expert reviews in molecular medicine 13:e4.

Connor JH, Weiser DC, Li S, Hallenbeck JM, Shenolikar S (2001) Growth arrest and DNA damage-inducible protein GADD34 assembles a novel signaling complex containing protein phosphatase 1 and inhibitor 1. Mol Cell Biol 21:6841-6850.

Costanzo RM (1991) Regeneration of olfactory receptor cells. Ciba Foundation symposium 160:233-242; discussion 243-238.

Cox JS, Walter P (1996) A novel mechanism for regulating activity of a transcription factor that controls the unfolded protein response. Cell 87:391-404.

Cox JS, Shamu CE, Walter P (1993) Transcriptional induction of genes encoding endoplasmic reticulum resident proteins requires a transmembrane protein kinase. Cell 73:1197-1206.

Cox JS, Chapman RE, Walter P (1997) The unfolded protein response coordinates the production of endoplasmic reticulum protein and endoplasmic reticulum membrane. Mol Biol Cell 8:1805-1814.

Cox LJ, Hengst U, Gurskaya NG, Lukyanov KA, Jaffrey SR (2008) Intra-axonal translation and retrograde trafficking of CREB promotes neuronal survival. Nat Cell Biol 10:149-159.

Cregg JM, DePaul MA, Filous AR, Lang BT, Tran A, Silver J (2014) Functional regeneration beyond the glial scar. Exp Neurol 253:197-207.

Cruickshank W (1795) Experiments on the nerves, particularly on their reproduction and on the spinal marrow of living animals. Philosophical Transactions of the Royal Society of London 85:177-189.

David S, Braun PE, Jackson DL, Kottis V, McKerracher L (1995) Laminin overrides the inhibitory effects of peripheral nervous system and central nervous system myelin-derived inhibitors of neurite growth. J Neurosci Res 42:594-602.

Deglincerti A, Jaffrey SR (2012) Insights into the roles of local translation from the axonal transcriptome. Open biology 2:120079.

DenBoer LM, Hardy-Smith PW, Hogan MR, Cockram GP, Audas TE, Lu R (2005) Luman is capable of binding and activating transcription from the unfolded protein response element. Biochem Biophys Res Commun 331:113-119.

DenBoer LM, Iyer A, McCluggage AR, Li Y, Martyn AC, Lu R (2013) JAB1/CSN5 inhibits the activity of Luman/CREB3 by promoting its degradation. Biochim Biophys Acta 1829:921-929.

Donnelly CJ, Park M, Spillane M, Yoo S, Pacheco A, Gomes C, Vuppalanchi D, McDonald M, Kim HK, Merianda TT, Gallo G, Twiss JL (2013) Axonally synthesized beta-actin and GAP-43 proteins support distinct modes of axonal growth. J Neurosci 33:3311-3322.

Donnelly CJ, Willis DE, Xu M, Tep C, Jiang C, Yoo S, Schanen NC, Kirn-Safran CB, van Minnen J, English A, Yoon SO, Bassell GJ, Twiss JL (2011) Limited availability of ZBP1 restricts axonal mRNA localization and nerve regeneration capacity. The EMBO journal 30:4665-4677.

Doster SK, Lozano AM, Aguayo AJ, Willard MB (1991) Expression of the growth-associated protein GAP-43 in adult rat retinal ganglion cells following axon injury. Neuron 6:635-647.

Doyle KM, Kennedy D, Gorman AM, Gupta S, Healy SJ, Samali A (2011) Unfolded proteins and endoplasmic reticulum stress in neurodegenerative disorders. Journal of cellular and molecular medicine 15:2025-2039.

Drerup CM, Nechiporuk AV (2013) JNK-interacting protein 3 mediates the retrograde transport of activated c-Jun N-terminal kinase and lysosomes. PLoS Genet 9:e1003303.

Dubacq C, Jamet S, Trembleau A (2009) Evidence for developmentally regulated local translation of odorant receptor mRNAs in the axons of olfactory sensory neurons. J Neurosci 29:10184-10190.

Eleveld-Trancikova D, Sanecka A, van Hout-Kuijer MA, Looman MW, Hendriks IA, Jansen BJ, Adema GJ (2010) DC-STAMP interacts with ER-resident transcription factor LUMAN which becomes activated during DC maturation. Mol Immunol 47:1963-1973.

Eng H, Lund K, Campenot RB (1999) Synthesis of beta-tubulin, actin, and other proteins in axons of sympathetic neurons in compartmented cultures. J Neurosci 19:1-9.

Espenshade PJ, Li WP, Yabe D (2002) Sterols block binding of COPII proteins to SCAP, thereby controlling SCAP sorting in ER. Proc Natl Acad Sci U S A 99:11694-11699.

Fainzilber M, Budnik V, Segal RA, Kreutz MR (2011) From synapse to nucleus and back again--communication over distance within neurons. J Neurosci 31:16045-16048.

Fawcett TW, Martindale JL, Guyton KZ, Hai T, Holbrook NJ (1999) Complexes containing activating transcription factor (ATF)/cAMP-responsive-element-binding protein (CREB) interact with the CCAAT/enhancer-binding protein (C/EBP)-ATF composite site to regulate Gadd153 expression during the stress response. Biochem J 339 (Pt 1):135-141.

Feng B, Yao PM, Li Y, Devlin CM, Zhang D, Harding HP, Sweeney M, Rong JX, Kuriakose G, Fisher EA, Marks AR, Ron D, Tabas I (2003) The endoplasmic reticulum is the site of cholesterol-induced cytotoxicity in macrophages. Nat Cell Biol 5:781-792.

Fernandes KJ, Fan DP, Tsui BJ, Cassar SL, Tetzlaff W (1999) Influence of the axotomy to cell body distance in rat rubrospinal and spinal motoneurons: differential regulation of GAP-43, tubulins, and neurofilament-M. J Comp Neurol 414:495-510.

Filbin MT (2003) Myelin-associated inhibitors of axonal regeneration in the adult mammalian CNS. Nature reviews Neuroscience 4:703-713.

Finelli MJ, Wong JK, Zou H (2013) Epigenetic regulation of sensory axon regeneration after spinal cord injury. J Neurosci 33:19664-19676.

Flores AJ, Lavernia CJ, Owens PW (2000) Anatomy and physiology of peripheral nerve injury and repair. Am J Orthop (Belle Mead NJ) 29:167-173.

Foretz M, Guichard C, Ferre P, Foufelle F (1999) Sterol regulatory element binding protein-1c is a major mediator of insulin action on the hepatic expression of glucokinase and lipogenesis-related genes. Proc Natl Acad Sci U S A 96:12737-12742.

Fox RM, Hanlon CD, Andrew DJ (2010) The CrebA/Creb3-like transcription factors are major and direct regulators of secretory capacity. J Cell Biol 191:479-492.

Freiman RN, Herr W (1997) Viral mimicry: common mode of association with HCF by VP16 and the cellular protein LZIP. Genes Dev 11:3122-3127.

Funfschilling U, Jockusch WJ, Sivakumar N, Mobius W, Corthals K, Li S, Quintes S, Kim Y, Schaap IA, Rhee JS, Nave KA, Saher G (2012) Critical time window of neuronal cholesterol synthesis during neurite outgrowth. J Neurosci 32:7632-7645.

Gardner BM, Walter P (2011) Unfolded proteins are Ire1-activating ligands that directly induce the unfolded protein response. Science 333:1891-1894.

Ghosh-Roy A, Wu Z, Goncharov A, Jin Y, Chisholm AD (2010) Calcium and cyclic AMP promote axonal regeneration in Caenorhabditis elegans and require DLK-1 kinase. J Neurosci 30:3175-3183.

Gill SR, Schroer TA, Szilak I, Steuer ER, Sheetz MP, Cleveland DW (1991) Dynactin, a conserved, ubiquitously expressed component of an activator of vesicle motility mediated by cytoplasmic dynein. J Cell Biol 115:1639-1650.

Giuditta A, Hunt T, Santella L (1986) Rapid important paper Messenger RNA in squid axoplasm. Neurochemistry international 8:435-442.

Goldfarb DS, Corbett AH, Mason DA, Harreman MT, Adam SA (2004) Importin alpha: a multipurpose nuclear-transport receptor. Trends Cell Biol 14:505-514.

Gonzalez C, Couve A (2014) The axonal endoplasmic reticulum and protein trafficking: Cellular bootlegging south of the soma. Seminars in cell & developmental biology 27C:23-31.

GrandPre T, Nakamura F, Vartanian T, Strittmatter SM (2000) Identification of the Nogo inhibitor of axon regeneration as a Reticulon protein. Nature 403:439-444.

Gumy LF, Tan CL, Fawcett JW (2010) The role of local protein synthesis and degradation in axon regeneration. Experimental Neurology 223:28-37.

Gumy LF, Yeo GS, Tung YC, Zivraj KH, Willis D, Coppola G, Lam BY, Twiss JL, Holt CE, Fawcett JW (2011) Transcriptome analysis of embryonic and adult sensory axons reveals changes in mRNA repertoire localization. RNA 17:85-98.

Gunstream JD, Castro GA, Walters ET (1995) Retrograde transport of plasticity signals in Aplysia sensory neurons following axonal injury. J Neurosci 15:439-448.

Hai TW, Liu F, Coukos WJ, Green MR (1989) Transcription factor ATF cDNA clones: an extensive family of leucine zipper proteins able to selectively form DNA-binding heterodimers. Genes Dev 3:2083-2090.

Han D, Lerner AG, Vande Walle L, Upton JP, Xu W, Hagen A, Backes BJ, Oakes SA, Papa FR (2009) IRE1alpha kinase activation modes control alternate endoribonuclease outputs to determine divergent cell fates. Cell 138:562-575.

Hanz S, Perlson E, Willis D, Zheng JQ, Massarwa R, Huerta JJ, Koltzenburg M, Kohler M, van-Minnen J, Twiss JL, Fainzilber M (2003) Axoplasmic importins enable retrograde injury signaling in lesioned nerve. Neuron 40:1095-1104.

Harding HP, Zhang Y, Ron D (1999) Protein translation and folding are coupled by an endoplasmic-reticulum-resident kinase. Nature 397:271-274.

Harding HP, Zhang Y, Bertolotti A, Zeng H, Ron D (2000) Perk is essential for translational regulation and cell survival during the unfolded protein response. Mol Cell 5:897-904.

Harrington AW, Ginty DD (2013) Long-distance retrograde neurotrophic factor signalling in neurons. Nature reviews Neuroscience 14:177-187.

Harris WA, Holt CE, Bonhoeffer F (1987) Retinal axons with and without their somata, growing to and arborizing in the tectum of Xenopus embryos: a time-lapse video study of single fibres in vivo. Development 101:123-133.

Hasler RM, Exadaktylos AK, Bouamra O, Benneker LM, Clancy M, Sieber R, Zimmermann H, Lecky F (2011) Epidemiology and predictors of spinal injury in adult major trauma patients: European cohort study. European spine journal : official publication of the European Spine Society, the European Spinal Deformity Society, and the European Section of the Cervical Spine Research Society 20:2174-2180.

Hayashi A, Kasahara T, Iwamoto K, Ishiwata M, Kametani M, Kakiuchi C, Furuichi T, Kato T (2007) The role of brain-derived neurotrophic factor (BDNF)-induced XBP1 splicing during brain development. J Biol Chem 282:34525-34534.

Haze K, Yoshida H, Yanagi H, Yura T, Mori K (1999) Mammalian transcription factor ATF6 is synthesized as a transmembrane protein and activated by proteolysis in response to endoplasmic reticulum stress. Mol Biol Cell 10:3787-3799.

Hollien J, Weissman JS (2006) Decay of endoplasmic reticulum-localized mRNAs during the unfolded protein response. Science 313:104-107.

Hong M, Luo S, Baumeister P, Huang JM, Gogia RK, Li M, Lee AS (2004) Underglycosylation of ATF6 as a novel sensing mechanism for activation of the unfolded protein response. J Biol Chem 279:11354-11363.

Honma Y, Kanazawa K, Mori T, Tanno Y, Tojo M, Kiyosawa H, Takeda J, Nikaido T, Tsukamoto T, Yokoya S, Wanaka A (1999) Identification of a novel gene, OASIS, which encodes for a putative CREB/ATF family transcription factor in the long-term cultured astrocytes and gliotic tissue. Brain Res Mol Brain Res 69:93-103.

Hoozemans JJ, van Haastert ES, Eikelenboom P, de Vos RA, Rozemuller JM, Scheper W (2007) Activation of the unfolded protein response in Parkinson's disease. Biochem Biophys Res Commun 354:707-711.

Hoozemans JJ, Veerhuis R, Van Haastert ES, Rozemuller JM, Baas F, Eikelenboom P, Scheper W (2005) The unfolded protein response is activated in Alzheimer's disease. Acta Neuropathol 110:165-172.

Horton JD, Shimomura I, Brown MS, Hammer RE, Goldstein JL, Shimano H (1998) Activation of cholesterol synthesis in preference to fatty acid synthesis in liver and adipose tissue of transgenic mice overproducing sterol regulatory element-binding protein-2. The Journal of clinical investigation 101:2331-2339.

Horton JD, Shah NA, Warrington JA, Anderson NN, Park SW, Brown MS, Goldstein JL (2003) Combined analysis of oligonucleotide microarray data from transgenic and knockout mice identifies direct SREBP target genes. Proc Natl Acad Sci U S A 100:12027-12032.

Hosokawa N, Wada I, Hasegawa K, Yorihuzi T, Tremblay LO, Herscovics A, Nagata K (2001) A novel ER alpha-mannosidase-like protein accelerates ER-associated degradation. EMBO Rep 2:415-422.

Hu Y, Park KK, Yang L, Wei X, Yang Q, Cho KS, Thielen P, Lee AH, Cartoni R, Glimcher LH, Chen DF, He Z (2012) Differential effects of unfolded protein response pathways on axon injury-induced death of retinal ganglion cells. Neuron 73:445-452.

Hua X, Nohturfft A, Goldstein JL, Brown MS (1996a) Sterol resistance in CHO cells traced to point mutation in SREBP cleavage-activating protein. Cell 87:415-426.

Hua X, Sakai J, Brown MS, Goldstein JL (1996b) Regulated cleavage of sterol regulatory element binding proteins requires sequences on both sides of the endoplasmic reticulum membrane. J Biol Chem 271:10379-10384.

Hua X, Wu J, Goldstein JL, Brown MS, Hobbs HH (1995) Structure of the human gene encoding sterol regulatory element binding protein-1 (SREBF1) and localization of SREBF1 and SREBF2 to chromosomes 17p11.2 and 22q13. Genomics 25:667-673.

Hua X, Yokoyama C, Wu J, Briggs MR, Brown MS, Goldstein JL, Wang X (1993) SREBP-2, a second basic-helix-loop-helix-leucine zipper protein that stimulates transcription by binding to a sterol regulatory element. Proc Natl Acad Sci U S A 90:11603-11607.

Huang CC, Li Y, Lopez AB, Chiang CM, Kaufman RJ, Snider MD, Hatzoglou M (2010) Temporal regulation of Cat-1 (cationic amino acid transporter-1) gene transcription during endoplasmic reticulum stress. Biochem J 429:215-224.

Huebner EA, Strittmatter SM (2009) Axon regeneration in the peripheral and central nervous systems. Results and problems in cell differentiation 48:339-351.

Jang SW, Kim YS, Lee YH, Ko J (2007) Role of human LZIP in differential activation of the NF-kappaB pathway that is induced by CCR1-dependent chemokines. Journal of cellular physiology 211:630-637.

Jankowski MP, McIlwrath SL, Jing X, Cornuet PK, Salerno KM, Koerber HR, Albers KM (2009) Sox11 transcription factor modulates peripheral nerve regeneration in adult mice. Brain Res 1256:43-54.

Jeong HJ, Lee HS, Kim KS, Kim YK, Yoon D, Park SW (2008) Sterol-dependent regulation of proprotein convertase subtilisin/kexin type 9 expression by sterol-regulatory element binding protein-2. Journal of lipid research 49:399-409.

Jha MK, Seo M, Kim JH, Kim BG, Cho JY, Suk K (2013) The secretome signature of reactive glial cells and its pathological implications. Biochim Biophys Acta 1834:2418-2428.

Ji C, Kaplowitz N, Lau MY, Kao E, Petrovic LM, Lee AS (2011) Liver-specific loss of glucose-regulated protein 78 perturbs the unfolded protein response and exacerbates a spectrum of liver diseases in mice. Hepatology 54:229-239.

Johnson EO, Zoubos AB, Soucacos PN (2005) Regeneration and repair of peripheral nerves. Injury 36 Suppl 4:S24-29.

Jung H, Yoon BC, Holt CE (2012) Axonal mRNA localization and local protein synthesis in nervous system assembly, maintenance and repair. Nature reviews Neuroscience 13:308-324.

Kammoun HL, Chabanon H, Hainault I, Luquet S, Magnan C, Koike T, Ferre P, Foufelle F (2009) GRP78 expression inhibits insulin and ER stress-induced SREBP-1c activation and reduces hepatic steatosis in mice. The Journal of clinical investigation 119:1201-1215.

Kar AN, MacGibeny MA, Gervasi NM, Gioio AE, Kaplan BB (2013) Intra-axonal synthesis of eukaryotic translation initiation factors regulates local protein synthesis and axon growth in rat sympathetic neurons. J Neurosci 33:7165-7174.

Karpova A, Mikhaylova M, Bera S, Bar J, Reddy PP, Behnisch T, Rankovic V, Spilker C, Bethge P, Sahin J, Kaushik R, Zuschratter W, Kahne T, Naumann M, Gundelfinger ED, Kreutz MR (2013) Encoding and transducing the synaptic or extrasynaptic origin of NMDA receptor signals to the nucleus. Cell 152:1119-1133.

Kim HC, Choi KC, Choi HK, Kang HB, Kim MJ, Lee YH, Lee OH, Lee J, Kim YJ, Jun W, Jeong JW, Yoon HG (2010) HDAC3 selectively represses CREB3-mediated transcription and migration of metastatic breast cancer cells. Cell Mol Life Sci 67:3499-3510.

Kim JE, Bonilla IE, Qiu D, Strittmatter SM (2003a) Nogo-C is sufficient to delay nerve regeneration. Mol Cell Neurosci 23:451-459.

Kim JE, Li S, GrandPre T, Qiu D, Strittmatter SM (2003b) Axon regeneration in young adult mice lacking Nogo-A/B. Neuron 38:187-199.

Kim TY, Kim E, Yoon SK, Yoon JB (2008) Herp enhances ER-associated protein degradation by recruiting ubiquilins. Biochem Biophys Res Commun 369:741-746.

Klinedinst S, Wang X, Xiong X, Haenfler JM, Collins CA (2013) Independent pathways downstream of the Wnd/DLK MAPKKK regulate synaptic structure, axonal transport, and injury signaling. J Neurosci 33:12764-12778.

Ko J, Jang SW, Kim YS, Kim IS, Sung HJ, Kim HH, Park JY, Lee YH, Kim J, Na DS (2004) Human LZIP binds to CCR1 and differentially affects the chemotactic activities of CCR1-dependent chemokines. FASEB J 18:890-892.

Lai CW, Otero JH, Hendershot LM, Snapp E (2012) ERdj4 protein is a soluble endoplasmic reticulum (ER) DnaJ family protein that interacts with ER-associated degradation machinery. J Biol Chem 287:7969-7978.

Lai KO, Zhao Y, Ch'ng TH, Martin KC (2008) Importin-mediated retrograde transport of CREB2 from distal processes to the nucleus in neurons. Proc Natl Acad Sci U S A 105:17175-17180.

Laplante M, Sabatini DM (2009) mTOR signaling at a glance. J Cell Sci 122:3589-3594.

Lasek RJ, Dabrowski C, Nordlander R (1973) Analysis of axoplasmic RNA from invertebrate giant axons. Nature: New biology 244:162-165.

Lee AH, Iwakoshi NN, Glimcher LH (2003) XBP-1 regulates a subset of endoplasmic reticulum resident chaperone genes in the unfolded protein response. Mol Cell Biol 23:7448-7459.

Lee JK, Geoffroy CG, Chan AF, Tolentino KE, Crawford MJ, Leal MA, Kang B, Zheng B (2010) Assessing spinal axon regeneration and sprouting in Nogo-, MAG-, and OMgp-deficient mice. Neuron 66:663-670.

Lee JN, Ye J (2004) Proteolytic activation of sterol regulatory element-binding protein induced by cellular stress through depletion of Insig-1. J Biol Chem 279:45257-45265.

Lee N, Neitzel KL, Devlin BK, MacLennan AJ (2004) STAT3 phosphorylation in injured axons before sensory and motor neuron nuclei: potential role for STAT3 as a retrograde signaling transcription factor. J Comp Neurol 474:535-545.

Li H, Korennykh AV, Behrman SL, Walter P (2010) Mammalian endoplasmic reticulum stress sensor IRE1 signals by dynamic clustering. Proc Natl Acad Sci U S A 107:16113-16118.

Liang G, Audas TE, Li Y, Cockram GP, Dean JD, Martyn AC, Kokame K, Lu R (2006) Luman/CREB3 Induces Transcription of the Endoplasmic Reticulum (ER) Stress Response Protein Herp through an ER Stress Response Element. Mol Cell Biol 26:7999-8010.

Lieberman A (1974) Some factors affecting retrograde neuronal responses to axonal lesions. In: Essays on the Nervous System: A Festschrift for Professor J. Z. Young (Bellairs R, Gray EG, eds), pp 71-105. Oxford: Clarendon Press.

Lin YZ, Yao SY, Veach RA, Torgerson TR, Hawiger J (1995) Inhibition of nuclear translocation of transcription factor NF-kappa B by a synthetic peptide containing a cell membrane-permeable motif and nuclear localization sequence. J Biol Chem 270:14255-14258.

Lindwall C, Kanje M (2005) Retrograde axonal transport of JNK signaling molecules influence injury induced nuclear changes in p-c-Jun and ATF3 in adult rat sensory neurons. Mol Cell Neurosci 29:269-282.

Liu K, Tedeschi A, Park KK, He Z (2011) Neuronal intrinsic mechanisms of axon regeneration. Annual review of neuroscience 34:131-152.

Lu PD, Harding HP, Ron D (2004) Translation reinitiation at alternative open reading frames regulates gene expression in an integrated stress response. J Cell Biol 167:27-33.

Lu R, Misra V (2000) Potential role for luman, the cellular homologue of herpes simplex virus VP16 (alpha gene trans-inducing factor), in herpesvirus latency. J Virol 74:934-943.

Lu R, Yang P, O'Hare P, Misra V (1997) Luman, a new member of the CREB/ATF family, binds to herpes simplex virus VP16-associated host cellular factor. Mol Cell Biol 17:5117-5126.

Lu R, Yang P, Padmakumar S, Misra V (1998) The herpesvirus transactivator VP16 mimics a human basic domain leucine zipper protein, luman, in its interaction with HCF. J Virol 72:6291-6297.

Lu X, Richardson PM (1991) Inflammation near the nerve cell body enhances axonal regeneration. J Neurosci 11:972-978.

Luciano RL, Wilson AC (2000) N-terminal transcriptional activation domain of LZIP comprises two LxxLL motifs and the host cell factor-1 binding motif. Proc Natl Acad Sci U S A 97:10757-10762.

Lunn ER, Perry VH, Brown MC, Rosen H, Gordon S (1989) Absence of Wallerian Degeneration does not Hinder Regeneration in Peripheral Nerve. Eur J Neurosci 1:27-33.

Ma Y, Hendershot LM (2003) Delineation of a negative feedback regulatory loop that controls protein translation during endoplasmic reticulum stress. J Biol Chem 278:34864-34873.

Mack TG, Reiner M, Beirowski B, Mi W, Emanuelli M, Wagner D, Thomson D, Gillingwater T, Court F, Conforti L, Fernando FS, Tarlton A, Andressen C, Addicks K, Magni G, Ribchester RR, Perry VH, Coleman MP (2001) Wallerian degeneration of injured axons and synapses is delayed by a Ube4b/Nmnat chimeric gene. Nat Neurosci 4:1199-1206.

Maiuolo J, Bulotta S, Verderio C, Benfante R, Borgese N (2011) Selective activation of the transcription factor ATF6 mediates endoplasmic reticulum proliferation triggered by a membrane protein. Proc Natl Acad Sci U S A 108:7832-7837.

Majumder M, Huang C, Snider MD, Komar AA, Tanaka J, Kaufman RJ, Krokowski D, Hatzoglou M (2012) A novel feedback loop regulates the response to endoplasmic reticulum stress via the cooperation of cytoplasmic splicing and mRNA translation. Mol Cell Biol 32:992-1003.

Mantuano E, Henry K, Yamauchi T, Hiramatsu N, Yamauchi K, Orita S, Takahashi K, Lin JH, Gonias SL, Campana WM (2011) The unfolded protein response is a major mechanism by which LRP1 regulates Schwann cell survival after injury. J Neurosci 31:13376-13385.

Mar FM, Bonni A, Sousa MM (2014) Cell intrinsic control of axon regeneration. EMBO Rep 15:254-263.

Maxfield FR, Tabas I (2005) Role of cholesterol and lipid organization in disease. Nature 438:612-621.

McKerracher L, David S, Jackson DL, Kottis V, Dunn RJ, Braun PE (1994) Identification of myelin-associated glycoprotein as a major myelin-derived inhibitor of neurite growth. Neuron 13:805-811.

Merianda TT, Lin AC, Lam JS, Vuppalanchi D, Willis DE, Karin N, Holt CE, Twiss JL (2009) A functional equivalent of endoplasmic reticulum and Golgi in axons for secretion of locally synthesized proteins. Mol Cell Neurosci 40:128-142.

Mhaille AN, McQuaid S, Windebank A, Cunnea P, McMahon J, Samali A, FitzGerald U (2008) Increased expression of endoplasmic reticulum stress-related signaling pathway molecules in multiple sclerosis lesions. J Neuropathol Exp Neurol 67:200-211.

Michaelevski I, Segal-Ruder Y, Rozenbaum M, Medzihradszky KF, Shalem O, Coppola G, Horn-Saban S, Ben-Yaakov K, Dagan SY, Rishal I, Geschwind DH, Pilpel Y, Burlingame AL, Fainzilber M (2010) Signaling to transcription networks in the neuronal retrograde injury response. Science signaling 3:ra53.

Mikenberg I, Widera D, Kaus A, Kaltschmidt B, Kaltschmidt C (2007) Transcription factor NF-kappaB is transported to the nucleus via cytoplasmic dynein/dynactin motor complex in hippocampal neurons. PLoS One 2:e589.

Ming GL, Wong ST, Henley J, Yuan XB, Song HJ, Spitzer NC, Poo MM (2002) Adaptation in the chemotactic guidance of nerve growth cones. Nature 417:411-418.

Miserez AR, Cao G, Probst LC, Hobbs HH (1997) Structure of the human gene encoding sterol regulatory element binding protein 2 (SREBF2). Genomics 40:31-40.

Misgeld T, Kerschensteiner M, Bareyre FM, Burgess RW, Lichtman JW (2007) Imaging axonal transport of mitochondria in vivo. Nature methods 4:559-561.

Misra V, Rapin N, Akhova O, Bainbridge M, Korchinski P (2005) Zhangfei is a potent and specific inhibitor of the host cell factor-binding transcription factor Luman. J Biol Chem 280:15257-15266.

Morgenstern DA, Asher RA, Fawcett JW (2002) Chondroitin sulphate proteoglycans in the CNS injury response. Progress in brain research 137:313-332.

Mori K (2009) Signalling pathways in the unfolded protein response: development from yeast to mammals. Journal of biochemistry 146:743-750.

Murphy PG, Borthwick LS, Johnston RS, Kuchel G, Richardson PM (1999) Nature of the retrograde signal from injured nerves that induces interleukin-6 mRNA in neurons. J Neurosci 19:3791-3800.

Nadanaka S, Okada T, Yoshida H, Mori K (2007) Role of disulfide bridges formed in the luminal domain of ATF6 in sensing endoplasmic reticulum stress. Mol Cell Biol 27:1027-1043.

Nagamori I, Yabuta N, Fujii T, Tanaka H, Yomogida K, Nishimune Y, Nojima H (2005) Tisp40, a spermatid specific bZip transcription factor, functions by binding to the unfolded protein response element via the Rip pathway. Genes Cells 10:575-594.

Nash M, Pribiag H, Fournier AE, Jacobson C (2009) Central nervous system regeneration inhibitors and their intracellular substrates. Mol Neurobiol 40:224-235.

Neumann S, Woolf CJ (1999) Regeneration of dorsal column fibers into and beyond the lesion site following adult spinal cord injury. Neuron 23:83-91.

Neumann S, Skinner K, Basbaum AI (2005) Sustaining intrinsic growth capacity of adult neurons promotes spinal cord regeneration. Proc Natl Acad Sci U S A 102:16848-16852.

Niemi JP, DeFrancesco-Lisowitz A, Roldan-Hernandez L, Lindborg JA, Mandell D, Zigmond RE (2013) A critical role for macrophages near axotomized neuronal cell bodies in stimulating nerve regeneration. J Neurosci 33:16236-16248.

Noble J, Munro CA, Prasad VS, Midha R (1998) Analysis of upper and lower extremity peripheral nerve injuries in a population of patients with multiple injuries. The Journal of trauma 45:116-122.

Nohturfft A, Yabe D, Goldstein JL, Brown MS, Espenshade PJ (2000) Regulated step in cholesterol feedback localized to budding of SCAP from ER membranes. Cell 102:315-323.

Novoa I, Zeng H, Harding HP, Ron D (2001) Feedback inhibition of the unfolded protein response by GADD34-mediated dephosphorylation of eIF2alpha. J Cell Biol 153:1011-1022.

Ochs S (1977) The early history of nerve regeneration beginning with Cruikshank's observations in 1776. Medical history 21:261-274.

Oikawa D, Kimata Y, Kohno K, Iwawaki T (2009) Activation of mammalian IRE1alpha upon ER stress depends on dissociation of BiP rather than on direct interaction with unfolded proteins. Exp Cell Res 315:2496-2504.

Ou WJ, Cameron PH, Thomas DY, Bergeron JJ (1993) Association of folding intermediates of glycoproteins with calnexin during protein maturation. Nature 364:771-776.

Papa FR, Zhang C, Shokat K, Walter P (2003) Bypassing a kinase activity with an ATP-competitive drug. Science 302:1533-1537.

Park KK, Liu K, Hu Y, Smith PD, Wang C, Cai B, Xu B, Connolly L, Kramvis I, Sahin M, He Z (2008) Promoting axon regeneration in the adult CNS by modulation of the PTEN/mTOR pathway. Science 322:963-966.

Perlson E, Hanz S, Ben-Yaakov K, Segal-Ruder Y, Seger R, Fainzilber M (2005) Vimentin-dependent spatial translocation of an activated MAP kinase in injured nerve. Neuron 45:715-726.

Perry RB, Doron-Mandel E, Iavnilovitch E, Rishal I, Dagan SY, Tsoory M, Coppola G, McDonald MK, Gomes C, Geschwind DH, Twiss JL, Yaron A, Fainzilber M (2012) Subcellular knockout of importin beta1 perturbs axonal retrograde signaling. Neuron 75:294-305.

Prinjha R, Moore SE, Vinson M, Blake S, Morrow R, Christie G, Michalovich D, Simmons DL, Walsh FS (2000) Inhibitor of neurite outgrowth in humans. Nature 403:383-384.

Qi M, Lei T, Zhou L, Chen XD, Long H, Long QQ, Zhang RR, Yang ZQ, Gan L (2009) Cloning, characterization, chromosomal mapping and tissue transcription analysis of porcine CREB2 and CREB3 genes. Folia biologica 55:137-144.

Raggo C, Rapin N, Stirling J, Gobeil P, Smith-Windsor E, O'Hare P, Misra V (2002) Luman, the cellular counterpart of herpes simplex virus VP16, is processed by regulated intramembrane proteolysis. Mol Cell Biol 22:5639-5649.

Raivich G, Bohatschek M, Da Costa C, Iwata O, Galiano M, Hristova M, Nateri AS, Makwana M, Riera-Sans L, Wolfer DP, Lipp HP, Aguzzi A, Wagner EF, Behrens A (2004) The AP-1 transcription factor c-Jun is required for efficient axonal regeneration. Neuron 43:57-67.

Raman M, Chen W, Cobb MH (2007) Differential regulation and properties of MAPKs. Oncogene 26:3100-3112.

Ramón y Cajal S, May RM (1928, reprinted in 1959) Degeneration and regeneration of the nervous system. New York: Hafner Publishing Company.

Rapallino MV, Cupello A, Giuditta A (1988) Axoplasmic RNA species synthesized in the isolated squid giant axon. Neurochem Res 13:625-631.

Rapiejko PJ, Gilmore R (1997) Empty site forms of the SRP54 and SR alpha GTPases mediate targeting of ribosome-nascent chain complexes to the endoplasmic reticulum. Cell 89:703-713.

Reiling JH, Olive AJ, Sanyal S, Carette JE, Brummelkamp TR, Ploegh HL, Starnbach MN, Sabatini DM (2013) A CREB3-ARF4 signalling pathway mediates the response to Golgi stress and susceptibility to pathogens. Nat Cell Biol 15:1473-1485.

Richardson PM, Issa VM (1984) Peripheral injury enhances central regeneration of primary sensory neurones. Nature 309:791-793.

Richardson PM, Verge VM (1986) The induction of a regenerative propensity in sensory neurons following peripheral axonal injury. J Neurocytol 15:585-594.

Richardson PM, McGuinness UM, Aguayo AJ (1980) Axons from CNS neurons regenerate into PNS grafts. Nature 284:264-265.

Richardson PM, Issa VM, Aguayo AJ (1984) Regeneration of long spinal axons in the rat. J Neurocytol 13:165-182.

Rishal I, Fainzilber M (2010) Retrograde signaling in axonal regeneration. Exp Neurol 223:5-10.

Rishal I, Fainzilber M (2014) Axon-soma communication in neuronal injury. Nature reviews Neuroscience 15:32-42.

Ron D, Walter P (2007) Signal integration in the endoplasmic reticulum unfolded protein response. Nature Reviews Molecular Cell Biology 8:519-529.

Ruff CA, Staak N, Patodia S, Kaswich M, Rocha-Ferreira E, Da Costa C, Brecht S, Makwana M, Fontana X, Hristova M, Rumajogee P, Galiano M, Bohatschek M, Herdegen T, Behrens A, Raivich G (2012) Neuronal c-Jun is required for successful axonal regeneration, but the effects of phosphorylation of its N-terminus are moderate. J Neurochem 121:607-618.

Sakai J, Duncan EA, Rawson RB, Hua X, Brown MS, Goldstein JL (1996) Sterol-regulated release of SREBP-2 from cell membranes requires two sequential cleavages, one within a transmembrane segment. Cell 85:1037-1046.

Samali A, Fitzgerald U, Deegan S, Gupta S (2010) Methods for monitoring endoplasmic reticulum stress and the unfolded protein response. International journal of cell biology 2010:830307.

Sano R, Reed JC (2013) ER stress-induced cell death mechanisms. Biochim Biophys Acta 1833:3460-3470.

Scheib J, Hoke A (2013) Advances in peripheral nerve regeneration. Nature reviews Neurology 9:668-676.

Schindler AJ, Schekman R (2009) In vitro reconstitution of ER-stress induced ATF6 transport in COPII vesicles. Proc Natl Acad Sci U S A 106:17775-17780.

Schnapp BJ, Reese TS (1989) Dynein is the motor for retrograde axonal transport of organelles. Proc Natl Acad Sci U S A 86:1548-1552.

Schuck S, Prinz WA, Thorn KS, Voss C, Walter P (2009) Membrane expansion alleviates endoplasmic reticulum stress independently of the unfolded protein response. J Cell Biol 187:525-536.

Schwaiger FW, Hager G, Schmitt AB, Horvat A, Hager G, Streif R, Spitzer C, Gamal S, Breuer S, Brook GA, Nacimiento W, Kreutzberg GW (2000) Peripheral but not central axotomy induces changes in Janus kinases (JAK) and signal transducers and activators of transcription (STAT). Eur J Neurosci 12:1165-1176.

Seidah NG, Khatib AM, Prat A (2006) The proprotein convertases and their implication in sterol and/or lipid metabolism. Biological chemistry 387:871-877.

Seijffers R, Mills CD, Woolf CJ (2007) ATF3 increases the intrinsic growth state of DRG neurons to enhance peripheral nerve regeneration. J Neurosci 27:7911-7920.

Seymour AB, Andrews EM, Tsai SY, Markus TM, Bollnow MR, Brenneman MM, O'Brien TE, Castro AJ, Schwab ME, Kartje GL (2005) Delayed treatment with monoclonal antibody IN-1 1 week after stroke results in recovery of function and corticorubral plasticity in adult rats. Journal of cerebral blood flow and metabolism : official journal of the International Society of Cerebral Blood Flow and Metabolism 25:1366-1375.

Shen J, Chen X, Hendershot L, Prywes R (2002) ER stress regulation of ATF6 localization by dissociation of BiP/GRP78 binding and unmasking of Golgi localization signals. Dev Cell 3:99-111.

Shen X, Ellis RE, Sakaki K, Kaufman RJ (2005) Genetic interactions due to constitutive and inducible gene regulation mediated by the unfolded protein response in C. elegans. PLoS Genet 1:e37.

Shimano H, Horton JD, Hammer RE, Shimomura I, Brown MS, Goldstein JL (1996) Overproduction of cholesterol and fatty acids causes massive liver enlargement in transgenic mice expressing truncated SREBP-1a. The Journal of clinical investigation 98:1575-1584.

Shimano H, Horton JD, Shimomura I, Hammer RE, Brown MS, Goldstein JL (1997) Isoform 1c of sterol regulatory element binding protein is less active than isoform 1a in livers of transgenic mice and in cultured cells. The Journal of clinical investigation 99:846-854.

Shin JE, Cho Y, Beirowski B, Milbrandt J, Cavalli V, DiAntonio A (2012) Dual leucine zipper kinase is required for retrograde injury signaling and axonal regeneration. Neuron 74:1015-1022.

Silver J, Miller JH (2004) Regeneration beyond the glial scar. Nature reviews Neuroscience 5:146-156.

Simonen M, Pedersen V, Weinmann O, Schnell L, Buss A, Ledermann B, Christ F, Sansig G, van der Putten H, Schwab ME (2003) Systemic deletion of the myelin-associated outgrowth inhibitor Nogo-A improves regenerative and plastic responses after spinal cord injury. Neuron 38:201-211.

Smith DS, Skene JH (1997) A transcription-dependent switch controls competence of adult neurons for distinct modes of axon growth. J Neurosci 17:646-658.

Sriburi R, Jackowski S, Mori K, Brewer JW (2004) XBP1: a link between the unfolded protein response, lipid biosynthesis, and biogenesis of the endoplasmic reticulum. J Cell Biol 167:35-41.

Stirling DP, Cummins K, Wayne Chen SR, Stys P (2014) Axoplasmic reticulum Ca(2+) release causes secondary degeneration of spinal axons. Ann Neurol 75:220-229.

Storlazzi CT, Mertens F, Nascimento A, Isaksson M, Wejde J, Brosjo O, Mandahl N, Panagopoulos I (2003) Fusion of the FUS and BBF2H7 genes in low grade fibromyxoid sarcoma. Hum Mol Genet 12:2349-2358.

Sung HJ, Kim YS, Kang H, Ko J (2008) Human LZIP induces monocyte CC chemokine receptor 2 expression leading to enhancement of monocyte chemoattractant protein 1/CCL2-induced cell migration. Experimental & molecular medicine 40:332-338.

Taylor AM, Berchtold NC, Perreau VM, Tu CH, Jeon NL, Cotman CW (2009) Axonal mRNA in uninjured and regenerating cortical mammalian axons. J Neurosci 29:4697-4707.

Tcherkezian J, Brittis PA, Thomas F, Roux PP, Flanagan JG (2010) Transmembrane receptor DCC associates with protein synthesis machinery and regulates translation. Cell 141:632-644.

Terzis JK, Sun DD, Thanos PK (1997) Historical and basic science review: past, present, and future of nerve repair. Journal of reconstructive microsurgery 13:215-225.

Teske BF, Wek SA, Bunpo P, Cundiff JK, McClintick JN, Anthony TG, Wek RC (2011) The eIF2 kinase PERK and the integrated stress response facilitate activation of ATF6 during endoplasmic reticulum stress. Mol Biol Cell 22:4390-4405.

Torgerson TR, Colosia AD, Donahue JP, Lin YZ, Hawiger J (1998) Regulation of NF-kappa B, AP-1, NFAT, and STAT1 nuclear import in T lymphocytes by noninvasive delivery of peptide carrying the nuclear localization sequence of NF-kappa B p50. J Immunol 161:6084-6092.

Towne C, Pertin M, Beggah AT, Aebischer P, Decosterd I (2009) Recombinant adeno-associated virus serotype 6 (rAAV2/6)-mediated gene transfer to nociceptive neurons through different routes of delivery. Molecular pain 5:52.

Travers KJ, Patil CK, Wodicka L, Lockhart DJ, Weissman JS, Walter P (2000) Functional and genomic analyses reveal an essential coordination between the unfolded protein response and ER-associated degradation. Cell 101:249-258.

Truettner JS, Hu K, Liu CL, Dietrich WD, Hu B (2009) Subcellular stress response and induction of molecular chaperones and folding proteins after transient global ischemia in rats. Brain Res 1249:9-18.

Tsujino H, Kondo E, Fukuoka T, Dai Y, Tokunaga A, Miki K, Yonenobu K, Ochi T, Noguchi K (2000) Activating transcription factor 3 (ATF3) induction by axotomy in sensory and motoneurons: A novel neuronal marker of nerve injury. Mol Cell Neurosci 15:170-182.

Tsukita S, Ishikawa H (1976) Three-dimensional distribution of smooth endoplasmic reticulum in myelinated axons. Journal of electron microscopy 25:141-149.

Van Minnen J, Bergman JJ, Van Kesteren ER, Smit AB, Geraerts WP, Lukowiak K, Hasan SU, Syed NI (1997) De novo protein synthesis in isolated axons of identified neurons. Neuroscience 80:1-7.

Vargas ME, Barres BA (2007) Why is Wallerian degeneration in the CNS so slow? Annual review of neuroscience 30:153-179.

Verge VM, Gratto KA, Karchewski LA, Richardson PM (1996) Neurotrophins and nerve injury in the adult. Philos Trans R Soc Lond B Biol Sci 351:423-430.

Verma P, Chierzi S, Codd AM, Campbell DS, Meyer RL, Holt CE, Fawcett JW (2005) Axonal protein synthesis and degradation are necessary for efficient growth cone regeneration. J Neurosci 25:331-342.

Vogelaar CF, Gervasi NM, Gumy LF, Story DJ, Raha-Chowdhury R, Leung KM, Holt CE, Fawcett JW (2009) Axonal mRNAs: characterisation and role in the growth and regeneration of dorsal root ganglion axons and growth cones. Mol Cell Neurosci 42:102-115.

Volmer R, van der Ploeg K, Ron D (2013) Membrane lipid saturation activates endoplasmic reticulum unfolded protein response transducers through their transmembrane domains. Proc Natl Acad Sci U S A 110:4628-4633.

Vuppalanchi D, Merianda TT, Donnelly C, Pacheco A, Williams G, Yoo S, Ratan RR, Willis DE, Twiss JL (2012) Lysophosphatidic acid differentially regulates axonal mRNA translation through 5'UTR elements. Mol Cell Neurosci 50:136-146.

Walker BA, Hengst U, Kim HJ, Jeon NL, Schmidt EF, Heintz N, Milner TA, Jaffrey SR (2012) Reprogramming axonal behavior by axon-specific viral transduction. Gene therapy 19:947-955.

Waller A (1850) Experiments on the Section of the Glossopharyngeal and Hypoglossal Nerves of the Frog, and Observations of the Alterations Produced Thereby in the Structure of Their Primitive Fibres. Philosophical Transactions of the Royal Society of London 140:423-429.

Waller AV (1861) The Nutrition and Reparation of Nerves: Being the Substance of a Lecture Delivered at the Royal Institution of Great Britain, Friday May 31, 1861. London: Read and Company.

Walter P, Ron D (2011) The unfolded protein response: from stress pathway to homeostatic regulation. Science 334:1081-1086.

Wang X, Sato R, Brown MS, Hua X, Goldstein JL (1994) SREBP-1, a membrane-bound transcription factor released by sterol-regulated proteolysis. Cell 77:53-62.

Wellmann H, Kaltschmidt B, Kaltschmidt C (2001) Retrograde transport of transcription factor NF-kappa B in living neurons. J Biol Chem 276:11821-11829.

Werstuck GH, Lentz SR, Dayal S, Hossain GS, Sood SK, Shi YY, Zhou J, Maeda N, Krisans SK, Malinow MR, Austin RC (2001) Homocysteine-induced endoplasmic reticulum stress causes dysregulation of the cholesterol and triglyceride biosynthetic pathways. The Journal of clinical investigation 107:1263-1273.

Wiessner C, Bareyre FM, Allegrini PR, Mir AK, Frentzel S, Zurini M, Schnell L, Oertle T, Schwab ME (2003) Anti-Nogo-A antibody infusion 24 hours after experimental stroke improved behavioral outcome and corticospinal plasticity in normotensive and spontaneously hypertensive rats. Journal of cerebral blood flow and metabolism : official journal of the International Society of Cerebral Blood Flow and Metabolism 23:154-165.

Wilkinson B, Gilbert HF (2004) Protein disulfide isomerase. Biochim Biophys Acta 1699:35-44.

Willis T, Feindel W (1681, reprinted in 1966) The anatomy of the brain and nerves. Montreal,: McGill University Press.

Xu CS, Shao HY, Liu SS, Qin B, Sun XF, Tian L (2009) Possible regulation of genes associated with intracellular signaling cascade in rat liver regeneration. Scandinavian journal of gastroenterology 44:462-470, 410 p following 470.

Yabe D, Brown MS, Goldstein JL (2002) Insig-2, a second endoplasmic reticulum protein that binds SCAP and blocks export of sterol regulatory element-binding proteins. Proc Natl Acad Sci U S A 99:12753-12758.

Yamada KM, Spooner BS, Wessells NK (1971) Ultrastructure and function of growth cones and axons of cultured nerve cells. J Cell Biol 49:614-635.

Yamamoto K, Sato T, Matsui T, Sato M, Okada T, Yoshida H, Harada A, Mori K (2007) Transcriptional induction of mammalian ER quality control proteins is mediated by single or combined action of ATF6alpha and XBP1. Dev Cell 13:365-376.

Yan D, Wu Z, Chisholm AD, Jin Y (2009) The DLK-1 kinase promotes mRNA stability and local translation in C. elegans synapses and axon regeneration. Cell 138:1005-1018.

Yang T, Espenshade PJ, Wright ME, Yabe D, Gong Y, Aebersold R, Goldstein JL, Brown MS (2002) Crucial step in cholesterol homeostasis: sterols promote binding of SCAP to INSIG-1, a membrane protein that facilitates retention of SREBPs in ER. Cell 110:489-500.

Yawo H, Kuno M (1985) Calcium dependence of membrane sealing at the cut end of the cockroach giant axon. J Neurosci 5:1626-1632.

Ye J, Rawson RB, Komuro R, Chen X, Dave UP, Prywes R, Brown MS, Goldstein JL (2000) ER stress induces cleavage of membrane-bound ATF6 by the same proteases that process SREBPs. Mol Cell 6:1355-1364.

Ying Z, Zhang R, Verge VM, Misra V (2014) Cloning and Characterization of Rat Luman/CREB3, A Transcription Factor Highly Expressed in Nervous System Tissue. J Mol Neurosci. DOI: 10.1007/s12031-014-0330-7.

Ylera B, Erturk A, Hellal F, Nadrigny F, Hurtado A, Tahirovic S, Oudega M, Kirchhoff F, Bradke F (2009) Chronically CNS-injured adult sensory neurons gain regenerative competence upon a lesion of their peripheral axon. Current biology : CB 19:930-936.

Yokoyama C, Wang X, Briggs MR, Admon A, Wu J, Hua X, Goldstein JL, Brown MS (1993) SREBP-1, a basic-helix-loop-helix-leucine zipper protein that controls transcription of the low density lipoprotein receptor gene. Cell 75:187-197.

Yoshida H, Oku M, Suzuki M, Mori K (2006) pXBP1(U) encoded in XBP1 pre-mRNA negatively regulates unfolded protein response activator pXBP1(S) in mammalian ER stress response. J Cell Biol 172:565-575.

Yoshida H, Haze K, Yanagi H, Yura T, Mori K (1998) Identification of the cis-acting endoplasmic reticulum stress response element responsible for transcriptional induction of mammalian glucose-regulated proteins. Involvement of basic leucine zipper transcription factors. J Biol Chem 273:33741-33749.

Yoshida H, Matsui T, Yamamoto A, Okada T, Mori K (2001) XBP1 mRNA is induced by ATF6 and spliced by IRE1 in response to ER stress to produce a highly active transcription factor. Cell 107:881-891.

Yoshida H, Okada T, Haze K, Yanagi H, Yura T, Negishi M, Mori K (2000) ATF6 activated by proteolysis binds in the presence of NF-Y (CBF) directly to the cis-acting element responsible for the mammalian unfolded protein response. Mol Cell Biol 20:6755-6767.

Yudin D, Fainzilber M (2009) Ran on tracks--cytoplasmic roles for a nuclear regulator. J Cell Sci 122:587-593.

Yudin D, Hanz S, Yoo S, Iavnilovitch E, Willis D, Gradus T, Vuppalanchi D, Segal-Ruder Y, Ben-Yaakov K, Hieda M, Yoneda Y, Twiss JL, Fainzilber M (2008) Localized regulation of axonal RanGTPase controls retrograde injury signaling in peripheral nerve. Neuron 59:241-252.

Zhang K, Shen X, Wu J, Sakaki K, Saunders T, Rutkowski DT, Back SH, Kaufman RJ (2006) Endoplasmic reticulum stress activates cleavage of CREBH to induce a systemic inflammatory response. Cell 124:587-599.

Zheng B, Ho C, Li S, Keirstead H, Steward O, Tessier-Lavigne M (2003) Lack of enhanced spinal regeneration in Nogo-deficient mice. Neuron 38:213-224.

Zheng JQ, Kelly TK, Chang B, Ryazantsev S, Rajasekaran AK, Martin KC, Twiss JL (2001) A functional role for intra-axonal protein synthesis during axonal regeneration from adult sensory neurons. J Neurosci 21:9291-9303.

Zhou J, Liu CY, Back SH, Clark RL, Peisach D, Xu Z, Kaufman RJ (2006) The crystal structure of human IRE1 luminal domain reveals a conserved dimerization interface required for activation of the unfolded protein response. Proc Natl Acad Sci U S A 103:14343-14348.

Zigmond RE (2012) Cytokines that promote nerve regeneration. Exp Neurol 238:101-106.

Zochodne DW (2012) The challenges and beauty of peripheral nerve regrowth. Journal of the peripheral nervous system : JPNS 17:1-18.

Zorner B, Schwab ME (2010) Anti-Nogo on the go: from animal models to a clinical trial. Ann N Y Acad Sci 1198 Suppl 1:E22-34.